# Elucidating conformational changes in Syntaxin-1a on different stages of SNAREs assembly using Electron Paramagnetic Resonance

Vanessa Amanda Bijak

Bachelor of Engineering in Chemistry, Warsaw University of Technology, 2014

Master of Science in Chemistry, Warsaw University of Technology, 2017

A Dissertation presented to the Graduate Faculty of the University of Virginia in Candidacy for the Degree of Doctor of Philosophy

Department of Chemistry

University of Virginia

July, 2022

July 2022

# ABSTRACT

When an action potential arrives at the axon terminal, it causes a local increase in intracellular $Ca^{2+}$ concentration that starts a cascade of molecular interactions leading to the fusion of synaptic vesicles with the plasma membrane. This process is called neuronal exocytosis and is mediated by SNARE proteins. SNAREs are a highly conserved group of proteins that interact to form a coiled-coil assembly called the SNARE complex. The assembly of this complex is believed to provide the driving force for the fusion of the neurotransmitter-carrying vesicles to the presynaptic membrane. In the neuronal system, the SNARE complex is formed by three proteins: synaptobrevin, syntaxin-1a, and SNAP25. In addition to the SNAREs, other proteins such as Complexin, Synaptotagmin, Munc13, and Munc18 serving regulatory roles by interacting with membranes or the SNAREs.

The primary goal of this study was to investigate Syntaxin-1a, which is known to play an essential role in the process of neuronal exocytosis and signal transduction. This protein has been studied for years; however, its exact function and mechanism of action are still not fully characterized. In this study, I investigated the conformations of the plasma membrane or t-SNARE Syntaxin-1a that are believed to occur during the priming steps leading to membrane fusion. Syntaxin-1a has several domains, including a transmembrane anchor, an H3 or SNARE motif, a regulatory Habc motif, a linker that connects the H3 and Habc domains, and a short N-terminal segment called N-peptide. During the SNARE assembly process, Syntaxin-1a interacts with the SNARE chaperone Munc18. When bound to Munc18 in solution, the Habc and H3 domains are brought into proximity leading to a closed state of Syntaxin-1a. In addition to this binding mode, Munc18 also binds to the assembled SNARE complex; however, neither the mode of this interaction nor the state of the Habc regulatory domain are well characterized in this complex.

Here, I examined Syntaxin-1a using two different approaches. In the first, I used CW-EPR spectroscopy to determine if Syntaxin-1a (alone and assembled into the t-SNARE or SNARE complex) and Munc18 interact with each other. In the second, DEER spectroscopy was used to determine the conformation of Syntaxin-1a at different stages during the SNARE assembly process and to determine how Munc18 changes the conformation of Syntaxin-1a in different environments, and when it is assembled into t-SNARE or cis-SNARE complexes.

It is generally believed that when Munc18 binds to a complex of Syntaxin-1a and SNAP25, SNAP25 is dissociated, and Syntaxin-1a assumes a closed state. However, work from our laboratory indicates that Munc18 converts a 2:1 complex of Syntaxin-1a and SNAP25 into a 1:1 complex, where Syntaxin-1a is in a closed state. The work presented here supports this earlier finding and indicates in the absence of an N-terminal fragment of Syntaxin-1a, Munc18 also binds to the t-SNARE complex. Moreover, Munc18 binds to the SNARE complex through the Habc domain of Syntaxin-1a. In the case of the SNARE complex, there is no interaction between the complex and Munc18 in the absence of an N-terminal domain of Syntaxin-1a, indicating that the N-terminal domain of Syntaxin-1a is required for Munc18 to associate with the SNARE complex.

I confirmed an equilibrium between an open and closed states of Syntaxin-1a for each stage of the SNAREs assembly process. For assembled Syntaxin-1a, the equilibrium is shifted primarily towards an open state. Munc18 binds to Syntaxin-1a at each step during assembly, and shifts the equilibrium towards the closed state of Syntaxin-1a.

# Table of Contents

# ACKNOWLEADGMENTS

The start and, more importantly, the conclusion of this graduate program would not have been possible without the strong support and encouragement of many people along this journey. I am very grateful to every person I meet along the way.

First and foremost, I would like to thank my advisor, prof. David Cafiso, for accepting me to join his group. First as a Visiting Student and then as a Graduate Student, for guiding me into the field, providing me with the opportunity to work and explore my ideas, to flourish with my research. I would like to thank you for being an understanding and compassionate PI when times were hard and for your encouragement when I had doubts about being in this program. Thanks to your guidance, I learned how to explore my ideas deeply and be patient in a field with many uncertainties and unanswered questions. The experience of being a member of this group has taught me far more than I was expecting about how to be a good scientist, the beautiful art of troubleshooting, and how to advocate for myself. Thank you for the past seven years. I could not have imagined a better advisor for my Ph.D. journey.

The time I spent in Cafiso Lab would not be so enjoyable without all my lab members, past and present. Whether it was through good or bad times, planned and surprise birthday parties, way too many lab floods, freezer emergencies, or endless nights in the lab, for all those thank you for standing by my side and for making sure that all is fine. Special thanks go to my always supportive dear friend Qian for sharing tears and laughs and always being there when needed.

I would not have been able to start my academic career in chemistry without the wonderful people I met along my journey in Poland and the United States. Thanks to my advisors at the Warsaw University of Technology for showing me the beauty of interdisciplinary research. I performed my first independent research under their guidance. I took my first steps at the

conferences with them and won my first oral and poster presentations. Without this experience, I would never have applied for the BioLab program. Thanks to dr. Carol Price, being her teaching assistant, was a wonderful experience. I would also like to acknowledge the directors of graduate studies, prof. Ian Harrison and prof. Thomas Brent Gunnoe, the department chair prof. Jill Venton and the graduate studies coordinator Susie Marshall for answering my questions along the way, being there when I needed help, and showing me your support and kindness.

Thank you to all of my committee members, prof. Zygmunt Derewenda, prof. Andreas Gahlmann and prof. Ken Hsu, for all the insightful comments, challenging questions, and kind feedback on my candidacy exam and all the committee meetings we had through the years. I appreciate your help in making this thesis the best it can be.

Thanks to all my friends worldwide who were always supportive.

Besides all these wonderful people, I would like to express my gratitude to those who were and are with me daily with endless support. From the bottom of my heart, I thank my Mom and Dad for their unconditional love, support, sacrifices, and blessings. Huge thank you to my little brother for all his “powodzenia siostra” along the way. All of these strengthened me never to give up pursuing a Ph.D. Heartful gratitude to my husband, Tomek, for being on the grad school roller-coaster for all these years and for helping me in every possible way.

Thank you!

## List of Figures

## List of Tables

## Abbreviations

AEBSF - 4-(2-aminoethyl)benzenesulfonyl fluoride hydrochloride

ATP - Adenosine triphosphate

bPC - Porcine brain L-$\alpha$-phosphatidylcholine

bPE - Porcine brain L- $\alpha$-phosphatidylethanolamine

bPS - Porcine brain L- $\alpha$-phosphatidylserine

CNS - Central nervous system

Cpx - Complexin

DNA - Deoxyribonucleic acid

dNTP – dinucleotidetriphosphate

DOPC - 1,2-Dioleoyl-sn-glycero-3-phosphocholine

DOPE - 1,2-Dioleoyl-sn-glycero-3-phospho-L-serine

DOPS - 1,2-Dioleoyl-sn-glycero-3-phosphoethanolamine

DPPC - 1,2-Dipalmitoyl-sn-glycero-3-phosphocholine

DPPE - 1,2-Dipalmitoyl-sn-glycero-3-phosphoethanolamine

DPPS - 1,2-Dipalmitoyl-sn-glycero-3-phospho-L-serine

DTT - Dithiothreitol

EDTA - Ethylenediaminetetraacetic acid

EPR - Electron paramagnetic resonance

HEPES - 2-[4-(2-hydroxyethyl)piperazin-1-yl]ethanesulfonic acid

IPTG - Isopropyl-β-D-thiogalacto-pyranoside

MOPS - 3-(N-morpholino)propanesulfonic acid

MTSL - S-(1-oxyl-2,2,5,5–tetramethyl-2,5–dihydro-1H–pyrrol–3yl) methylmethanethiosulfonate

Munc13 - Mammalian uncoordinated-13

Munc18 - Mammalian uncoordinated 18

NMR - Nuclear magnetic resonance

PIP2 - Porcine brain L-α-phosphatidylinositol-4,5-bisphosphate

POPC - 1-Palmitoyl-2-oleoyl-sn-glycero-3-phosphocholine

POPE - 1-Palmitoyl-2-oleoyl-sn-glycero-3-phosphoethanolamine

POPG - 1-palmitoyl-2-oleoyl-sn-glycero-3-phospho-(glycerol)

POPS - 1-Palmitoyl-2-oleoyl-sn-glycero-3-phospho-L-serine

Q-SNAREs - Proteins that contribute a glutamine (Q) residue in the assembled core SNARE complex, such as syntaxin and SNAP25

R-SNARE - Proteins that contribute a glutamine (Q) residue in the assembled core SNARE complex, such as synaptobrevin

SDSL - Site directed spin labeling

SM - Sec-1/Munc18

SNAP25 - Synaptosome associated protein 25

SNARE - Soluble N-ethylmaleimide–sensitive factor attachment protein receptors

Syx-1a - Syntaxin-1a

t-SNARE - Target SNARE

Tris - tris(hydroxymethyl)aminomethane hydrochloride

v-SNARE - Vesicle SNARE

# I. INTRODUCTION

## 1.1 Neuronal Exocytosis

Exocytosis and endocytosis are processes that either release material from the cell interior or take in material from the external environment, respectively. Both processes involve the remodeling of membranes. They are vital for all living cells, require energy, and are a form of active transport. During exocytosis, intracellular vesicles fuse with a plasma membrane releasing the vesicle contents to the extracellular space[1].

Neuronal exocytosis is the basis for neurotransmission. It involves the fusion of synaptic vesicles with the presynaptic membrane, thereby releasing neurotransmitter molecules into the synaptic cleft. Neurotransmission is the fundamental and highly regulated process underlying information transfer between nerve cells. This process is responsible for all functions in the central nervous system (CNS), which monitors and coordinates internal organ function and responds to all changes in the external environment in all species, from invertebrates to highly evolved mammals. Dysfunction in neurotransmission is involved in various neurological disorders[2,3], including autism, Alzheimer's, bipolar disorder[4], dementia, depression[5], epilepsy, and schizophrenia[6,7]. Thus, it is essential to understand the complex and sophisticated molecular mechanisms and interactions underlying synaptic transmission.

Neurotransmission is a multistage regulated process that occurs at specific regions between two neurons. This region is called a synapse. Synaptic transmission is mediated by repeated cycles of exocytosis of neurotransmitters followed by the endocytosis of plasma membrane material at the nerve terminus. It relies on proper protein-protein and protein-lipid interactions in a time-sensitive manner in the complex neuronal wiring scheme.

Despite considerable progress in understanding the molecular level events that underlie neuronal exocytosis, the roles of individual proteins remain unknown especially the sequence and kinetics of protein-protein interactions that drive the vesicle cycle[2,3,5].

In this section, nerve cells and synapses, the process of intracellular vesicle trafficking, and the basics of membrane fusion will be introduced. Then, we will take a closer look at the presynaptic active zone, which consists of unique protein components that accomplish synaptic vesicle fusion and neurotransmitter release. Among these proteins, are the SNARE proteins: Syntaxin-1a (Syx), SNAP-25, and Synaptobrevin (Syb), and complexes that they form. Finally, we will describe regulatory proteins like synaptotagmin-1, complexin-1, and Munc18 which are neuron-specific and indispensable for proper synaptic function. Synaptotagmin-1 serves as the $Ca^{2+}$ -sensor by coupling $Ca^{2+}$ -influx tightly with vesicle fusion, and complexin-1 modulates neuronal exocytosis by suppressing spontaneous vesicle fusion (in the absence of $Ca^{2+}$) and facilitating $Ca^{2+}$ -evoked release. Munc18 acts as a chaperon for Syx to prevent unspecific interactions. This chapter will allow us to have a better molecular view of the fusion site.

### 1.1.1 The nervous system and the neuron

The nervous system consists of the central nervous system (CNS) and the peripheral nervous system. There are two components of the CNS, the brain and the spinal cord, while the peripheral nervous system is composed of a complex network of neurons[8]. The nervous system is a two-way pathway responsible for sending, receiving, and interpreting information from all body parts, with the CNS being its processing center. The nervous system monitors and coordinates internal organ function by integrating all information received from the

environment with the proprioceptive information to produce and send an appropriate response in the form of physiological change or a change in motion[8,9]. Understanding many functions of this fascinating organ entails exploring the interconnections of many nerve cells organized in neural networks. This process is the key to understanding the cause of diseases and neurological disorders. Even the slightest change at any stage of the neurotransmission process can cause significant changes in overall mind and body function. Sleep disorders, impaired learning/thinking/memory, impaired motor capacity, and chronic pain are among the general examples mentioned before[3,10]. They all are linked to pathological changes on several levels, including the molecular. Unfortunately, many neurological conditions are still not fully understood on the neuronal level, not to mention the molecular level, and there is a need to understand neurotransmission at the basic chemical level[11].

The basic functional unit of the nervous system is the nerve cell or neuron. There are 86 billion of neurons in the brain alone[12]. They were first described by Ramón y Cajal in 1888. They may assume different shapes and sizes, and they have unique functions in the brain, spinal cord, and muscle[13]. All neurons are highly specialized and responsible for different functions in human body. We usually classify neurons based on function (motor, sensory, and interneurons) or structural differences (multipolar, unipolar, bipolar, pseudo-unipolar)[14]. Despite this variability, all neurons have the same essential components that enable them to receive and transmit signals through the body. Neurons are typically composed of a cell body (soma), one axon, and many highly branched, thin dendrites (see Figure 1)[15]. Axons and dendrites are bundled together into what are called nerves. There is one particular case where there is no axon, and such neuron is called anaxonic. This neuron can be found in some brain regions.

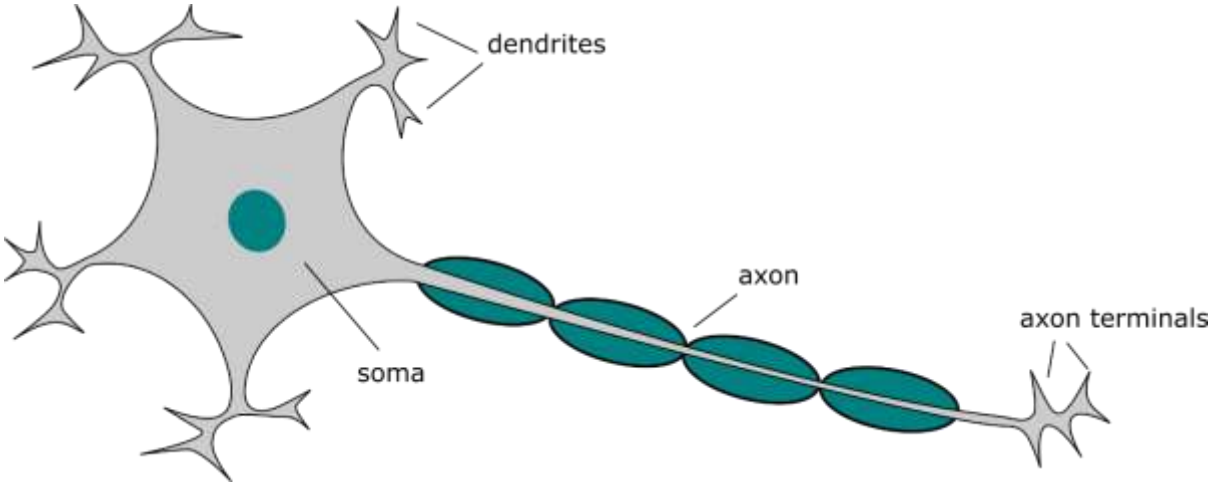


***Figure 1.*** *Illustration of the single motoneuron. A neuron cell body (soma) is a compact structure that extrudes two types of filaments: axon and dendrites. Dendrites are typically highly branched and are responsible for receiving information from other neurons. The axon leaves the soma as a single filament that branches at the end. Axon's branches are called axon terminals. The axon sends information received by dendrites to the next neuron in line.*

The flow of information in the neuron is unidirectional, from the dendrites through the cell body to the axon. In this case, dendrites are the primary input center of the neuron, and they receive signals from the preceding neuron's axon terminal. They are usually more numerous, significantly shorter, and more highly branched than the axon. The extensive branching can substantially increase the contact surface with other neurons[16]. The neuron's axon is a thin extension downward from the cell body, and it carries signals away from the cell body. In contrast to dendrites, the branching of the axon occurs at its very end. The branched part of the axon, or telodendrion, ends in structures called axon terminals.

Action potential plays a central role in the cell's communication in the nerve cells. The action potential is a fast (up to 100m/s) electrical impulse that originates at the axon's initial segment and travels along the axon length[17]. Upon reaching the axonal terminal, the action potential causes a cascade of molecular changes that eventually lead to the transfer of information to the next downstream cell. The action potential in the neuron is also called a nerve impulse or spike.

### 1.1.2 Synapses

As mentioned earlier, the human brain contains about 86 billion neurons, and every single one can influence many other cells in the whole human body. A highly specialized mechanism is required to enable communication between the elements of the nervous system. Passing information between two neurons or a neuron and effector cell is called neurotransmission. Neurotransmission takes place through synapses, the functional contact points between neurons. In synapses, neurons can pass electrical and chemical signals between each other. Synapses are composed of a presynaptic neuron terminus, a synaptic cleft, and a postsynaptic

neuron surface (Figure 2)[18]. Although there are many subtypes of synapses within the brain, the primary two general classes are electrical and chemical synapses.

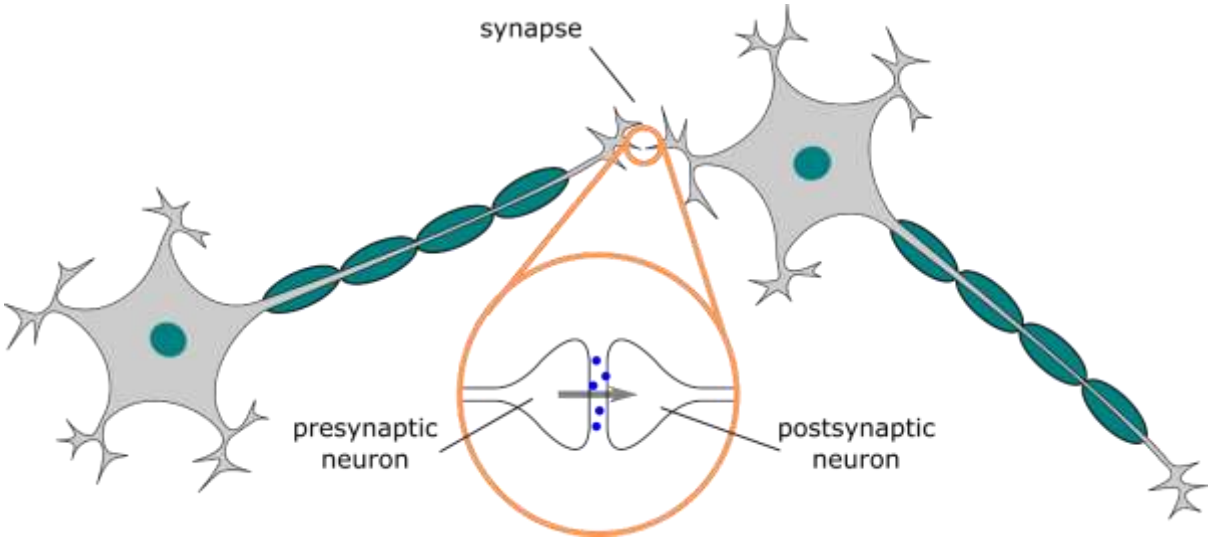


***Figure 2.*** *A synapse is a junction between the dendrites of one neuron and the axon terminal of another. The synapse is the region where nerve impulses are transmitted.*

#### 1.1.2.1 Electrical synapses

Despite being in the minority of synapses, electrical synapses are widely distributed in the mammalian brain[19,20]. Electrical synapse are defined by how the two contacting neurons are linked. This particular kind of intercellular connection is called a gap junction (Figure 3B). Gap junctions contain precisely aligned paired channels in the membrane of each neuron so that each pair forms a pore. The size of these pores is large enough to allow molecules with a molecular weight of up to several hundred Daltons to diffuse between the cytoplasm of the pre- and postsynaptic neurons[21]. In this way, electrical synapses provide a pathway for both ionic current and small organic molecules. The direct connection between two neurons allows for the uninterrupted and bidirectional spread of electrical changes[22]. The nature of the electrical synapses allows signals to travel much faster than in chemical synapses. However, the structural organization of the electrical synapse does not allow for signal amplification or modulation. Also, a signal might diminish from one neuron to the next. Both of these factors make them less effective. Despite mentioned limitations, electrical synapses are essential for the proper and unmodified function of the nervous system[23].

#### 1.1.2.2 Chemical synapses

Chemical synapses are the most common of all neuronal communication in mammals. The synaptic complex consists of three essential elements (Figure 3A):

- A presynaptic element (e.g., axon terminal)
- A synaptic cleft
- A postsynaptic element (e.g., dendritic spine)

This structure is the basic unit of a chemical synapse, and it is required for effective neurotransmission[24].

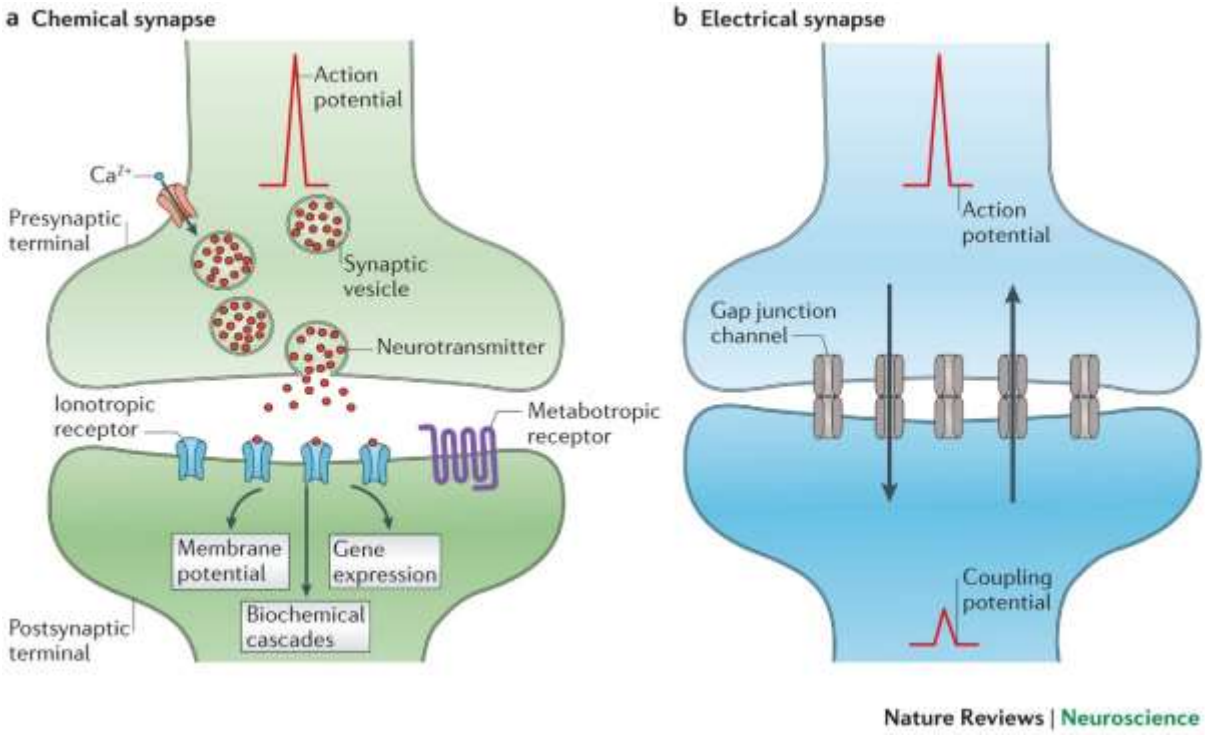


***Figure 3.*** *<u>Two main classes of synapses.</u>* ***A.*** *Chemical synapse - The presynaptic neuron contains synaptic vesicles loaded with neurotransmitters. The postsynaptic neuron is equipped with neurotransmitter binding channels on its surface. The synaptic cleft separates both neurons.* ***B.*** *Electrical synapse. The presynaptic and postsynaptic neurons are connected by intercellular channels called gap junctions. Electrical synapses are bidirectional. (Figure source: Pereda, 2014)*[21]

Two elements characterize the presynaptic element. The first one is an active zone with a high density of $Ca^{2+}$ channels. The fusion of synaptic vesicles (exocytosis) occurs in this zone, and the whole process is described later in this chapter. The second element is a region where all synaptic vesicles containing neurotransmitters are close to the presynaptic membrane. In contrast, the postsynaptic element is characterized by a high density of receptors specific for certain neurotransmitters. The morphology of the presynaptic and postsynaptic neurons ensure that synaptic transmission occurs only in one direction, from the presynaptic element to the postsynaptic element. The separation between two neurons (synaptic cleft) is significantly more prominent than the gap junction in electrical synapses, with an average distance of about 20 nm[25]. The synaptic cleft is filled with proteins responsible for maintaining proper position, orientation, and distance between two neurons[26].

Although chemical synapses are slower than electrical synapses, their ability to amplify, modulate and adapt the synaptic signal is much greater. These features and the large number of chemical synapses in the nervous system make them intensive area research and is one reason that they are better understood than electrical synapses[21].

The work presented in this dissertation focuses on the proteins responsible for the events that facilitate the synaptic vesicle fusion with the plasma membrane. That is why, the following sections will address the pre-synapse and membrane fusion in more detail.

#### 1.1.2.3 Pre-synapse

One of the most characteristic features that differentiates the pre-synapse from post-synapse is the presence of numerous synaptic vesicles. Synaptic vesicles are spherically shaped organelles with an average diameter of ~40 nm[27,28,29]. They can be divided into different populations: the

readily releasable pool, the recycling pool, and the reserve pool[30]. The differences between these pools are based on their functions and localization in the pre-synapse. Every single synaptic vesicle contains a large number of molecules of neurotransmitter. Neurotransmitters are released in a controlled manner into the synaptic cleft during neuronal exocytosis, the final step in the cycle that leads to information transfer between two neurons[31].

#### 1.1.2.4 Vesicle cycle

Vesicle trafficking is a highly regulated process that is assisted by vesicular and plasma membrane proteins that function at various steps in this process. These steps include loading neurotransmitter into the synaptic vesicle, docking the vesicle, priming, $Ca^{2+}$-sensing, exocytosis, and later vesicle recycling to restart the whole process (see Figure 4 for reference)[30].

Once at the synapse, each vesicle is loaded with neurotransmitter. These vesicles are translocated to the active zone that is localized directly at the plasma membrane of the presynaptic cleft. Each synapse can have from 1 to nearly 1000 active zones forming a region where fusion occurs[32]. The first process in the active zone is docking. The loaded vesicle must be docked appropriately near the release site. Although many proteins have been identified on synaptic vesicles and at the release site, a knowledge of their role in docking is not well understood. Mutations in Munc18 alter docking and vesicle organization, but they do not entirely block this process[33]. Also, SNARE proteins, especially Syntaxin-1a, appear to be involved in the docking[34]. After proper docking and prior to fusion, the vesicle must be primed. At this stage, the vesicle is being prepared to undergo membrane fusion in response to an influx of $Ca^{2+}$ and an increase in intracellular $Ca^{2+}$ levels. This step is believed to involve already

partially assembled SNARE complexes (v-SNARE or t-SNARE). Munc13 participates in this process by stimulating changes in the closed conformation of Syntaxin-1a, which leads to the assembly of v-SNARE or t-SNARE complexes[35]. Upon the arrival of the action potential at the axon terminal, voltage-dependent $Ca^{2+}$ channels open, causing a sudden $Ca^{2+}$ influx. $Ca^{2+}$ ions play a role as signaling molecules, and the increase in $Ca^{2+}$ levels puts in motion all the necessary protein-protein and protein-lipid interactions that lead to the fusion of the synaptic vesicle with the plasma membrane. This results is the release of neurotransmitter into the synaptic cleft. The $Ca^{2+}$ sensor in this system is a protein called Synaptotagmin. The free energy released from the assembly of the SNARE complex is believed to be a driving force of fusion. Released neurotransmitter binds to receptors in the postsynaptic membrane and enables activation and signaling in the postsynaptic neuron. When vesicles fuse with the membrane, the plasma membrane expands. In order to maintain the size, composition, and full functionality of synapse, an opposite process to exocytosis – endocytosis recreates the vesicles. The vesicle trafficking process is finished when an empty vesicle is retrieved from the membrane in clathrin-mediated endocytosis[27,30]. However, this is not the only mechanism by which the vesicles are recycled.

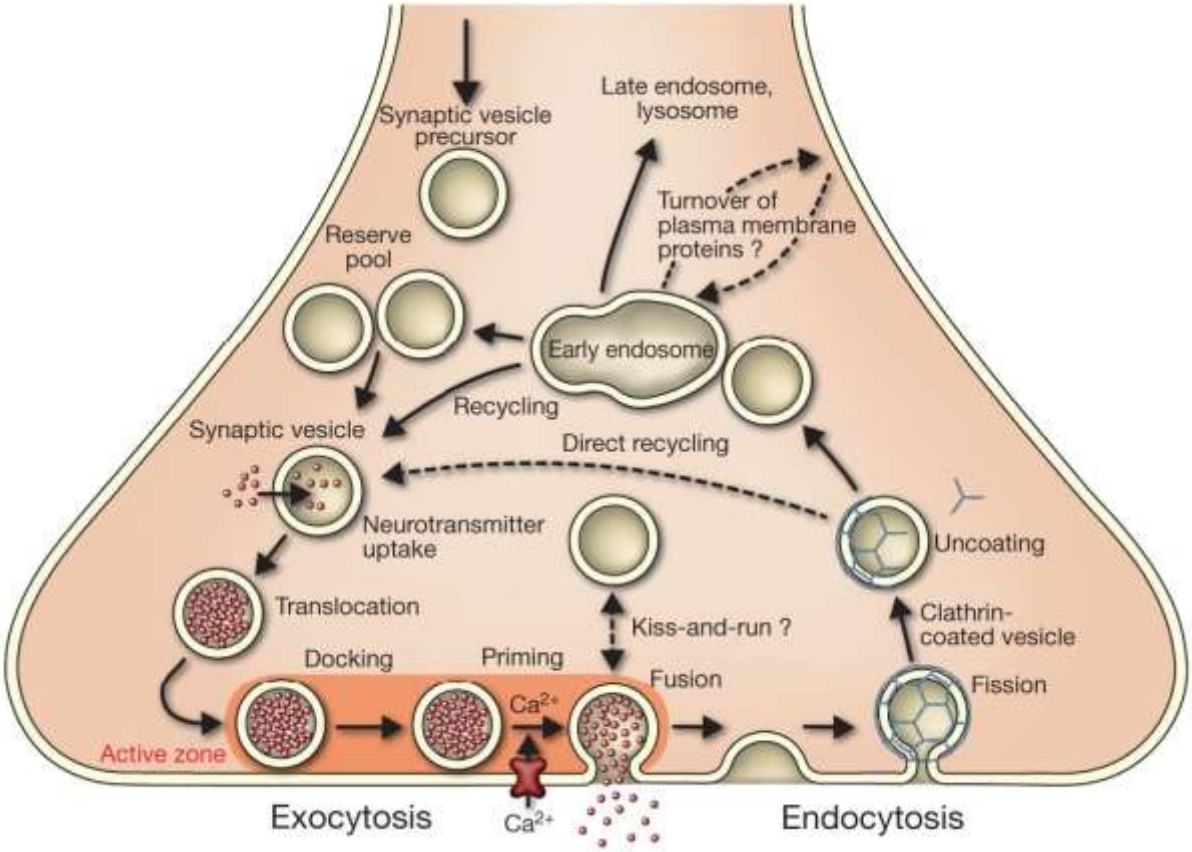


***Figure 4.*** *Synaptic vesicle cycle in the nerve terminal. Synaptic vesicles loaded with neurotransmitters are translocated into the active zone (orange area), where they dock and prime. Upon $Ca^{2+}$ influx, vesicle fuse with the plasma membrane and release its content into the synaptic cleft. Membranes and proteins at the presynaptic plasma membrane after synaptic vesicle fusion are retrieved by endocytosis. The retrieved vesicles are ready to be refilled with neurotransmitter molecules and again participate in the fusion reaction. (Figure source: Jahn&Fasshauer, 2012)*[30]

For the past couple of decades, general exocytotic and vesicle recycling mechanisms have been investigated[36]. A brief description of vesicle recycling is as follows. A loaded vesicle docks to the plasma membrane and releases its content into the synaptic cleft. The molecular details regarding the fusion process and how the empty vesicle is recycled are still not understood. Two main mechanisms proposed for vesicle recycling are full collapse[30,37] and kiss-and-run[31,38,39]. The former involves the full merging of the vesicle and plasma membrane followed by clathrin mediated endocytosis, and the latter is a ultrafast endocytosis which is an energy-efficient pathway[39]. In the full collapse mechanism, the recovery of proteins and lipids that form synaptic vesicle occurs in neuronal endocytosis as a clathrin-mediated pathway[40] requiring a clathrin coat formation around the recovered vesicle[30]. The clathrin coat consists of two layers. The outer layer is composed of clathrin, and the inner layer is formed by clathrin adaptors[41]. The full collapse recovery mechanism is a relatively slow process and is thought to be too slow to be consistent with the activity of a fast synapse[38,42]. The second vesicle recycling concept described by a kiss-and-run model is a quick and energy-efficient pathway characterized by the lack of a full merging of the vesicle with the membrane. The synaptic vesicle must dock and prime in the active zone in this type of event. Afterward, it releases its content to the presynaptic cleft through a fusion pore. The empty vesicle disengages from the membrane and is ready to be re-loaded with neurotransmitter[43].

Due to the high level of exo- and endocytosis happening in the plasma membrane, the presynaptic plasma membrane is specialized and ready for a continuous change in membrane conformation, whether it is a kiss-and-run or full collapse fusion model. Both models explain the basis of neuronal communication.

## 1.2 Membrane Fusion

Membrane fusion is a process that involves two separate lipid bilayers merging their hydrophobic cores to form a single bilayer. Several factors might influence fusion, such as charge, curvature, lipid composition, specific proteins (i.e., SNAREs) present on the membrane surface, laser radiation, or electric pulses[44]. Scientists have established that membrane fusion occurs through a sequence of consecutive events[45,46,47]. Initially, two lipid bilayers are brought together in a process called docking, where the two membranes are separated by a distance that ranges from 0 nm to 50 nm[48,49,50,51]. When they are in close contact, the water that is associated with the opposing monolayers must be removed and the surfaces dehydrated. According to the generally accepted model, membrane fusion proceeds through a stalk intermediate where one of the monolayers is destabilized. Some of the lipid acyl chains reorient to face the opposing monolayer. This local defect causes the two lipid monolayers to come in contact and merge to form a hemifusion diaphragm[52]. Finally, the fusion of the outer leaflets forms a fusion pore. Figure 5 illustrates the proposed chain of events[53,54]. All these stages are associated with an energy barrier that must be overcome for fusion to occur. Unfortunately, it is still not clear how high these energy barriers are.

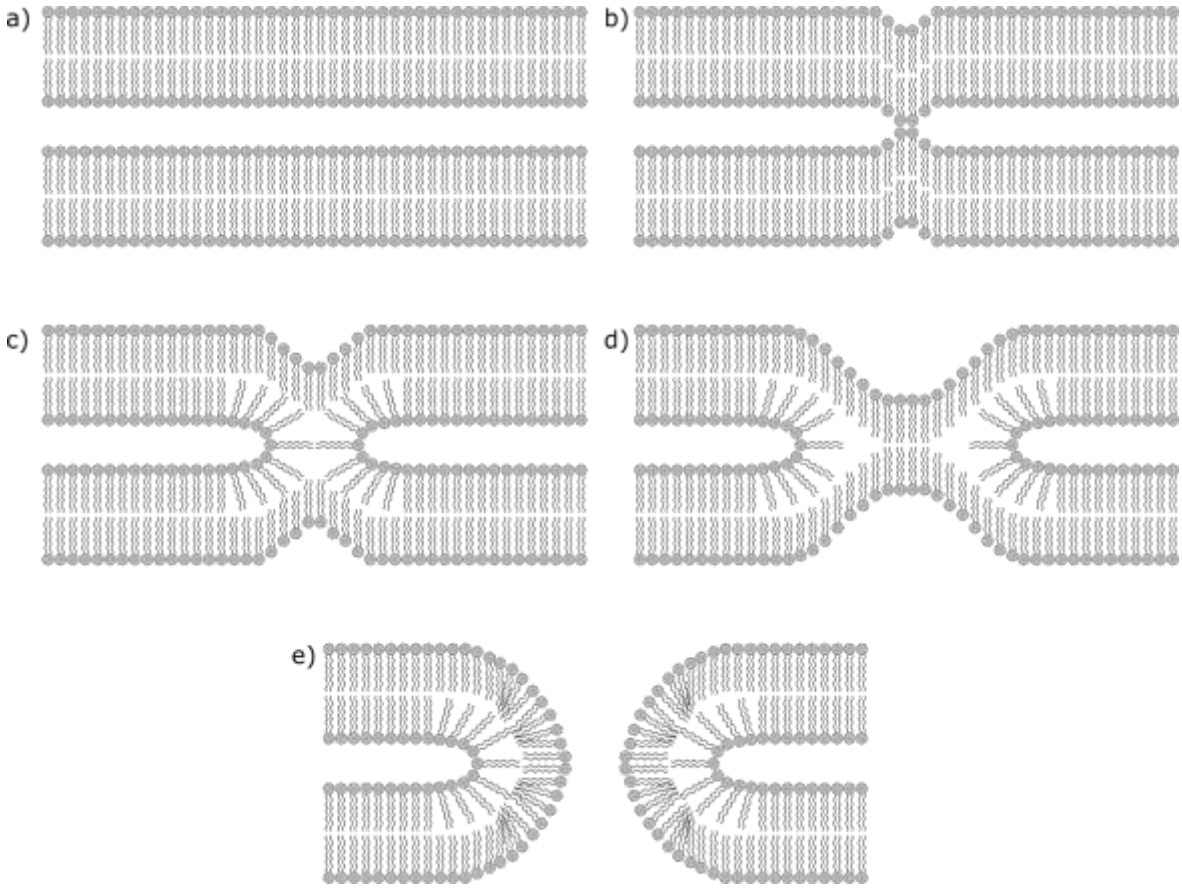


***Figure 5.*** *Stalk hypothesis for the mechanism of lipid fusion: a. two membranes come in close contact b. local disturbance of the membranes c. stalk intermediate d. hemifusion diaphragm e. fusion pore. According to the model, fusion is initiated by contact between the two opposing lipid bilayers, termed the stalk. Then, the stalk intermediate expands to form a hemifusion state, leading to the fusion pore. Figure was based on Figure 1 from (Chernomordik et al., 1985)*[55] *and Figure 1 from (Chernomordik and Kozlov, 2008)*[56].

## 1.3 The SNARE proteins

Since researchers first began to investigate neuroscience, many biomolecules responsible for the proper function of the neuronal system have been identified. As scientific techniques evolved and different approaches were taken, more and more information was collected about biomolecules in the neurology field. In this dissertation, the focus is directed at the molecules, primarily proteins, that are generally responsible for directing vesicles to the presynaptic membrane and, in the following steps, docking and triggering the fusion once the action potential arrives. Among other roles, these proteins bring two opposite membranes together, disturb the lipid bilayer, and decrease the energy barrier to allow fusion to occur. Another fact suggesting a significant role in the regulatory system is the speed at which $Ca^{2+}$-triggered membrane fusion happens, just a few hundred microseconds[57]. Two main contributions made it possible to identify the proteins involved in neurotransmission. One, published in 1974, described the genetic screens[58,59]. A second, published in the 1980s, followed and added genetic screening experiments in Saccharomyces cerevisiae[59]. The second one described the development of a cell-free *in vitro* fusion system[60]. Work based on the results of these experiments led to the discovery of the active zone SNARE proteins. SNAREs, an abbreviation for soluble NSF attachment receptor proteins, are often called a 'minimal membrane fusion machinery' primarily because they are sufficient and necessary in the synaptic vesicle cycle, especially for events in the active zone[61,31].

The SNARE protein superfamily has been identified as essential for intracellular fusion events in all Eukarya. This superfamily includes proteins involved in both exocytic and endocytic pathways. The members of the SNARE superfamily have been identified in different cellular compartments; however, the best characterized are the SNAREs involved in the neuronal exocytosis. The undisputed importance of SNAREs in neuronal fusion was disclosed when

these proteins were identified as the target of *Clostridium* toxins. Neurotoxins produced by *Clostridium botulinum* and *Clostridium tetani* can cleave the SNAREs, which leads to blockage of fusion events and impairs communication between neurons[62,63,64]. Among 36 small proteins that are a member of the SNARE superfamily in humans[65], most are transmembrane proteins containing a transmembrane domain at their C-terminus. SNAP25 (synaptosome-associated protein of 25 kDa) is one of the exceptions to this rule and does not contain a transmembrane domain. These are docked to the membrane by the attachment of acyl chains[66].

Additionally, some SNAREs have additional N-terminal α-helical domains. The unique sign of all SNARE proteins across different organisms is an evolutionarily conserved stretch of 60-70 amino acids composed of heptad repeats called the SNARE domain. The heptad repeat is the repetition of hydrophobic residues and the SNARE motif, which is the most characteristic feature of this domain[67].

There are three neuronal SNAREs. First to be discovered was Synaptobrevin (or VAMP-2 for vesicle-associated membrane protein 2), localized on the surface of the neurotransmitter-carrying vesicle. Syntaxin-1a and SNAP-25 were discovered shortly after[64] and they are both located on the presynaptic membrane. Moreover, all three proteins possess highly conserved SNARE motifs that are primarily unstructured when in the monomeric state. Through these domains, SNAREs can interact with each other to form a coiled-coil tetra-helical bundle called the SNARE complex[68]. It is currently proposed that the complex formation starts from the N-terminal end of the SNARE motifs of the three SNARE proteins, which then proceeds to their C-terminus. This process is also called SNARE zippering[69,70,71,72,73]. Upon zippering hydrophobic amino acids associate with layers of interacting residues[74]. The interacting residues at the center of the SNARE complex form 16 layers labeled from -7 to +8 (Figure 6)[75]. The exception is the 0 layer which is composed of hydrophilic amino acids. The “0-layer”, present in the center of the site of interaction between helices, contains one conserved arginine

(R) and three conserved glutamine (Q) residues which provide an alternative classification for the SNARE proteins giving R- and Q-SNAREs (Figure 6)[76].

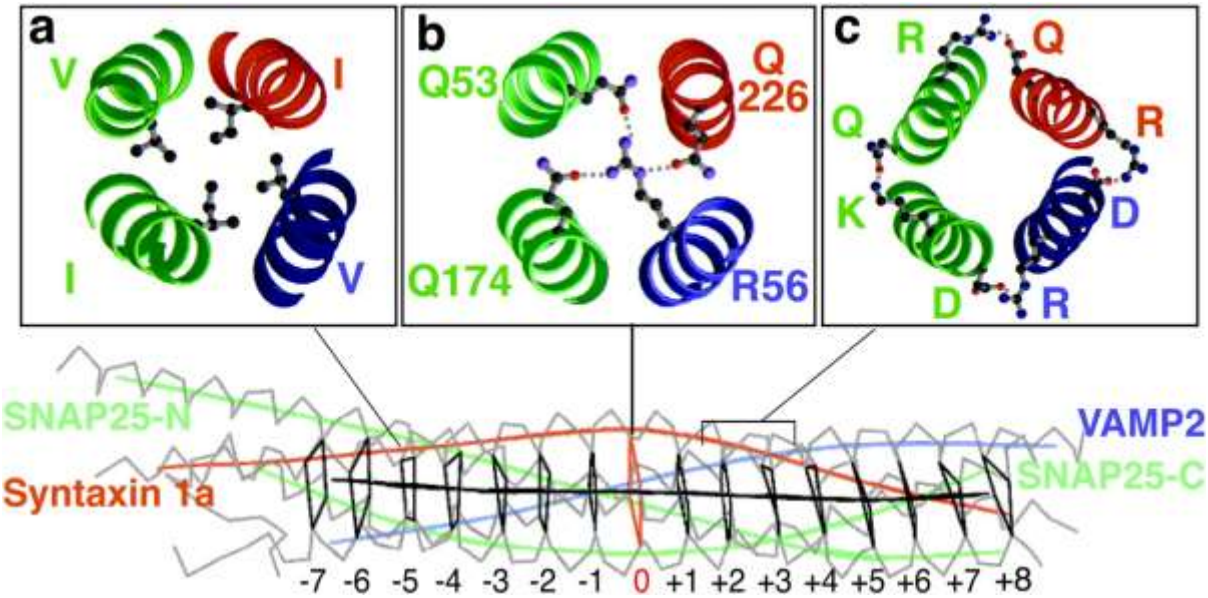


***Figure 6***. *<u>The layers of the SNARE complex</u>. At the bottom there is structutre of the four-helical bundle of the* cis-*SNARE core complex*[68]. *The central black polygons represent the highly conserved residues of three neuronal SNAREs. (a) Representation of a cross section of a typical (here the −5) hydrophobic layer, ball and stick structures representing the amino acids. (b) The central red layer, called the 0-layer is composed of charged residues. (c) Charged residues form hydrogen bonds outside the layer. (Figure source Scales et al. 2001)*[75]

Originally it was believed that SNARE-mediated fusion is NSF-dependent, and disassembly of the SNARE complex would trigger fusion[77]. Nevertheless, later studies proved that the process of NSF disassembly is independent of fusion initiation and that the SNARE complex formation promotes fusion[78]. The SNARE zippering is proposed to provide the force to overcome the energy barrier and bring to oppose membrane close enough to enable fusion[69]. The alternative way in which the SNARE complex could facilitate membrane fusion is by destabilizing the membrane surface with Syntaxin-1a and Synaptobrevin transmembrane domains. SNARE proteins are essential but not sufficient to mediate the synaptic vesicle cycle. Other proteins in the active zone play crucial roles in mediating the synaptic vesicle fusion[65].

### 1.3.1 Syntaxin-1a

Syntaxin-1a is a transmembrane protein categorized as Qa SNARE protein (thanks to the glutamine residue in its zero layers) or t-SNARE protein (target SNARE). It is a 33 kDa protein localized in the presynaptic membrane through a single-span C-terminal transmembrane region (266 – 288)[79]. The SNARE domain of Syntaxin-1a (192 – 254 residues), called the H3 domain[80], is partially unstructured and gains further alpha-helical character upon assembly in a heterodimer with only SNAP-25 or into a full SNARE complex[68]. The H3 and C-terminal transmembrane domains are connected by a short linker (255 – 265 residues)[81,82] (see Figure 7 for reference).

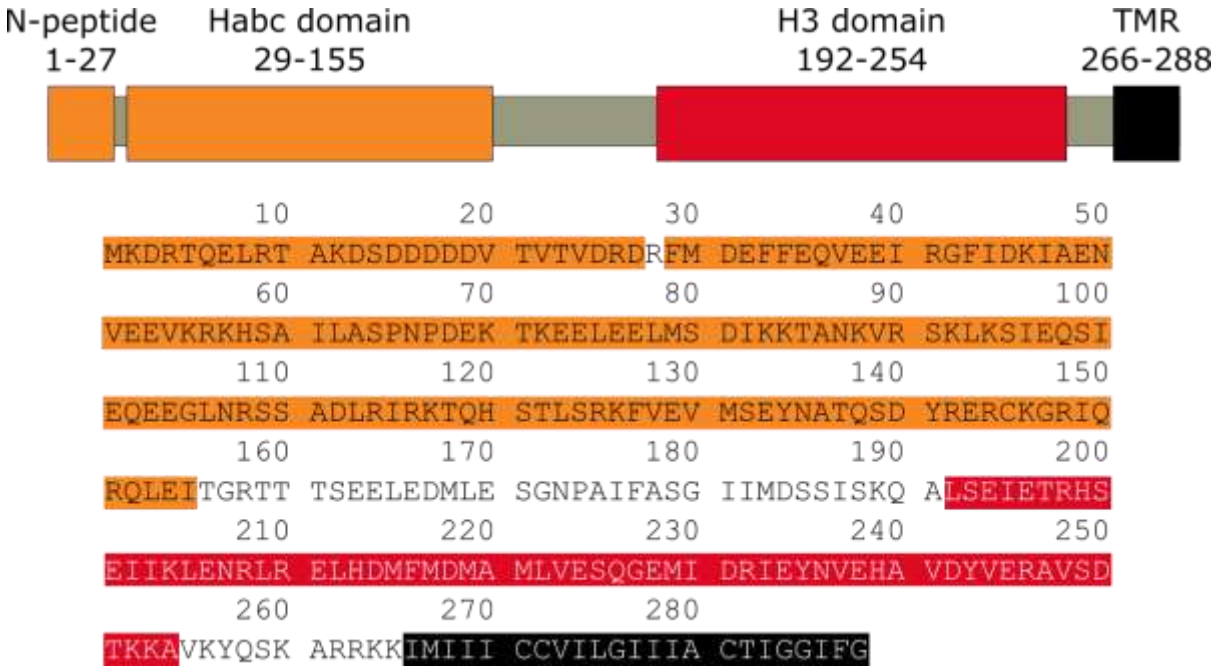


***Figure 7****. Amino acid sequence and domains of Rattus norvegicus Syntaxin-1a.*

From previous work on Syntaxin-1a in solution, the H3 segment tends to homo-oligomerize and form dimers or tetramers when it exceeds concentrations of 2 μM[83,84,85]. Two helices of Syntaxin-1a are in a parallel alignment in the dimer form; however, there are conflicting results reported for the tetramer conformation. From studies using EPR, all Syntaxin-1a molecules are parallel in the tetrameric complexes[85]. In contrast, two Syntaxin-1a dimers forming a tetramer were observed in antiparallel orientation in the crystal structure, where a Phe217 was observed to generate steric hindrance to parallel orientation[83]. Syntaxin-1a molecules form much bigger oligomers that do not appear to be randomly distributed in the plasma membrane[86]. Instead, Syntaxin-1a is organized in 50 to 60 nm average diameter clusters, where the average density is 19.6 clusters/$\mu m^2$. Each cluster contains about 90 molecules, which suggests a dense packing of monomers[87]. Imaging using dSTORM showed that the clusters are not evenly packed. The cluster is more tightly packed at the center, and the density gradually decreases from the center to the periphery. There is a dynamic equilibrium between proteins in clusters and free proteins in the surrounding membrane[88]. The Syntaxin-1a clustering is driven by at least two separate mechanisms. The first involves ionic interactions between the polybasic linker region and lipids in the plasma membrane, especially phosphatidyl inositol phosphates (PIPs)[89,90]. PIP2 sequesters the protein into larger, more loose clusters. In addition to PIP2[91,92], cholesterol is reported as a stabilizing agent for Syntaxin-1a clusters[93,94,95]. This mechanism is called "lipid-mediated pre-clustering." The second clustering mechanism, called "cluster tightening by protein-protein interactions," involves the SNARE domain of Syntaxin-1a[90,96]. In addition to the SNARE domain, Syntaxin -1a has a C-terminal transmembrane region, an α-helical Habc domain(28-105) and so-called N-peptide (1 – 27 residues)[97]. The Habc domain is composed of three antiparallel α-helices, Ha (29-66), Hb (70-105), and Hc (110-155)[68,84,98]. The Habc and the H3 domains of Syntaxin-1a interact with each other resulting in a closed conformation[63,99,100,101,102].

Current literature extensively documents the interaction between Habc and H3 domains and its impact on the ability of Syntaxin-1a to interact with SNAP-25 and Synaptobrevin. In the closed conformation, Syntaxin-1a cannot interact with other SNARE proteins and thus cannot participate in SNARE complex formation[100,103]. The open and closed conformations are in dynamic equilibrium, and there are conflicting reports about which conformation dominates[99,104,105]. In order to interact with other SNARE proteins, only the H3 domain is necessary[80]. Two mutations, called LE mutation, L165A and E166A were found to disrupt the interdomain H3-Habc interaction, which as a result, shifts equilibrium towards an open state of Syntaxin-1a[103,106]. Moreover, with the LE mutation, Syntaxin-1a is more effective at SNARE complex formation[103,107,108].

The H3 and Habc domains are connected through a long, unstructured linker (156 – 191) that appears to affect the open-close equilibrium[109]. And the LE mutation mentioned above lies in the linker region[103]. The Habc domain and the N-peptide are necessary to bind Syntaxin-1a to the SM protein (Sec1/Munc18 family) Munc18 protein when Syntaxin-1a is alone or when it is assembled with other SNARE proteins. Munc18 binds to Syntaxin-1a through its N-peptide, Habc, and H3 domains with high affinity[110,111]. Upon binding, Munc18 stabilizes the closed conformation[112]. This interaction inhibits the formation of the SNARE complex but also prevents Syntaxin-1a from unspecific interactions with other proteins. The Syntaxin-1a conformation observed in the crystal structure of the Syntaxin-1a-Mucn18 complex is believed to represent the closed state (Figure 8)[102]. Munc18 is able to bind to the acceptor and assembled SNARE complexes, but the binding affinity to these complexes is much weaker than to Syntaxin-1a alone[107,113]. The shorter, unstructured N-peptide is not required for Munc18 to bind Syntaxin-1a, although it does contribute to the affinity between these proteins[107]. However, this N-peptide segment is crucial for Munc18 to interact with the SNARE complex, suggesting at least two possible modes of Munc18 binding to Syntaxin-1a[107,114].

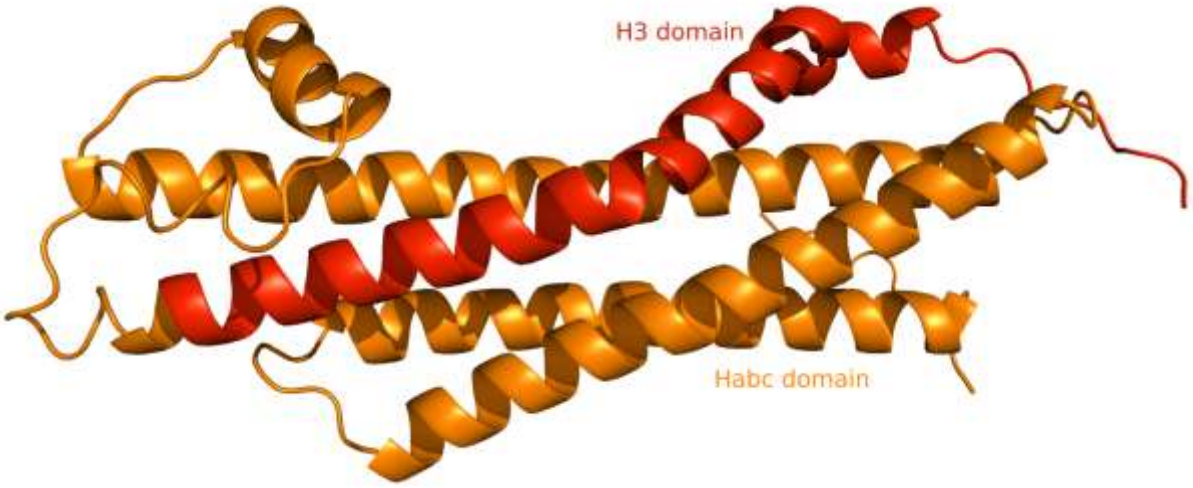


***Figure 8.*** *Representation of the closed state of Syntaxin-1a. When the H3 (red) and Habc (orange) domains come into proximity, Syntaxin-1a adapts to a closed state. Fragment of the crystal structure of Syntaxin-1a-Munc18 complex (PDB ID: 3C98*

Lastly, Syntaxin-1a is one of two isoforms of Syntaxin-1 expressed in neurons. The second one is Syntaxinaxin-1b. They share a 84% sequence identity and are considered functionally equivalent[115]. Deleting one of these isoforms has little to no effect because the other isoform will compensate for the lack of the first one. However, the deletion of both isoforms is prenatally lethal[116]. Moreover, experiments performed on the double knock-out mice for both Syntaxin-1a and Syntaxin-1b underline the importance of Syntaxin-1 in neuronal maintenance through a neuronal lifetime[116,50].

### 1.3.2 SNAP-25

SNAP-25 (Synaptosomal-associated protein 25) is the first member of the large SNAP-25 subfamily and is categorized as Q-SNARE. It is a 24 kDa protein with two unique features that distinguish it from the other two SNARE proteins. The first feature is the lack of a transmembrane domain, and the second is the presence of not one but two SNARE motifs, which is a feature found only within the SNAP-25 subfamily[117]. Two SNARE domains are denoted SN1 (7- 83) and SN2 (141-204), and they belong to Qb, and Qc SNAREs, respectively; they are connected through a long, flexible linker[118]. The linker is palmitoylated and anchors the protein to the membrane[119].

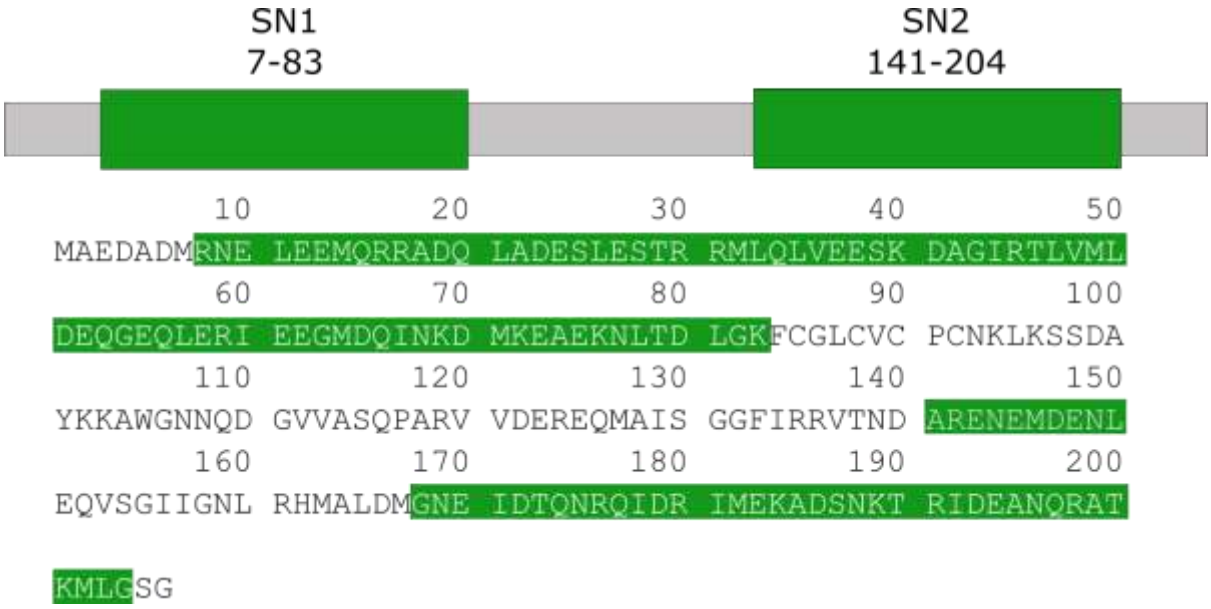


***Figure 9.*** *Amino acid sequence and domains of Rattus norvegicus SNAP-25.*

Like Syntaxin-1a, SNAP-25 is organized into clusters on the presynaptic plasma membrane[86,93,120]. These clusters are positioned in close proximity to Syntaxin-1a clusters. SNAPE-25 clusters are elliptical in shape and cover an area 28 percent bigger than the area covered by Syntaxin-1a clusters[88]. The cluster's center is more tightly packed, and the density gradually decreases from the center to its periphery, in much the same manner as observed for Syntaxin-1a clusters[88]. The individual molecules of SNAP-25 and Syntaxin-1a that surround the protein clusters can interact with each other. Work reported by Rickman et al. suggests that protein clusters serve as a reservoir pool for both Syntaxin-1a and SNAP-25, from which isolated and reactive proteins can form a Syntaxin-1a – SNAP-25 complex[120].

SNAP-25 is mostly unstructured[68]. Both SN1 and SN2 become α-helical when interacting with Syntaxin-1a or when assembled in the SNARE complex while the linker stays disordered and flexible[68,121]. The helicity of the SNARE domains of SNAP-25 is dependent upon ionic strength, and helicity increases with an increasing amount of NaCl, $MgCl_2$, and $CaCl_2$[121]. It was observed by Fasshauer *et al*. that a high concentration of NaCl is the cause of SNAP-25 oligomerization[121]. It is still not known if the increased helicity with ionic strength of isolated SNAP-25 is physiologically relevant or if it impacts interactions with other proteins. SNAP-25 can also adopt a conformation where both its SNARE motifs come in contact, and other regulatory proteins can stabilize this state[122].

Lastly, there are two isoforms of SNAP-25, SNAP-25a and SNAP-25b, with only nine amino acid differences between them. SNAP-25a has two additional charged amino acids compared to SNAP-25b[123]. Both isoforms are able to drive vesicle fusion. Despite the minimal differences between these isoforms, both are critical for neurons to function properly. Experiments performed on mice expressing only the SNAP-25a isoform show that the lack of the SNAP-25b isoform causes defect in spatial learning, higher anxiety, and pathological changes in the stratum lucidum of the hippocampus[124]. The importance of SNAP-25 in neurotransmitter

release is well documented. Vesicle fusion is blocked when SNAP-25 is cleaved by botulinum toxins[63,64]. In addition, neuron arborization and neuron survival are decreased by SNAP-25 deletion[125]. Last but not least, SNAP-25 knockout neurons have been reported to have impaired vesicle docking[50].

### 1.3.3 Synaptobrevin-2

Synaptobrevin-2, also called VAMP-2 (from vesicle-associated membrane protein 2), is classified as R-SNARE or v-SNARE (vesicle SNARE). Synaptobrevin-2 is a 13 kDa transmembrane protein anchored in the synaptic vesicle membrane through a single pass C-terminal transmembrane helical region (97 – 116). About 70 molecules of Synaptobrevin-2 can be found on the synaptic vesicle[29]. The SNARE motif of Synaptobrevin-2 (30 – 85) is connected to the transmembrane domain by a short linker (86 – 96) (Figure 10). This linker contains basic residues that are reported to bind negatively charged lipids[126]. This protein-lipid interaction slightly tilts Synaptobrevin-2, and places the SNARE domain closer to the vesicle membrane. The SNARE domain of the intact protein is unstructured on the lipid bilayer[127,128]. However, studies performed on the full-length protein resuspended in detergent buffer show a tendency for helical structure[129,130]. Similar to other SNAREs, the SNARE motif of Synaptobrevin-2 turns into a full α−helix during the SNARE complex formation. There are also reports that the SNARE domain of Synaptobrevin-2 dynamically binds to lipids with relatively low affinity[127,130,131,132]. This protein-lipid interaction promotes an increase in α-helicity, which is hypothesized to modulate the ability of Synaptobrevin-2 to assemble into the SNARE complex. Helical structure in the N-terminal fragment may be essential to initiate SNARE zippering[133]. On the other hand, the interaction between the C-terminal segment of the

SNARE domain with lipids and the formation of α-helical structure can lower the energy barrier for fusion to occur by increasing the rate of the SNARE complex assembly[130,132].

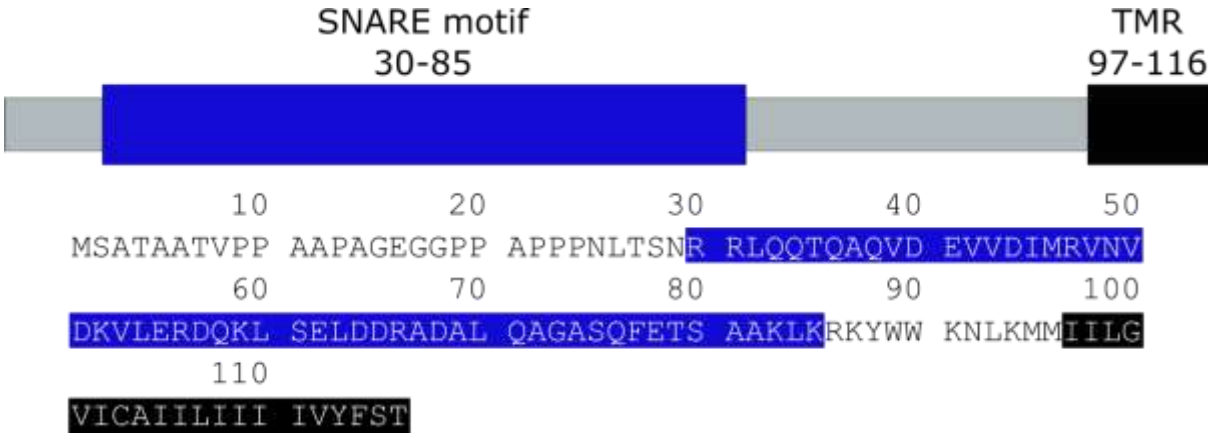


***Figure 10**. Amino acid sequence and domains of Rattus norvegicus Synaptobrevin-2.*

Lastly, the cleavage of Synaptobrevin-2 by botulinum or tetanus neurotoxins stops neurotransmitter exocytosis, causing flaccid or spastic paralysis[63,134]. The importance of the Synaptobrevin-2 vesicle trafficking cycle was described by Imig *et al*[50]. They performed electron tomography experiments on Synaptobrevin-2 knockout neurons and found that synaptic vesicle docking was drastically lower. Moreover, the a lack of Synaptobrevin-2 causes a 25% increase in the synaptic vesicle volume[50].

### 1.3.4 SNARE complex

The SNARE complex is a three-molecule (Syntaxin-1a, SNAP25, Synaptobrevin-2), highly stable four-helical bundle[135,136,137]. It is also termed the core complex or the 'SNAREpin' that forms a bridge between the synaptic vesicle and the plasma membrane[61,68,70]. The core complex is composed of SNARE helical domains, each of approximately 60 amino acids, Syntaxin-1a and Synaptobevin-2 each contribute one helix, with SNAP-25 contributing two helices[68]. The SNARE complex formation starts from the N-terminal end of the SNARE motifs and proceeds towards the C-terminus. It is composed of helical SNARE motifs. This complex has been crystallized, resulting in a high-resolution structure (Figure 11)[68,73]. An analysis of the structure reveals that the helices twist around each other and create a leucine-zipper-like assembly with an embedded ionic layer consisting of repeating modules of an arginine residue and three glutamine residues[68]. The ionic layer is called the zero layer.

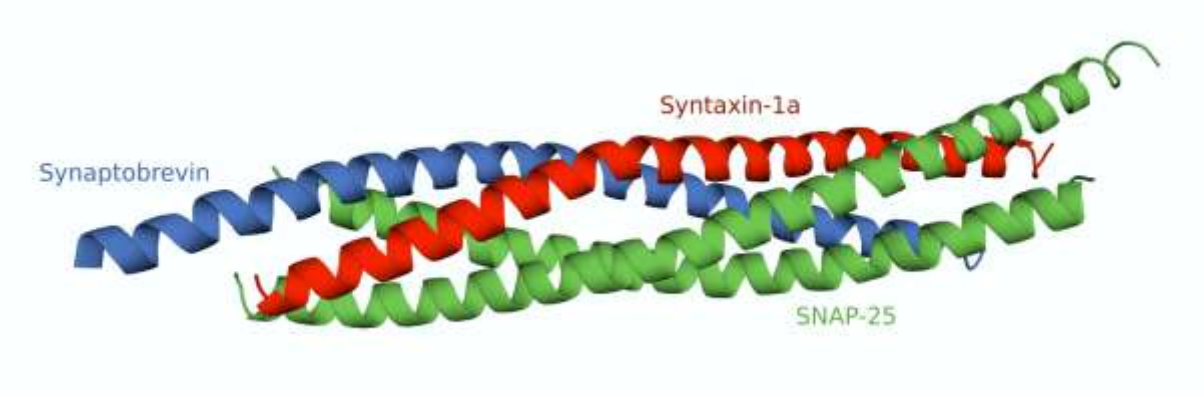


***Figure 11***. *The crystal structure of the SNARE complex. The SNARE domains of Syntaxin-1a (red), SNAP-25 (green) and Synaptobrevin-2 (blue) form a four-helix bundle called the SNARE complex (PDB ID: 1SFC)*[68].

Once assembled, the SNARE complex is very stable. Disassembly of the SNARE complex requires energy and it is mediated by SNAPs (soluble NSF attachment proteins) and ATP-hydrolyzing NSF (N-ethylmaleimide-sensitive factor), leading to the recycling of the SNAREs for another round of membrane fusion[138]. The process of SNAREs assembly and disassembly is presented in Figure 12[65].

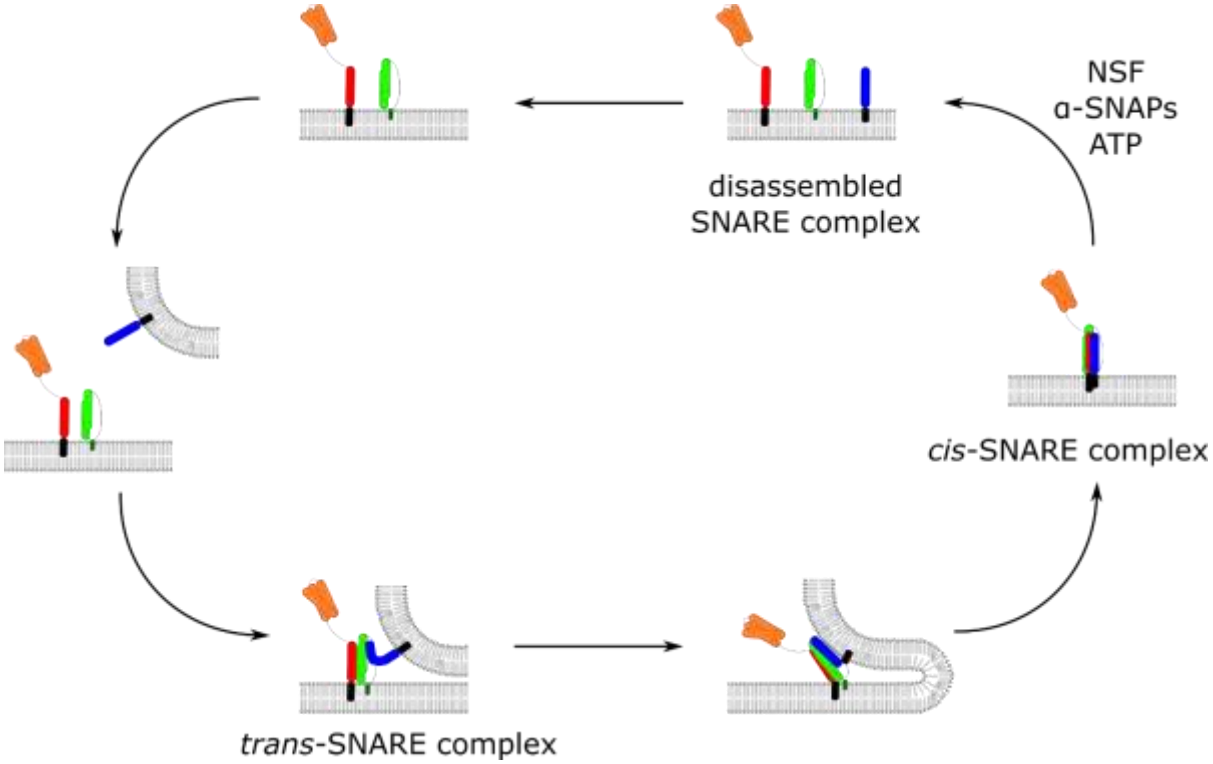


***Figure 12***. *The SNARE assembly and disassembly cycle. Synaptobrevin-2 (blue) located at the synaptic vesicle interacts with the plasma membrane target SNARE proteins (Syntaxin-1 and SNAP25). Interaction starts when proteins are in a different membrane, and it can be referred as trans position. As proteins zippering proceeds two opposing membranes are brought close together. Once membrane fusion is complete, the fully formed SNARE complex is located in the plasma membrane and it is called cis-SNARE complex. The cis-SNARE complex is disassembled by AAA+ ATPase NSF with the help of adaptor proteins, SNAPs, and with hydrolysis of ATP. In a final step all proteins are separated and redistributed to their corresponding membranes and ready participate in a new fusion cycle. Figure is based on Figure 3 from (Jahn and Scheller, 2006)*[65].

The results from experiments performed on isolated and assembled SNARE complexes in aqueous solution suggest that the SNARE complex is not present as a single monomer. The size of the SNARE complex has been measured by multiangle laser light scattering (MALLS), gel filtration, analytical ultracentrifugation, and mobility of SDS-resistant complexes on gels. In each case, the size of the measured sample appears to be bigger than anticipated for a monomeric SNARE complex[80,85,139,140,141]. Based on these results, the SNARE complex is thought to be present as a dimer or trimer[141]. The interactions and structural features that drive core complex oligomerization are not fully understood, but a number of models have been proposed. One model involves interactions between the transmembrane domains[142]. The specific amino acid residues in the trans membrane domain of Synaptobrevin (Leu99, Ile102, Cys103, Leu107, Ile110, and Ile111) and Syntaxin-1a (Ile270, Cys271, Leu275, Ile278, and Ile-279) found to be responsible for heterodimerization[142]. However, whether these interactions are a driving force for SNARE complex oligomerization is unclear. Moreover, some EPR studies performed on the synaptic four-helix bundle show that the spin-label is immobile at sites that should be exposed to soluiton[85]. These data imply that contact between surface residues on the neighboring bundles might exist. It is suggested that interactions between SNARE complex molecules may be critical for catalyzing fusion. It even seems possible that a single SNARE complex might actually prevent the fusion when the helical bundle blocks the contact between two opposing membranes. Formation of an organized pattern of SNARE complexes surrounding a patch of SNARE-free membrane can avoid the steric problem. In this patch, lipid mixing could occur. SNARE complex oligomerization in neuronal exocytosis might be regulated by a several factors including $Ca^{2+}$, Synaptotagmin, and Complexin/Synaphin[140,143,144,145,146]. Littleton et al. suggested that purified Synaptotagmin is able to dimerize the purified SNARE complex in a $Ca^{2+}$-dependent manner[144]. Tokumaru *et al.* discovered that the protein Complexin binds to the assembled the core complex[146]. Upon

binding, Complexin mediates SNARE complex oligomerization which was confirmed by the formation of a higher-order SDS-resistant structure.

Lastly, experimental evidence shows that assembled SNARE proteins are protected from clostridial neurotoxin cleavage, which is not the case for the SNAREs in their monomeric form. In synapses, a partially zippered SNARE complex protects only the membrane-distal portion of the Synaptobrevin SNARE motif. Later, upon competition of zippering, the whole domain is protected[147]. Additionally, experiments performed in chromaffin cells yield similar results where the SNAREs are protected from cleavage when assembled into the core complex. In this system, free, loosely assembled, and fully assembled SNARE complexes display different reactions and sensitivity to an anti-SNAP-25 monoclonal antibody[148].

### 1.3.5 Binary Syntaxin-1a-SNAP25 interaction

SNAP-25 binds to Syntaxin-1a. They coexist on the presynaptic membrane, and it is generally believed that interactions between these two proteins are an essential step that precedes SNARE complex formation and membrane fusion itself. It turns out that out of three possible binary SNARE interactions (Syntaxin-1a – SNAP-25, Syntaxin-1a – Synaptobrevin2, Synaptobrevin2 – SNAP-25), the interaction between Syntaxin-1a and SNAP-25 results in the most stable complex[71]. This interaction has been extensively studied over the past decades and it appears to be quite complex. At least two possible products are formed by the interaction between these two proteins[61,149,150]. The first one is a 1:1 SNAP-25 – Syntaxin-1a complex often referred to as the t-SNARE complex or acceptor complex[122]. The second is the 2:1 complex, in which two syntaxin molecules are bound to one SNAP25 molecule[151]. It is generally believed that the 1:1 acceptor complex represents the state of the SNARE proteins before the arrival of the $Ca^{2+}$

trigger, and it serves as a starting point for the SNARE complex formation upon Synaptobrevin2's arrival. However, results obtained from work performed *in vitro* indicate that the 2:1 complex is the dominant form. Both SNARE domains of SNAP-25 and SNARE domains from the two Syntaxin-1a molecules are in parallel orientation, resembling the full SNARE complex. This 2:1 complex is often referred to as a "dead-end complex" because it is does not appear to provide a pathway to SNARE complex formation[71]. Results from lipid fusion assays show that the presence of a 2:1 complex drastically decreases fusion efficiency. There are two possible pathways for the non-productive 2:1 complex during fusion in an *in-vivo* system. In the first, the unproductive complex is disassembled by NSF and α-SNAP to free up the SNARE proteins[152,153]. In the second, the assembly of the 2:1 complex is prevented by the accessory proteins in the active zone[71,154,155].

## 1.4 Other proteins

### 1.4.1 Munc18

The precise control of the SNARE proteins and their assembly is essential for fusion, and a family of SM (Sec1/Munc18- like) proteins – Munc18 and their orthologues - serve to regulate the SNAREs[156,157]. The SM proteins contain a highly conserved polypeptide chain with a molecular weight of 60-70 kDa and a length of ~600 amino acids[158], and they are essential for membrane fusion. The absence of the SM proteins can inhibit membrane fusion in different systems, such as the endocrine and the vascular system. Munc18 is a key regulatory protein of neurotransmission, and its physiological functions are well researched. The abnormal expression of Munc18 is involved in various neurological diseases; for example, it is associated with epileptic encephalopathy, autism, schizophrenia, Parkinson’s disease, Alzheimer’s disease, multiple sclerosis, Duchenne’s muscular dystrophy, and neuronal ceroid

lipofuscinosis[159]. Moreover, an *in vivo* study of neurons with a Munc18 knock-out revealed that fusion was inhibited at an early state of vesicle priming.

Munc18 is an arch-shaped, evolutionarily conserved, cytosolic protein that was initially discovered based on its affinity for Syntaxin-1a[102]. Munc18's tertiary structure is complex, consisting of four closely connected domains named 1, 2, 3a, and 3b (domains 1, 2, 3a, and 3b form the arch), domains 1 and 3a form an arched gap, domains 3a contacts with the Habc of Syntaxin-1a, domain 1 is located on the other side of the arched gap and binds to the n-terminal peptide of Syntaxin-1a[160]. The crystal structure of the Syntaxin-1a – Munc18 complex[102] (Figure 13) indicates one primary role of Munc18: to stabilize the Syntaxin-1a closed conformation and protecting it from non-specific interactions. Since Syntaxin-1a is a core protein of the SNARE complex, Munc18 may regulate fusion by its interaction with Syntaxin-1a through its N-terminal peptide, Habc domain, and H3 domain[161,162,163,164].

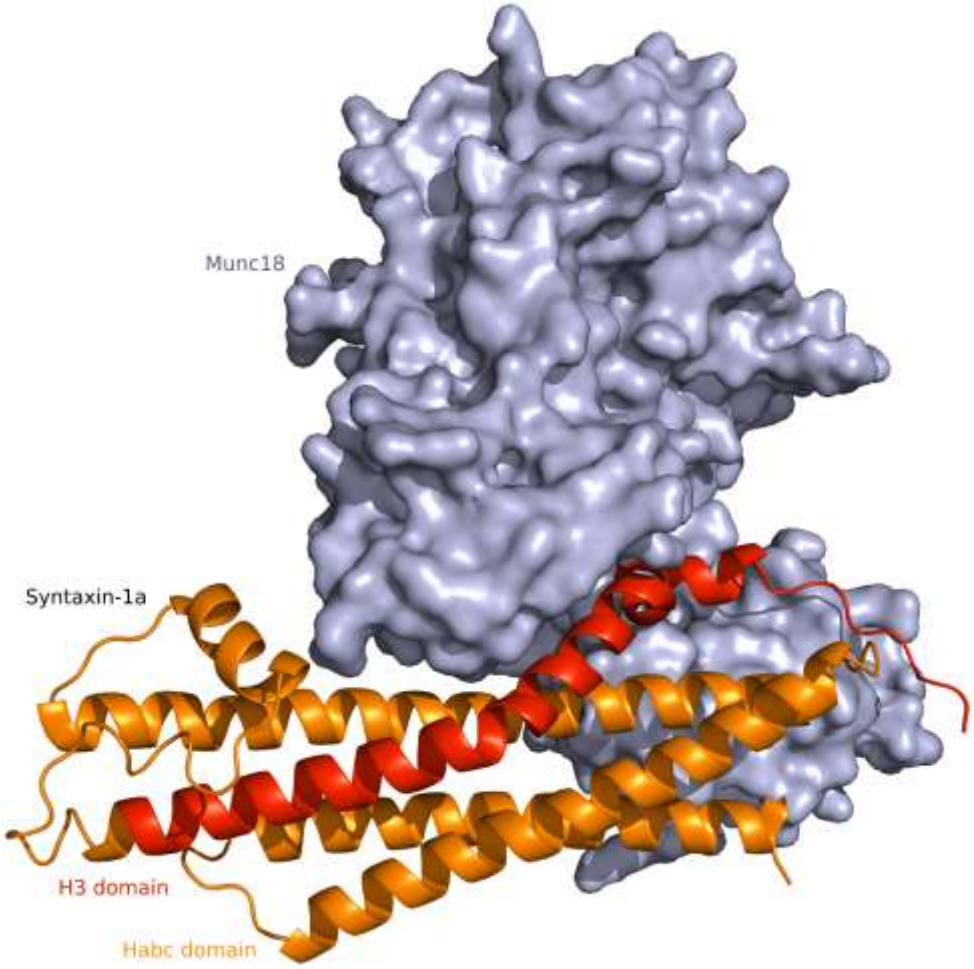


***Figure 13.*** *<u>The crystal structure of Syntaxin-1a – Munc18 complex</u>. Munc18 (grey) binds simultaneously to the H3 (red) and Habc (orange) domains of Syntaxin-1a, stabilizing closed conformation of Syntaxin-1a (PDB ID: 3C98)*[102].

Due to its importance in neurotransmission, the interaction between Munc18 and Syntaxin-1a has been well-investigated. Thus far, it has been shown that both the N-terminal peptide and Habc domain of Syntaxin-1a play a vital role in synaptic membrane fusion. The N-terminal peptide is essential for vesicle fusion, and the Habc domain regulates fusion by actively participating in the formation of the closed conformation of Syntaxin-1a. The closed conformation makes the Syntaxin-1a H3 domain less accessible for SNARE complex formation and prevents non-specific interactions. The current thinking about Munc18 – Syntaxin-1a interactions is that these two proteins have several binding modes[165]. The first and best defined mode, is one in which Munc18 binds to Syntaxin-1a via its N-peptide, Habc, and H3 domains arresting Syntaxin-1a in a closed conformation and inhibiting the formation of the SNARE complex[112,160]. The second binding mode is based upon the hypothesis that Munc18 - when bound to closed Syntaxin-1a - forms a template complex for SNAREs assembly. In this binding mode Munc13, another regulatory protein, plays an important role by helping to open Syntaxin-1a for SNARE assembly. Munc13 also bridges the synaptic vesicle and presynaptic membranes, and together with Munc18 it primes the assembly of the t-SNARE complex[166]. Finally, there is a binding mode in which Munc18 interacts only with the N-terminal peptide of Syntaxin-1a. This binding mode involves a smaller protein-protein interface and includes only the outer surface of domain 1 or Munc18-1 and an the Syntaxin-1a N-terminal peptide. In this binding mode, the H3 domain of Syntaxin-1a is not blocked, making it available for core SNARE complex assembly. This interaction may have two functions[160]. First, upon binding to the N-terminal peptide of Syntaxin-1a, Munc18 closes Syntaxin-1a, regulates its accessibility, and finally assists Syntaxin-1a in forming the SNARE complex when it disassociates from the N-terminal peptide. Another function of this N-terminal binding mode may not be to bind free Syntaxin-1a but to bind Syntaxin-1a when it is fully assembled in the SNARE complex[167].

All binding modes appear to be vital in the process, and it is highly likely that Munc18 acts by keeping Syntaxin-1a in an inactive state, where it is unable to assemble into a SNARE complex until an appearance of the activation signal. Studies of the interaction between Munc18 and the SNARE complex have presented some evidence regarding this interaction. For example, work performed by Zillyet *et al*. has shown that Munc18 binding to closed Syntaxin-1a does not prevent the formation of the core complex on the plasma membrane[168]. However, at the same time, Burkhard *et al*., based on the results from an assay that measures the formation of sodium dodecyl sulfate-resistant SNARE complexes, stated that Munc18 inhibits SNARE complex formation[107]. It seems, that the N-terminal peptide of Syntaxin-1a is essential for Munc18 to bind the SNARE complex, as deletion of the N-terminus of Syntaxin-1a tends to eliminate of this interaction[167]. At the same time, the results obtained from FRET experiments show that the Syntaxin-1a N-terminal region competes with the SNARE four-helix bundle for Munc18 binding, suggesting yet another possible binding mode of Munc18[114].

Most of the findings strongly support the idea that the binary Syntaxin-1a – Munc18 interaction and its closed Syntaxin-1a product is essential for efficient Syntaxin-1a trafficking, dense-core vesicle docking, and neuronal exocytosis. At the same time, the results suggest that the effect of Munc18 on fusion may extend past binary Syntaxin-1a – Munc18 interactions. Therefore, it is crucial to investigate further and define the binding mode between Munc18 and assembled SNARE complex and its functional significance better to understand the role of Munc18 in neuronal exocytosis.

### 1.4.2 Synaptotagmin-1

Synaptotagmins are a family of proteins with an N-terminal transmembrane domain and two C2 domains. Neuronal Synaptotagmin-1 is the $Ca^{2+}$ sensor for synchronous neurotransmitter release. It is anchored to the synaptic vesicle through a single N-terminal transmembrane domain, and it has two cytosolic C2 domains: C2A and C2B, connected by a flexible linker[169,170,171]. $Ca^{2+}$-binding loops present within C2A and C2B allow for the coordination of up to five $Ca^{2+}$ ions[170]. Synaptotagmin-1 function as a $Ca^{2+}$ sensor has been extensively studied in both, *in vitro* and *in vivo*. Even a single mutation disturbing $Ca^{2+}$-binding without any conformational changes in Synaptotagmin-1 decreases the $Ca^{2+}$ sensitivity of neurotransmitter release. Also, knockout experiments confirmed Synaptotagmin-1's role as the key regulator for synchronous synaptic vesicle exocytosis[170,172].

Synaptotagmin-1a interacts with membranes in various ways. The C2B domain has a polybasic region that is reported to be involved in a $Ca^{2+}$-independent interaction with negatively charged lipids in the membrane[173]. The electrostatic interactions between Synaptotagmin-1 and membrane are more pronounced in the presence of the polyvalent lipid phosphatidylinositol-(4,5)-bisphosphate (PI(4,5)P2)[174]. Moreover, recent EPR work shows that a region with conserved arginine residues (often referred to as the arginine apex) opposite the $Ca^{2+}$-binding loops in the C2B domain make contact with the membrane. These multiple sites of interaction suggest that the C2B domain binds to bilayer surfaces that are curved[175].

In addition to $Ca^{2+}$-sensing and membrane binding, Synaptotagmin-1 interacts with the SNARE proteins directly[176,177,178]. These interactions include Syntaxin-1a, SNAP-25, Syntaxin-1a – SNAP-25 heterodimers, and the fully assembled SNARE complex[143,179]. The binding of Synaptotagmin-1a with SNARE proteins involves the polybasic face and the arginine apex in the C2B domain. It occurs in a $Ca^{2+}$-free environment, although the presence

of $Ca^{2+}$ enhances the affinity. The interaction between Synaptotagmin-1a and SNARE complex is structurally heterogeneous[180] and can be disrupted by polyvalent ions such as ATP and Mg2+ at physiologically relevant concentrations[181].

Although the interactions of Synaptotagmin-1 with membranes and SNAREs have been well described, the actual mechanism of action of this protein as the $Ca^{2+}$ sensor in neuronal exocytosis is not yet been resolved. Models involving either SNARE interactions, membrane interactions, or both, have been proposed; however, there is no general agreement on the mechanism by which Synaptotagmin 1 regulates fusion.

### 1.4.3 Complexin

Complexin (also called Synaphin) was discovered because of its ability to bind to the assembled SNARE complex[182]. Binding between Complexin and SNARE complex happens through the conserved central helix region of Complexin[183]. Moreover, a crystal structure obtained of the Complexin - SNARE complex shows that Complexin binds as an α-helix, antiparallel to the SNARE helices in the groove between Synaptobrevin and Syntaxin-1a. The structure indicates that there are ionic interactions, hydrophobic interactions, and hydrogen bonding between Complexin 48-70, Synaptobrevin-2 47-68, and Syntaxin-1a 214-232 (Figure 14)[183]. An independent X-ray and TROSY-based NMR study confirmed the interaction between Complexin and SNARE complex[183].

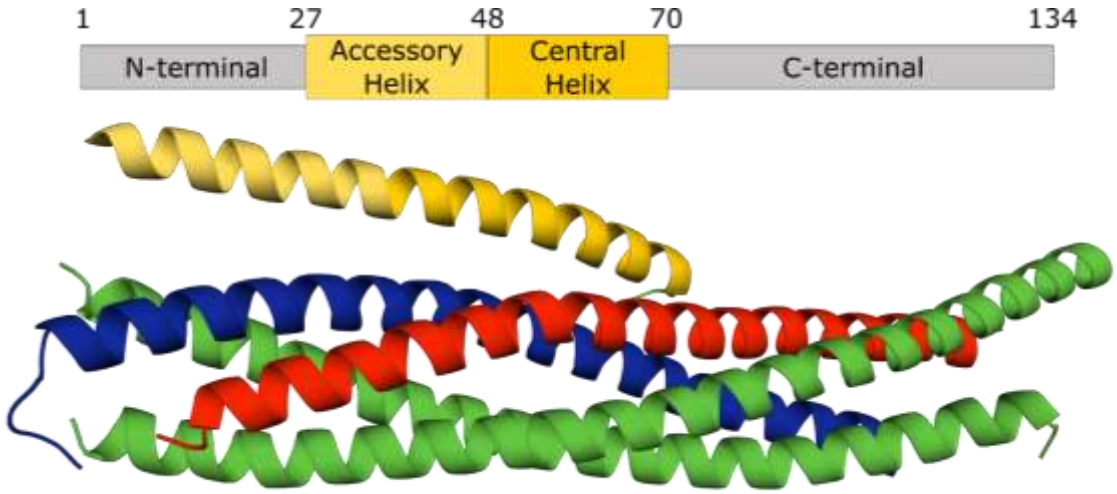


***Figure 14.*** *Domain diagram of Rattus norvegicus Complexin. The central helix (48- 70) binds to the SNARE complex and the accessory helix (27-48) might stabilize the binding of the central helix with the SNARE complex. On the bottom the Complexin – SNARE complex bound structure. Shown in the yellow is the Complexin fragment of the central helix and the accessory helix only. The central helix domain binds to Synaptobrevin-2 (blue) and Syntaxin-1 (red). Structure deposited in PDB as 1KIL*[183]*. Secondary structure was calculated with STRIDE*[184]

Complexin, in a manner similar to Synaptotagmin, can bind to both membranes and SNARE complex[185,186,187]. Complexin and the membrane interact through its unstructured N- and C-terminal domains. Complexin's role in fusion has been extensively studied using different techniques. Complexin has been studied in liposomes, neurons, and neuroendocrine cells across several species via techniques including a lipid mixing assay, reconstituted vesicle fusion, antibody perturbation, gene knockout, and overexpression. Although the results are reproducible, the conclusions reached are contradictory, suggesting that Complexin has both a facilitatory role and an inhibitory effect on vesicle fusion[188,189]. The fusion facilitating role was confirmed in experiments in PC12 cells and chromaffin cells[190,191].

Lastly, a recent report shows that the acute genetic deletion of Cpx decreases the rates of all forms of neurotransmitter release in forebrain neurons in the mouse. Additionally, altered expression levels of Complexin have been proposed to contribute to many psychiatric disorders, including Alzheimer's disease, Huntington's disease, and Parkinson's disease[188].

## 1.4 Electron Paramagnetic Spectroscopy

Spectroscopy is a vast field of study focused on generating and interpreting spectra obtained from the interactions of electromagnetic radiation with matter.

One of the spectroscopic methods widely used in chemistry, biology, physics, and medicine to study paramagnetic materials is Electron Paramagnetic Resonance (EPR), also called Electron Spin Resonance (ESR). Paramagnetic materials have unpaired electrons, and the magnetic moment of the electron spin will align in the presence of an external magnetic field. The EPR technique requires a paramagnetic center, and biomolecules like proteins usually do not have one. However, there are some proteins that have metal centers that are paramagnetic[192], and

some intermediates in electron transport (like flavins or tyrosine radicals)[193] are paramagnetic, thus can be studied with EPR. However, we do not see these in the proteins we study. To enable proteins to be examined by the EPR, we utilize paramagnetic probe molecules. We call them spin labels when they are chemically attached to the specific site in the system or spin probes when they interact non-covalently with the system[194]. Due to the requirement of a paramagnetic center for EPR spectroscopy, this method is a highly selective technique.

EPR spectroscopy and the Site Direct Spin Labeling (SDSL) are well-established and powerful biophysical techniques to study local structure and dynamics within protein systems. SDSL utilizes mutagenesis to allow us to introduce cysteine into the part of the protein that we need to examine. Afterward, a paramagnetic probe is attached to the introduced cysteine during spin-labeling, creating a spin-label site in a specific place in a protein[195]. An accurate analysis of the spin-label dynamics gives valuable data describing the local environment, the protein secondary structure, or tertiary contacts made at the labeled site. The depth of the protein's membrane penetration can be determined by a continuous-wave (CW) EPR experiment[196]. Pulse EPR approach provides additional structural information about distances and conformations of proteins and fill in the gaps and is complementary to data obtained from the CW EPR experiment[197]. The range of information provided by those two types of EPR experiments creates an extensive information mosaic. The datasets obtained from the EPR experiments enable mapping the local steric accessibility, mobility, conformational changes, or interactions within the protein or with other proteins or components in the solution (or membrane). Moreover, we can measure the protein oligomerization, tumbling, and stability, giving us a more precise picture of the proteins' structure and overall function[196].

The characteristics of the EPR experiment allow it to be used under a wide range of conditions with a range of solvents and substances in a protein samples, provided the protein is stable. One can even mimic the physiological conditions closely. There is no molecular size limit on

the protein samples, which allows for an extensive range of protein sizes to be examined[198]. Measurements can be performed with minimal sample volumes and with relatively low concentrations. This method is nondestructive, so samples can be reused for additional experiments if needed. EPR spectra (CW-EPR) may be recorded in solution at room temperature which allows one to sample dynamics and examine conformational equilibria. The EPR features mentioned above give the method some unique advantages compared to other biophysical techniques when proteins are characterized. Methods like X-ray crystallography[199], Nuclear Magnetic Resonance (NMR)[200], or Fluorescence Microscopy[201] often require usual and sometimes non-physiological experiment conditions. With methods like fluorescence, sometimes the addition of labels is required that are larger than tested proteins. NMR can require high sample concentrations that may create problems with protein stability, and NMR is limited in the molecular weight range that can be examined. X-ray crystallography is a very powerful method to determine high-resolution structures, but sometimes it requires an unusual sample conditions which may alter protein structure that would be present under more physiological conditions. The limitations make EPR the method of choice for some experiments, and particularly when the experiments require physiologically relevant condiitons[202]. EPR spectroscopy is not a method for obtaining a complete three-dimensional structure, but EPR is an excellent technique to test protein structural changes and function when an initial structure is known. EPR can often be combined with computational methods to test structures or modify existing high-resolution structures.

### 1.5.1 Fundamental Theory and Continuous Wave EPR (CW EPR)

The essence of the EPR lies in the ability of the unpaired electron to adopt one of two energy states in the presence of an external magnetic field. It is called Zeeman Effect or Zeeman Splitting, and it is represented by Equation 1:

$$Hz = g\,\beta\,S_z\,B_0 \quad (1)$$

Where g is the *g-factor* and is equal to 2.002 for a free electron[203], β is the Bohr magneton ($9.274 \times 10^{-21}$ erg Gauss), $S_z$ is the spin angular momentum and $B_0$ is the applied magnetic field. The spin angular momentum is quantized, and along the z-axis or the direction of the applied magnetic field, there are two possible values of $S_z$: -1/2 and +1/2. Therefore, the spin energies are:

$$E = \pm\tfrac{1}{2}\,g\,\beta\,B_0 \quad (2)$$

The energy difference between the two states is linear with the field B0 and is given by:

$$\Delta E = g\,\beta\,B_0 \quad (3)$$

If an alternating electromagnetic field is applied to the sample at a frequency $\nu$ that corresponds to the energy difference (ΔE) between these states, transitions are induced between these energy states. For typical EPR experiments these frequencies are in the microwave frequency range. Transitions to a higher energy state absorb energy and transitions to the lower energy state release energy as given by:

$$\Delta E = h\nu \quad (4)$$

Where h is the *Plank's* constant and $\nu$ is the frequency the radiation. In the EPR experiment, the magnetic field component of the microwave radiation is applied perpendicular to the static magnetic field ($B_0$). Combining equations 3 and 4, the resonance condition can be written as:

$$g \beta B_0 = h\nu \quad (5)$$

The resonance condition is met, and the absorption power takes place when with the proper selection of the electromagnetic radiation frequency and static magnetic field. From the equation above that we can obtain the resonance condition in two ways:

1) By changing the frequency of an alternating magnetic field at a fixed magnetic field induction $B_0$

2) By changing the magnetic field at a fixed frequency.

In the EPR, the second way is utilized. When a sample is exposed to a magnetic field of varying $B_0$ and a constant microwave radiation frequency, the value of $B_0$ is found at which resonance occurs, and a single line for a CW EPR spectrum is produced (Figure 15)[204].

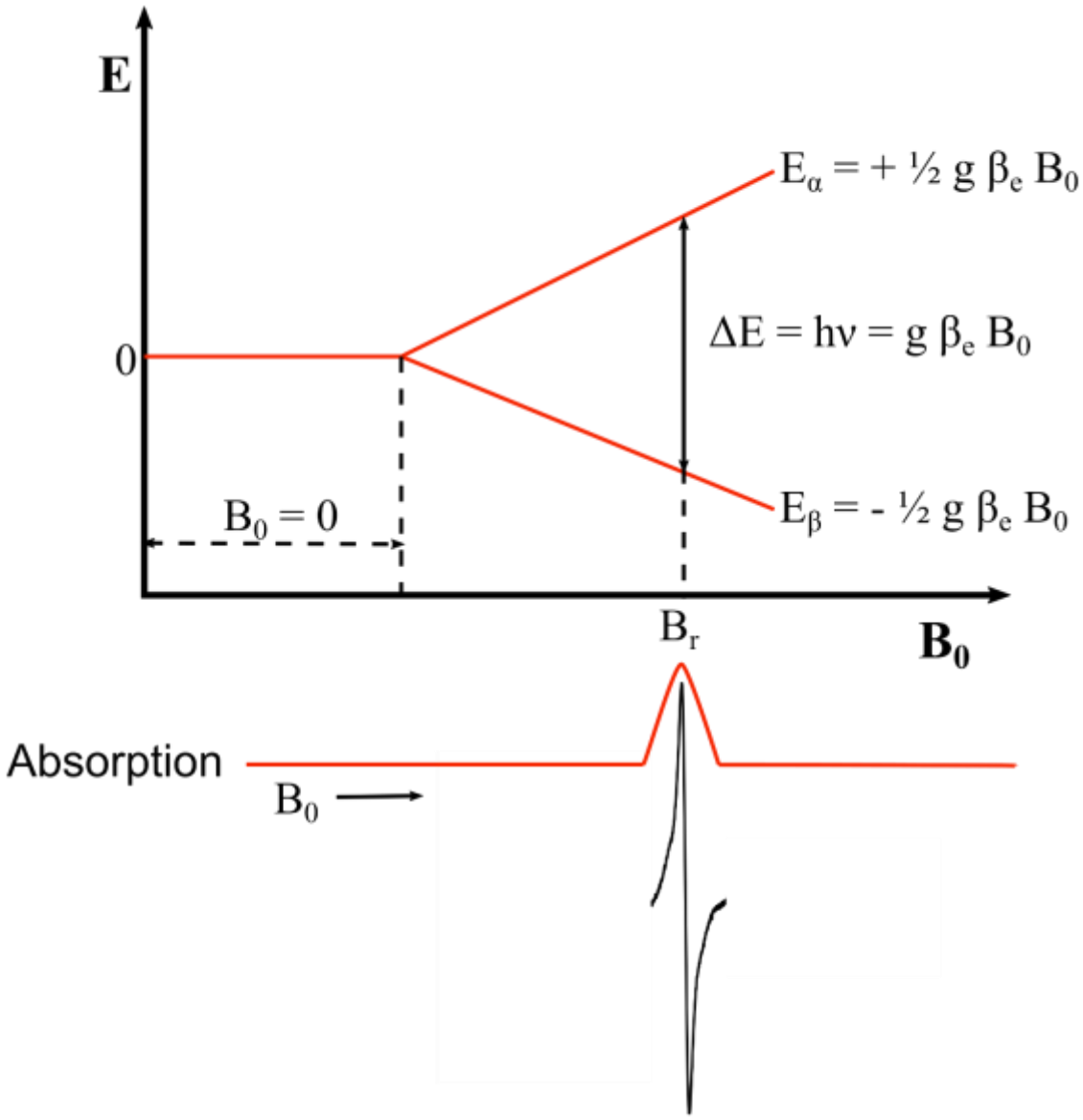


***Figure 15.*** *The Zeeman Effect. In the presence of the external magnetic field B, the unpaired electron can adopt two distinct energy levels. The transition from the ground to the excited state (ms = - ½ to ms = ½) occurs at the resonant magnetic field (Br) upon energy absorption. The absorption signal is recorded as the first derivative due to the modulation of a magnetic field.*

There are typically three lines in the EPR spectrum of a nitroxide label. In a nitroxide, this characteristic splitting of the signal results from the interaction between the unpaired electron on the oxygen atom with the neighboring nitrogen nucleus. A free electron will yield a single resonant peak; however, this is not typically observed in organic free radicals. The additional three resonance peaks arise from a hyperfine interaction with the nitrogen nucleus, which has nuclear spin states of $M_I$=-1, 0, +1. These spin states generate three values of the local magnetic field BI yielding three resonance peaks. In general, the addition peaks due to hyperfine interactions can be utilized to identify paramagnetic species and collect information about the environment of the spin[205,206,207]. In the CW EPR spectrum of a nitroxide, these are frequently referred to as the low field, center field, and high field lines from left to right. (Figure 16)[204].

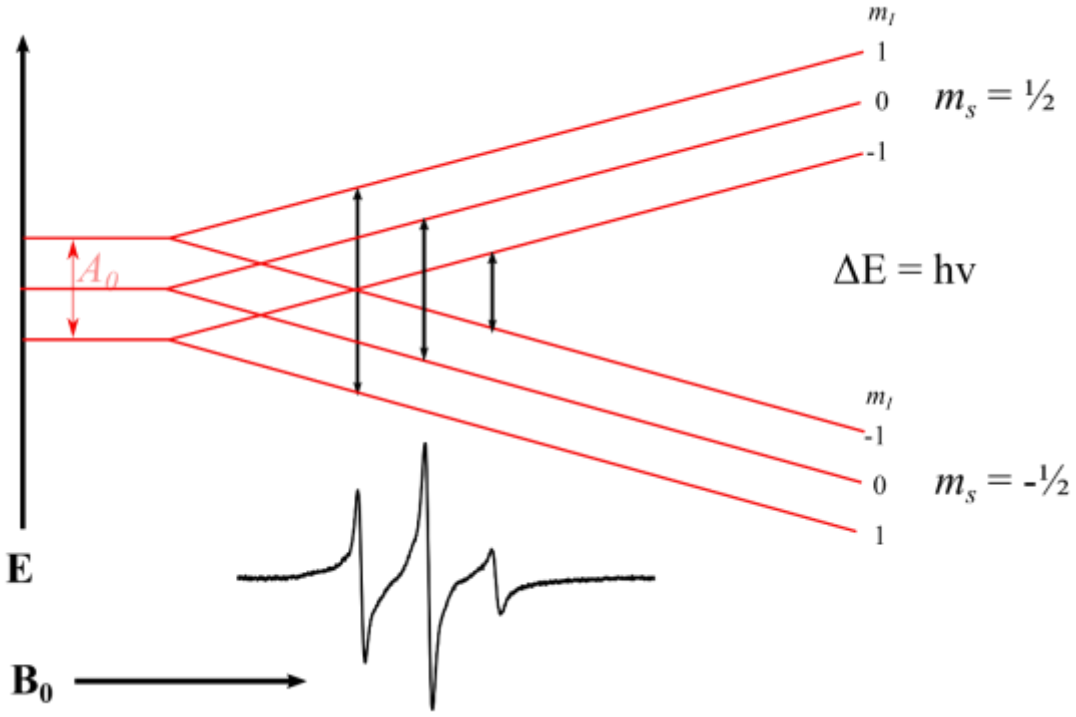


***Figure 16****. The hyperfine interaction. Diagram presenting splitting of energy levels upon the interaction between an electron (ms = 1/2) and a nitrogen nucleus (nuclear spin I = 1) at the constant frequency with a swept magnetic field (B0). Vertical arrows indicate allowed transitions between the energy levels of the same nuclear spin. Also shown is the first derivative of the absorption profile: three possible energy transitions shown by black arrows, which will produce CW EPR peaks (low field, center field, high field, from left to right).*

### 1.5.2 Site-Directed Spin Labeling (SDSL)

Initially, the EPR technique had minimal application and was used only to study naturally occurring paramagnetic systems, radicals, and transition metal complexes with a residual electron spin. This fundamental feature was the primary limitation of the technique in studying biological systems, as unpaired electrons are not commonly found in biomolecules due to their high reactivity and instability. However, with the advent of spin-labeling, and biochemical techniques to place stable radicals at specific locations on biological macromolecules, the potential use of EPR has been extended to virtually any molecular system[208]. That said, proteins and protein complexes can be studied through artificially introduced paramagnetic centers.

There are several approaches that can be used to attach spin labels to proteins. First, a spin label can be attached to a biomolecules through click chemistry[209], in a similar manner that is used to attach a fluorescent probe. Second, the intein-mediated protein ligation (IPL) method produces semi-synthesized proteins with spin labels where spin-labeled synthesized peptides are incorporated into proteins[210]. Thirdly, tRNAs with attached spin-labeled amino acids are used to insert labels during translation in nonsense repressor technology[211]. Last but not least, a widely used tool to introduce a spin-label is site-directed spin labeling (SDSL)[212,213,214]. This method is based on cysteine chemistry. All native reactive cysteines, if they are present, are eliminated by replacement with other amino acids (the most common is alanine). Then, a unique cysteine residue is introduced to the protein at the DNA level. Both steps are performed *via* site-directed mutagenesis. The mutated gene expression follows this in a chosen expression system. After the gene expression, protein isolation and purification, the mutated cysteine site is labeled with the EPR spin-label of choice typically by creating a disulfide bond between the protein and the spin-label. However, there are spin labels that can be attached through non reversible bond such a maleimide based labels that reacts with cysteine to form a thio-ether

bond. Acetamide-functionalized spin labels also react with cysteine via a C–S bond. These reagents can be used under mild reducing conditions that would lead to cleavage of the typical disulfide bond[215,216].

One of the most prominent spin-label families comprises nitroxide spin-labels based on the nitroxyl(N–O) radicals[217,218]. These radicals are five- or six-membered heterocyclic derivatives of piperidine, pyrrolidine, isoindoline, and other heterocycles containing two heteroatoms. Figure 3 presents some of the typical nitroxide families. One of the most classic nitroxides with many chemical and materials application is the piperidine-based 2,2,6,6-tetra-methyl piperidine 1-oxyl (TEMPO, Figure 17 a)

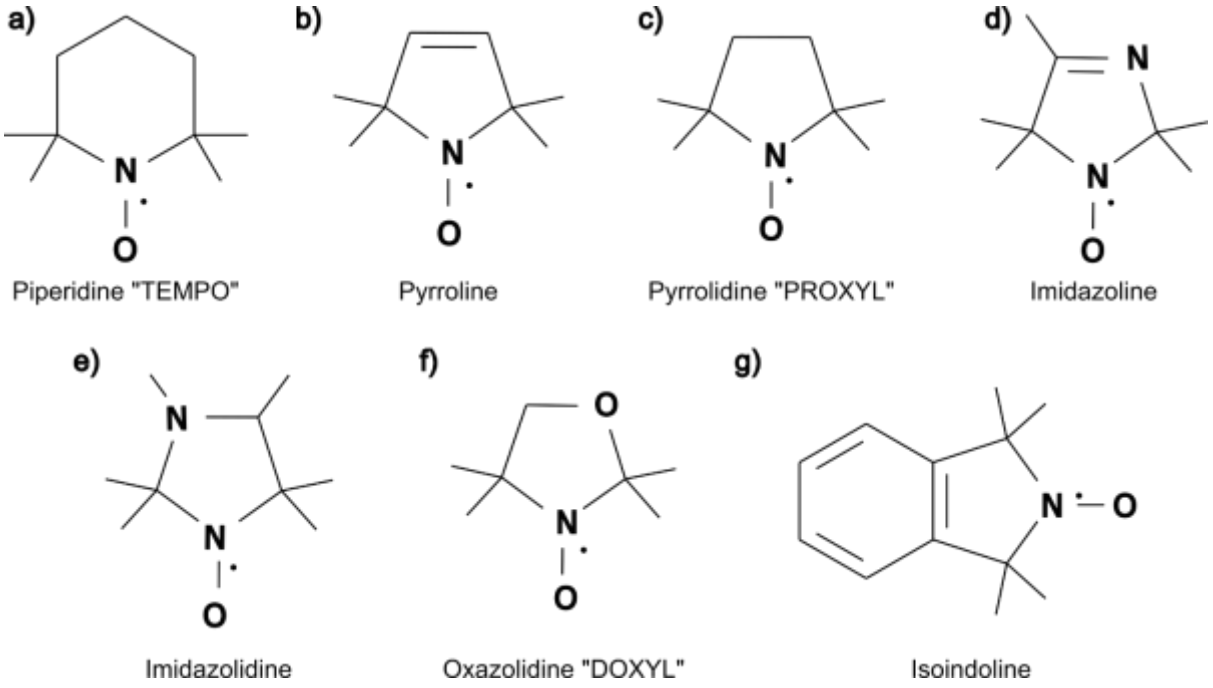


***Figure 17****. Structure of examples of nitroxide spin labels used in the site-directed spin labeling (SDSL) EPR*[218].

The most commonly used spin-label is the nitroxide reagent – (1-oxyl-2,2,5,5-tetramethylpyrroline-3-methyl) methanethiosulfonate spin-label (MTSL) [212,219], which yields a so-called R1 side chain (see Figure 18). It is small, very selective, quickly reacting, with a side chain area similar to a tryptophan side chain[220]. The features of MTSL, like its sulfhydryl specificity, small size, and structural similarity to tryptophan, made it one of the most popular spin labels employed in SDSL EPR experiments.

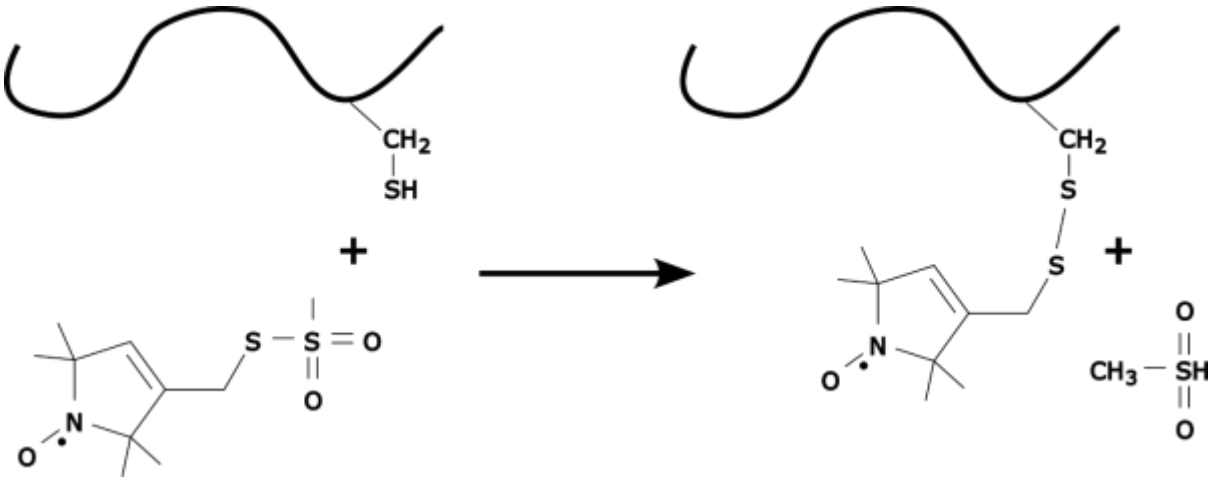


***Figure 18**. Reaction of the methanethiosulfonate spin-label (MTSL) with a cysteine residue via disulfide bond formation generates an R1 side chain*[221].

MTSL is usually the spin-label of choice due to several reasons, mentioned above. The unique dynamic properties of this label side chain provide detailed structural information from the lineshape of its EPR spectrum. The EPR spectra are susceptible to even small changes in the overall motion of the spin label side chain. EPR spectra from the R1 side chain are very sensitive to the rates and amplitudes of motion of R1 on the ns time scales. This motion is dictated by the local structure around the nitroxide; and as a result, spectra vary depending upon the site to which they are attached. Figure 19 shows characteristic spectra that arise when the label is placed at different sites within T4 lysozyme[222].

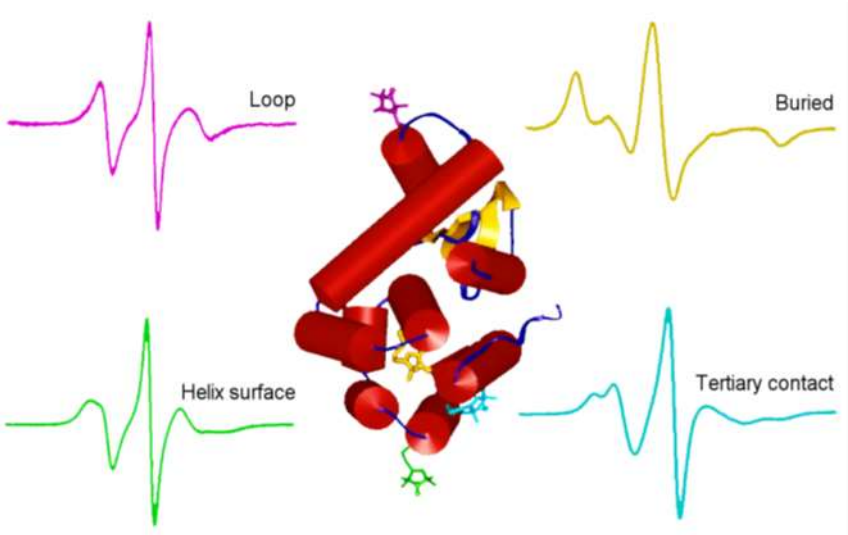


***Figure 19.*** *The illustration of the CW EPR spectra obtained in different protein structural environments. The CW study on the T4 lysozyme's secondary structure produces unique EPR spectra. The particular nitroxide used in the experiment, MTSSL, is very sensitive to the motion of the protein backbone, and it explains the spectra' uniqueness (Figure source: Mchaourab et all, 1996)* [222].

### 1.5.3 Double Electron-Electron Resonance DEER

Double Electron-Electron Resonance (DEER), also called Pulsed Electron Double Resonance (PELDOR) spectroscopy, is a rapidly emerging, powerful structural biology technique in which we measure the dipolar coupling between two unpaired electron spins (usually site-directed nitroxide spin labels). In the majority of cases, the spin probe is introduced into two different sites, but it is also possible to test single labeled samples, i.e. when studying protein aggregation or protein-protein interactions. The dipolar coupling between the two spins can then be used to determine the distance between the two spin probes ranging between 1.5 and 8 nm[223,224].

Two paramagnetic molecules can interact via exchange interactions or dipolar interactions. The exchange interaction decreases when the distance between two species increases, which leaves it with only dipole-dipole coupling between two unpaired electron spins (S1 and S2 in Figure 20).

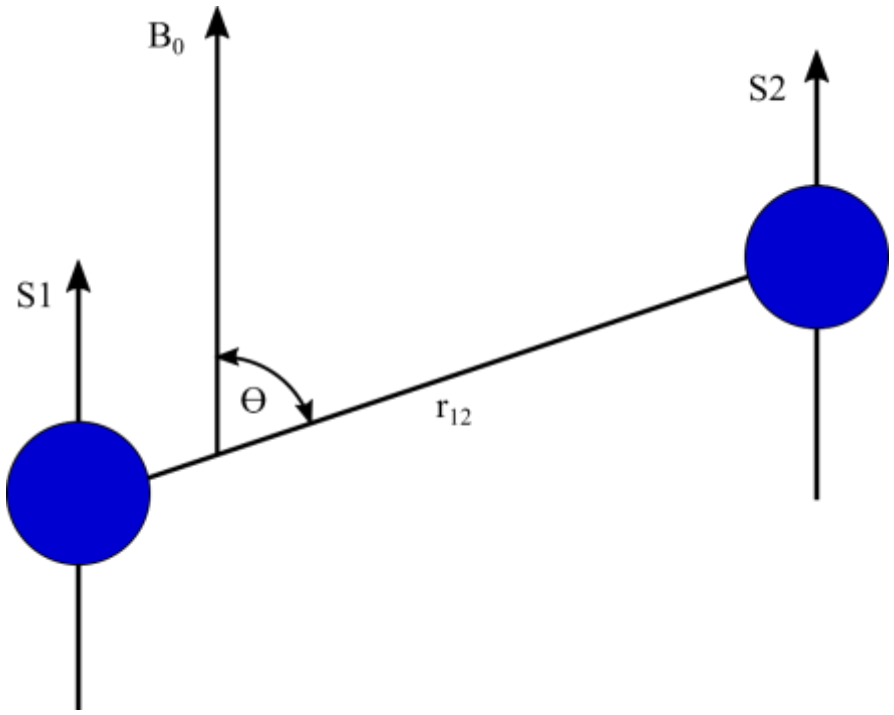


***Figure 20.*** *Dipolar interactions between two paramagnetic centers.*

The dipolar interaction depends on two factors. The first factor is the distance $r_{12}$ between two paramagnetic centers. The second factor is the angle Θ formed between the interspecies vectors $S_1$ and $S_2$ and the applied magnetic field B0. Equation 6 describes this interaction:

$$v_{dd}(r,\theta) = \frac{\mu_0 g_1 g_2 \mu_B}{2h} * \frac{1}{r^3} * (3cos\theta^2 - 1) \quad (6)$$

Where $v_{dd}$ is the dipolar coupling, $\mu_0$ is the permeability of a vacuum, h is the Planck constant, $g_1$ and $g_2$ represent the isotropic g-values of the respective paramagnetic molecules, and $\mu_B$ is the Bohr magneton.

These measurements are typically conducted with Q-band (~34 GHz) but can also be performed at X-band (~9.4 GHz) microwave excitation using the 4-pulse DEER sequence. For a biological sample, the experiment may require up to 12+ hours of signal averaging, and this depends on the sample and, more precisely, spin label concentration.

The magnetic field is kept fixed in a pulse EPR experiment, the opposite of the CW EPR experiment. In principle, an EPR spectrum may be recorded by exciting over a broad frequency range with a single high-power MW pulse and recording the free-induction decal. But this is difficult to do because of the fast relaxation time of the nitroxide and the power required to excite the entire spectrum (Figure 21)[225]. Since the relaxation times of nitroxides is too short in most biological systems to execute the DEER experiment at room temperature, pulsed EPR measurements such as DEER usually require cryogenic temperatures.

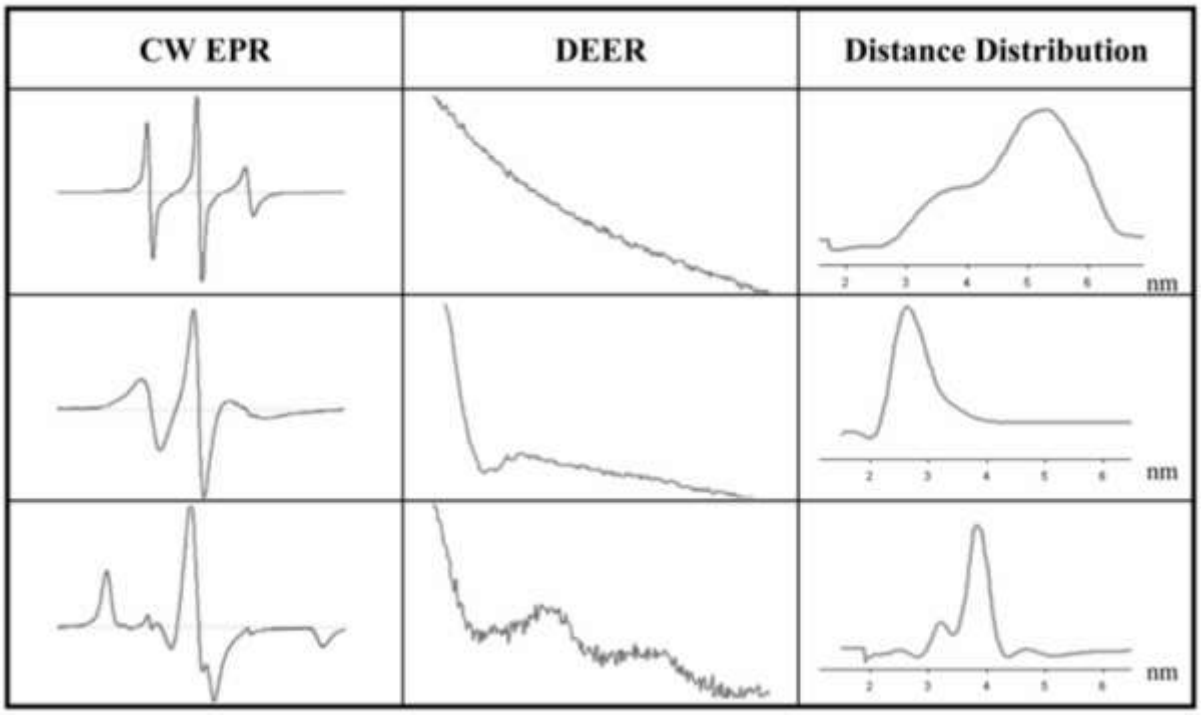


***Figure 21**. Comparison of spin label mobility CW EPR, DEER spectra, and distance distribution. Decreasing mobility of spin labels results in larger modulation depth of the dipolar evolution and narrower distance distribution (Figure source: Fajer, 2006)*[225].

The DEER technique carefully manipulates two groups of spins: A spins that are exited at the *observe* position or frequency and B spins at the *pump* position. These two positions are selected from different locations on the absorption spectrum of the nitroxide. The two groups of nitroxides can be selectively excited in the 4-pulse DEER experiment, an example of which is shown schematically in Figure 22 [219]. During the experiment, after the first π pulse that flips the A spins, there is a π pulse applied to the B spins. This pulse will change the dipolar contribution from the B spins felt by the A spins. This way, there will be a phase shift that will influence the refocusing of the A spins. The final π pulse on those spins will yield an echo recorded in the experiment. This experiment is then repeated by changing the time of the pump pulse influencing the B spins. The final result will be the echo intensity.

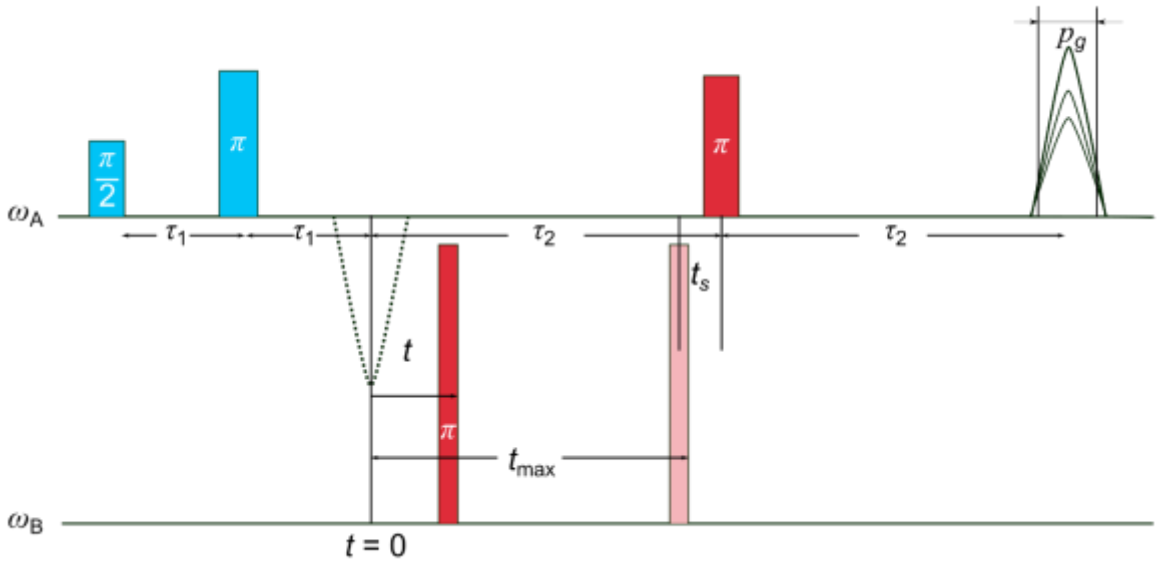


***Figure 22**. The four-pulse sequence of the DEER experiment. The primary echo sequence with observer frequency (ω1) is refocused by applying pump frequency (ω2) at time t after the undetected first echo. Times τ1 and τ2 are kept constant, while t can vary (Figure inspired by Jeschke, 2012)*[219]

The DEER signal that is obtained consists of two types of interactions - intra- and intermolecular[226]. The former describes the interactions between the spin pair and the latter between other spin-labeled molecules in the sample. Thus, the echo signal, V(t), is composed of a spin pair interaction contribution, F(t), and a background contribution, B(t), where B(t) needs to be subtracted to obtain F(t) (Figure 23 A). After fitting the background, B(t), F(t) can be obtained by dividing V(t) by B(t) (Figure 23 B), and F(t) is converted into distance distribution P(r).

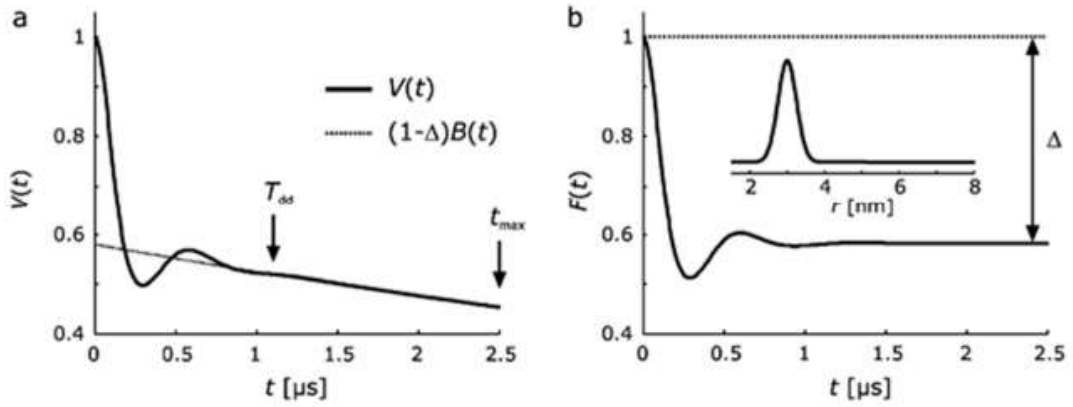


***Figure 23.*** *Obtaining F(t) from DEER signal. (a) The echo signal is observed until tmax. F(t) has a damped oscillation shape, completely decaying at Tdd. The rest of the signal is B(t). Thus, B(t) is fitted in V(t). (b) F(t) is obtained after removing B(t) from V(t) and renormalized to time zero, and F(t) is used to obtain the corresponding Gaussian distribution (Figure source: Jeschke, 2007 )* [197].

The CW EPR and pulsed EPR with SDSL have become widely used in biophysical research. The SDSL CW EPR and DEER create a powerful pair of tools where an electron spin introduced into diamagnetic proteins provides information on their local environment and the mobility of the protein domain. As a result, we obtain information on secondary structures, structural changes associated with protein dynamics, protein-protein interactions, distances between two spin-labeled sites, and protein backbone dynamics. The distance distributions obtained will reflect the true conformational heterogeneity of the protein and the spin-label sidechains. The work presented here features proteins labeled with the MTSL label (which may contribute approximately 30-40 nm to the distance distribution). By utilizing these techniques in this work, we can better describe the sophisticated interactions between SNARE proteins, visualize this protein itself, and learn about higher organization among them.

## II. RESEARCH AIMS

The work presented in this dissertation had four main objectives.

- The first objective was to explore how the chemical and physical environment impacts the proteins from the SNARE complex, if the impact is significant, and whether we can observe these proteins' aggregation. The first part of chapter four of this work contains a detailed description of these findings.
- The second objective was to shed light on the states of Syntaxin-1a in different stages of SNAREs assembly. It is a well-established fact that Syntaxin-1a exists in equilibrium between an open and a close state. In this work, I focused on Syntaxin-1a assembled into Syntaxin-1a – SNAP25 complex (also called t-SNAREs or acceptor complex) and SNARE complex. I confirmed that Syntaxin-1a remains open in the SNARE complex with the 6 nm distance between the Glu52 in the Habc and Arg210 in the H3 domain when there is no mutations in the Habc domain. Syntaxin-1a in the acceptor complex remains open with the 6 nm distance. However, another set of distance populations, of about 4 nm, suggests a slightly shorter distance between the Glu52 in the Habc and Arg210 in the H3 domain.
- The third aim of this work was focused on the interaction between Munc18 and Syntaxin-1 during SNAREs assembly. Munc18 binds to Syntaxin-1a alone, disassociates its aggregates, and shifts it in to the closed state. Therefore, it was essential to investigate this interaction to explain the details of the assembly process of Syntaxin-1a into the t-SNARE or SNARE complex.
- The final aim was to analyze how lipid bilayer membrane presence affected Syntaxin-1a and its assembled complexes, as well as its interaction with Munc18. Most of the Syntaxin-1a studies are conducted on a water-soluble part of the protein. That includes the aspects of this work focused on this protein. At the same time, Syntaxin-1a is a

membrane protein, and it was essential to analyze its conformational changes and interactions with other proteins in the presence of the lipid membrane. These findings allow for a better understanding of what happens during in the neuronal fusion system orchestrated by SNARE proteins.

At this point, all of the proteins involved in neuronal fusion have been identified and analyzed in some detail. Still, many studies yield contrary results. Moreover, while functional assay studies dominate the research on neuronal fusion, they lack information on the process on a biomolecular level. Therefore, the work's overall goal was to expand the existing models of neuronal fusion and confirm some of the published earlier hypotheses. At the same time, the EPR study was used to provide more detailed insight into the interaction between SNARE proteins and accessory proteins.

# III. MATERIALS AND METHODS

## 3.1 Materials

Plasmids

Plasmids containing sequences encoding wild-type SNARE proteins, Complexin-1 and Munc18-1 were generously provided by the Cafiso laboratory and Tamm laboratory members at the University of Virginia. All the sequences originate from Rattus norvegicus. The full-length sequence of SNAP-25, full-length sequence of Munc18-1, full-length sequence of Complexin-1, full-length sequence of syntaxin-1a, 1-262, and 27-262 residues fragments of Syntaxin-1a and the 1–96 residues synaptobrevin-2 fragment were cloned into the pET-28a vectors, whereas the 180–253 residues syntaxin-1 fragment was cloned into the pET-15b vector. All recombinant fusion proteins carried a thrombin-cleavable amino-terminal His6 tag to facilitate the purification procedure.

Syntaxin-1a constructs: full length (1-288), soluble (1-262), ΔN (27-262), H3 (180-253). Native cysteines were mutated using the standard PIPE site-directed. For EPR CW and DEER measurements, single and double cysteine mutations were introduced into cysteine-free construct.

The correct sequence of all mutants was confirmed by DNA sequencing (GENEWIZ).

***Table 1****. General supplies used in the laboratory*

| **SUPPLIES** | **SOURCE** |
|---|---|
| BUFFERS AND GENERAL CHEMICAL REAGENTS | |
| Ethylenediaminetetraacetic acid (EDTA) | Bio Basic |
| calcium chloride | IBI Scientific |
| potassium chloride | IBI Scientific |

| | |
|---|---|
| sodium chloride | IBI Scientific |
| tris(hydroxymethyl)aminomethane hydrochloride (Tris) | Sigma |
| 3-(N-morpholino)propanesulfonic acid (MOPS) | Bio Basic |
| glycerol | Research Products International |
| 2-[4-(2-hydroxyethyl)piperazin-1-yl]ethanesulfonic acid (HEPES) | Bio Basic |
| Chloroform | Sigma |
| methanol | LabChem |
| sucrose | Sigma |
| Bacto Agar | BD |
| acetic acid | Bio Basic |
| DDT (Ditiothrietol) | G Biosciences |
| urea | Sigma-Aldrich |
| SDS PAGE & DNA gel | |
| Loading buffer | Amresco |
| Loading buffer for native page | Amresco |
| 2-mercaptoethanol | Sigma |
| 12 % Mini-PROTEAN TGX gels | BioRad |

| | |
|---|---|
| 4-20 % Mini-PROTEAN TGX gels | BioRad |
| Protein ladder standard | Goldbio |
| agarose | Invitrogen |
| DNA ladder standard | Goldbio |
| Loading buffer | Lonza |
| LIPIDS AND DETERGENTS | |
| triton X-100 | Sigma |
| sodium cholate | |
| n-Dodecylphosphocholine (DPC) | Antracen |
| 1-palmitoyl-2-oleoyl-sn-glycero-3-phosphocholine (POPC) | Avanti Polar Lipids Inc |
| 1-palmitoyl-2-oleoyl-snglycero-3-phosphoethanolamine (POPE) | |
| 1-palmitoyl-2-oleoyl-sn-glycero-3-phospho-L-serine (POPS) | |
| 1-palmitoyl-2-oleoyl-sn-glycero-3-phospho-(1′-rac-glycerol) (POPG) | |
| porcine brain L-α-phosphatidylcholine (brain PC) | |

| | |
|---|---|
| porcine brain L-α-phosphatidylethanolamine (brain PE) | |
| porcine brain L-αphosphatidylserine (brain PS) | |
| phosphatidylinositol 4,5-bisphosphate (PIP2) | |
| 1,2-dipalmitoyl-snglycero-3-phosphocholine (DPPC) | |
| 1,2-dipalmitoyl-sn-glycero-3-phosphoethanolamine (DPPE) | |
| 1,2-dipalmitoyl-sn-glycero-3-phospho-L-serine (DPPS) | |
| 1,2-dioleoyl-sn-glycero-3- phosphocholine (DOPC) | |
| 1,2-dioleoyl-sn-glycero-3-phosphoethanolamine (DOPE) | |
| 1,2-dioleoylsn-glycero-3-phospho-L-serine (DOPS) | |
| cholesterol | EMD Millipore/Sigma |
| BioBeads | Bio-Rad |
| PCR AND MINI PREP REAGENTS | |

| | |
|---|---|
| Primers for PCR | Integrated IDT Technologies |
| PfuUltra High-Fidelity DNA Polymerase | Agilent |
| 10 X Pfu Turbo polymerase reaction buffer | Agilent |
| DpnI restriction endonuclease | New England Biolabs |
| dNTP mixes | Bio Basic |
| QIAprep spin miniprep kit | Qiagen |
| GeneJET PCR Purification Kit | Thermo Scientific |
| PROTEIN EXPRESSION AND PURIFICATION | |
| Top10 competent cells | Invitrogen |
| BL21(DE3) cells | |
| Yeast | IBI Scientific |
| Tryptone | |
| Isopropylβ-D-thiogalacto-pyranoside (IPTG) | Goldbio |
| ampicillin sodium salt | IBI Scientific |
| kanamycin | Boston BioProducts |
| Benzonase nuclease | EMD Millipore |
| 4-(2-aminoethyl) benzenesulfonyl fluoride hydrochloride (AEBSF) | Indofine Chemical Company |

| | |
|---|---|
| Aprotinin | Research Products International |
| Leupeptin | Roche |
| Thrombin | Sigma-Aldrich |
| PierceTM Coomassie<br><br>Plus (Bradford) Assay reagent | Thermo Fisher Scientific |
| NiNTA agarose | Qiagen |
| Profinity IMAC Ni-Charged Resin | Biorad |
| EPR | |
| MTSL (S-(1-oxyl-2,2,5,5 – tetramethyl - 2,5 – dihydro - 1H – pyrrol – 3 - yl) methyl methanethiosulfonate) | Santa Cruz Biotech |
| chromium (III) oxalate | |
| deuterated glycerol | Cambridge Isotopes |

General Lab Equipment and accessories

***Table 2.*** *General Lab accessories*

| **SUPPLIES** | **SOURCE** |
|---|---|
| GENERAL SUPPLY | |
| Syringes | BD Medical |
| Syringe filters | CELLTREAT |

| | |
|---|---|
| Needles | BD Medical |
| Nanopure system | Dubuque |
| borosilicate tubes | DWK Life Sciences (Kimble) |
| Culture flasks (2.8L and 500mL) | Corning |
| General glass and plasticware | mainly from Fisher Scientific |
| Hamilton Syringes | Hamilton |
| SDS PAGE & DNA gel | |
| T100 thermal cycler | BioRad |
| Gel box | BioRad |
| Power source | BioRad |
| Protein Purification | |
| Dialysis tubing | Spectra/Por |
| Dialysis cassettes | Fisher Scientific |
| Amicon Ultra Concentrators | EMD Millipore/Sigma |
| Columns: | |
| HiTrap SP | GE Healthcare |
| HiTrap Q HP | |
| HiPrep 26/10 Desalting | |
| HiTrap 16/60 Sephacryl S-100 HR | |

| | |
|---|---|
| MonoQ 5/50 | |
| Superdex75 10/30 | |
| Superdex200 10/30 | |
| Superdex200 Increase 10/30 | |
| DP-10 Desalting | GE Healthcare Life Science |
| EPR | |
| 0.6IDx0.84OD-100 mm Borosilicate capillaries | VitroCom |
| 1.5IDx1.8OD-100 mm Quartz capillaries | |

ÄKTA™ lab-scale protein purification systems

These protein purification systems are designed to purify biomolecules, providing speed, performance, and flexibility in the research process. ÄKTA systems use intelligent UNICORN™ system control software to combine simplicity with power in protein purification. Currently, in the laboratory, we are using:

- ÄKTAprime plus
- ÄKTApurifier 100 plus

NGC Quest 10 Plus Chromatography System

This system is designed to suit labs with basic purification needs. The NGC Quest 10 Plus instrument has automated 10 ml/min pumps that provide accurate gradients for high-resolution separations for any application. The NGC Quest 10 Plus system has a multi-wavelength

detector with simultaneous four-wavelength monitoring for high-accuracy detection of proteins, peptides, and nucleic acids combined with conductivity measurements. Fractionated samples can be easily collected from analytical- to preparative-scale purifications using the NGC Fraction Collector and BioFrac Fraction Collector.

NanoDrop Spectrophotometer ND-1000

Ultracentrifuges:

- Beckman Coulter with 70 Ti and 45 Ti rotors

Centrifuges:

- SORVALL with SLA-3000 rotor
- Sorvall Tabletop Centrifuge

EPR Instrumentation:

- Bruker EMX Xband EPR spectrometer
- Bruker ELEXSYS E580 Q-band with a EN5107D2dielectric resonator

## 3.2 Methods

### 3.2.1 Site-directed mutagenesis

Site-directed mutagenesis is a technique based on PCR (polymerase chain reaction) with precisely modified primers. This technique was utilized to obtain the mutated versions of all Syntaxin-1a constructs. All used primers were ordered from IDT Technologies.

The reaction was driven by PfuUltra high-fidelity DNA polymerase in a BioRad T100 thermal cycler. The cysteine free Syntaxin-1a was used as a matrix in the following PCR reactions

leading to the acquisition of modified sequences containing a cysteine coding codon at the site of interest. The PCR samples were prepared according to Table 3 and the PCR cycle (Figure 24) used in PIPE PCR mutagenesis with selected annealing temperatures based on the melting temperatures of the primers used.

***Table 3**. Stock and final concentrations of reagents used in PCR mutagenesis*

| Reagent | Stock concentration | Final concentration in individual PCR reaction tube |
|---|---|---|
| Template DNA | 3 ng/µL | 0.06 ng/µL |
| 10 X Pfu Turbo polymerase reaction buffer (100 mM KCl, 100 mM $(NH_4)SO_4$, 200 mM Tris-Cl pH 8.8, 20 mM $MgSO_4$, 1 % Triton® X-100 and 1 mg/ml BSA)[11] | 10 X | 1 X |
| Forward primer | 10 µM | 1 µM |
| Reverse primer | 10 µM | 1 µM |
| dNTP mix | 10 mM each | 200 µM each |
| Pfu Turbo polymerase | 2.5 U/µL | 0.05 U/µL |
| $ddH_2O$ | | To bring final volume to 50 µL |

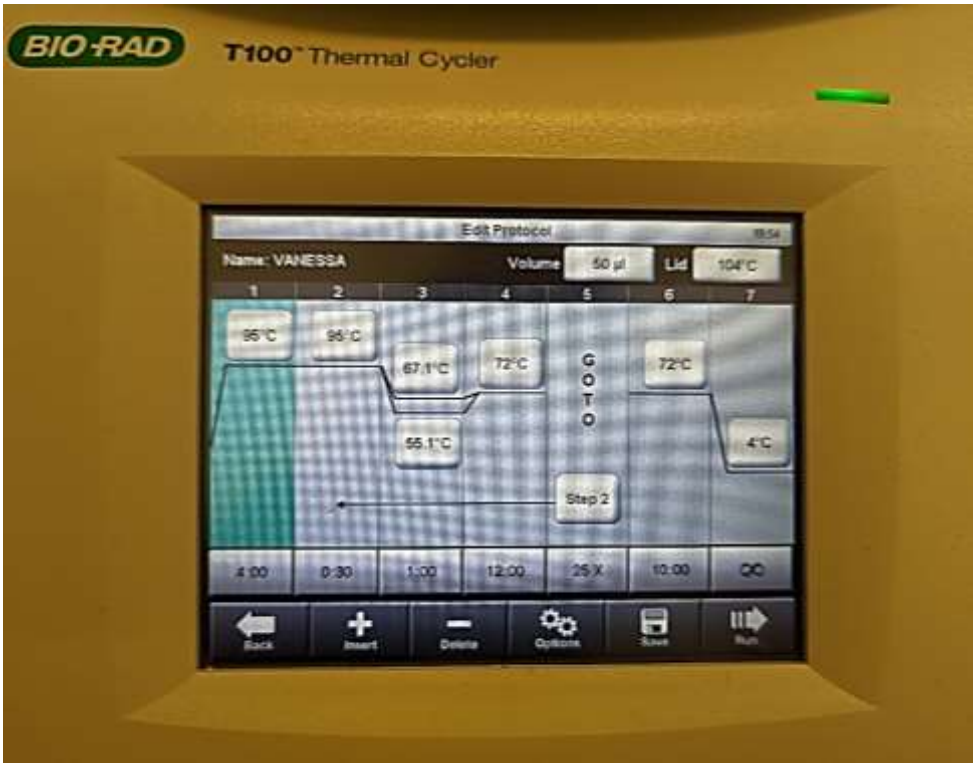


***Figure 24.*** *Example BioRad Thermocycler method used for PIPE Mutagenesis of Syntaxin-1a. Steps 1 and 2 are denaturation steps, Step 3 is Annealing over a gradient according to the placement of the tube in the thermocycler, Step 4 is extension time and temperature, Step 5 lists the number of cycles performed, Step 6 is final extension, step 7 cools the reaction and holds temperature. The conditions in the image are optimized for the standard reactions for Syntaxin-1a.*

As a last step, samples were incubated for 1h at 37 ºC with 20 U of DpnI, a restriction enzyme that cleaves the template DNA within its methylated recognition site. After incubating the PCR samples with Dpn1, samples were analyzed using 1 % agarose gel electrophoresis (Figure 25).

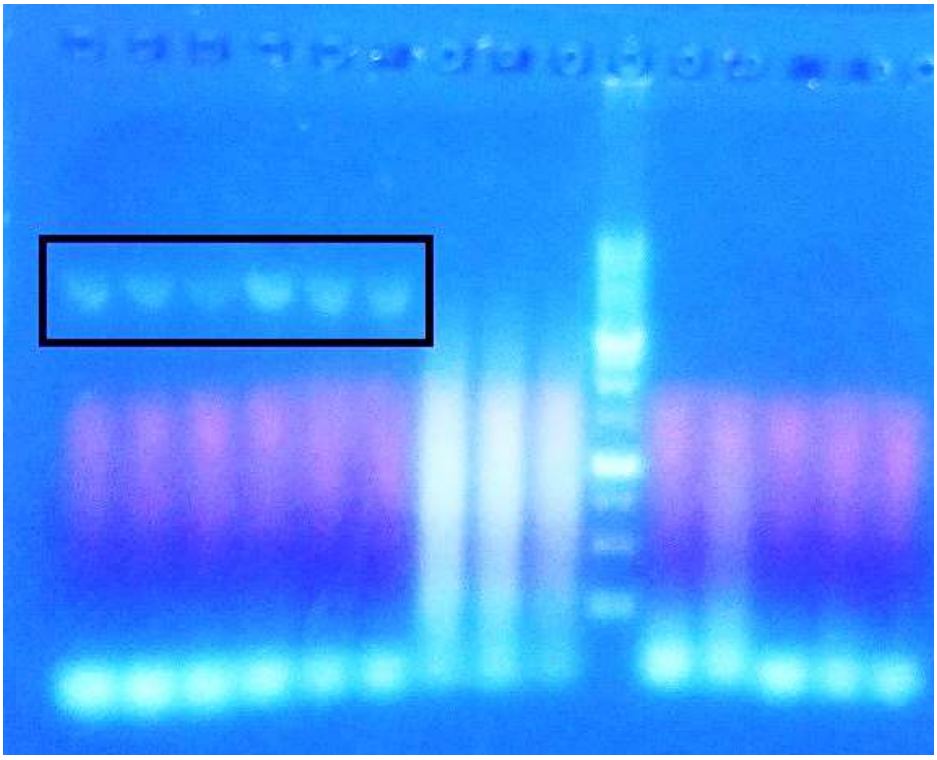

***Figure 25****. An image of a gel post electrophoresis, bands in the black box show successful reaction.*

The TOP10 chemically competent cells were transformed with plasmids containing the obtained mutated sequences and plated on antibiotic-containing LB-agar plates to amplify and subsequently isolate plasmids. Plasmids were purified from 5 ml cultures using either QIAprep Spin Miniprep Kit or GeneJET PCR Purification Kit. The NanoDrop was employed to monitor DNA concentration and purity. The correct sequence of all mutants was confirmed by DNA sequencing (GENEWIZ).

### 3.2.2 Protein expression and purification

#### Protein expression

All recombinant proteins were expressed in BL21 (DE3) cells. A standard heat-shock procedure was used to transform the competent E. coli cells with pET-28a or pET-15b vectors. Then cells were incubated for 1h at 37ºC to develop antibiotic resistance. After the incubation, cells were plated on the kanamycin/ampicillin LB-agar plates and left for overnight incubation at 37ºC. Grown colonies were used to inoculate 50ml LB media cultures supplied with kanamycin (40µg/ml) or ampicillin (50µg/ml). Cultures were incubated in a shaker overnight at 37ºC and used to inoculate 1L of LB media culture containing the desired antibiotic. When OD was measured at OD600 ≈ 1.0 culture was induced with 0.5mM IPTG. Cells were grown for 4h at 37ºC or overnight at 20ºC, leading to similar yields.

#### Protein purification

Following induction, cells were collected via centrifugation (7,000rpm, 10min, 4ºC) and resuspended in Extraction buffer (20mM Hepes, 500mM NaCl, 8mM imidazole, pH = 7.4). Leupeptin and AEBSF in a concentration of 10µg/ml were added to prevent protein degradation, cell lysis, and the release of proteases. Additionally, 1000U of benzonase nuclease

was added to remove nucleic acid contaminants. Cells were lysed using the French press and pelleted during ultracentrifugation (35,000rpm, 4ºC, 1h). For all SNARE proteins, 6M urea was added before centrifugation. Additionally, 2% of Triton-X 100 was added to full-length Syntaxin-1. The supernatant was applied on a Ni-Charged Resin column equilibrated beforehand with the Extraction buffer and incubated for 2 hours at 4ºC. Before proteins could be eluted, the column was washed with wash buffer (20mM HEPES, 500mM NaCl, 20mM imidazole, pH = 7.4). The washing step for full-length syntaxin-1 was different because of the presence of the transmembrane region. It involved rinsing the resin successively with the Wash buffer containing 1 % Triton-X100, 6M urea, and 10% Glycerol, the Wash buffer containing 20% glycerol, and 1% Triton-X100, the Wash buffer with 1% Triton-X100, and finally the Wash buffer containing 0.1% DPC. All soluble fragments of Syntaxin-1a, SNAP-25, Synaptobrevin-2, and Complexin were eluted with the elution buffer (20mM HEPES, 500mM NaCl, 400mM imidazole, pH = 7.4). Full-length syntaxin was eluted with the elution buffer containing 0.1% DPC, and the content in each fraction was assessed by SDS polyacrylamide gel electrophoresis (Figure 26).

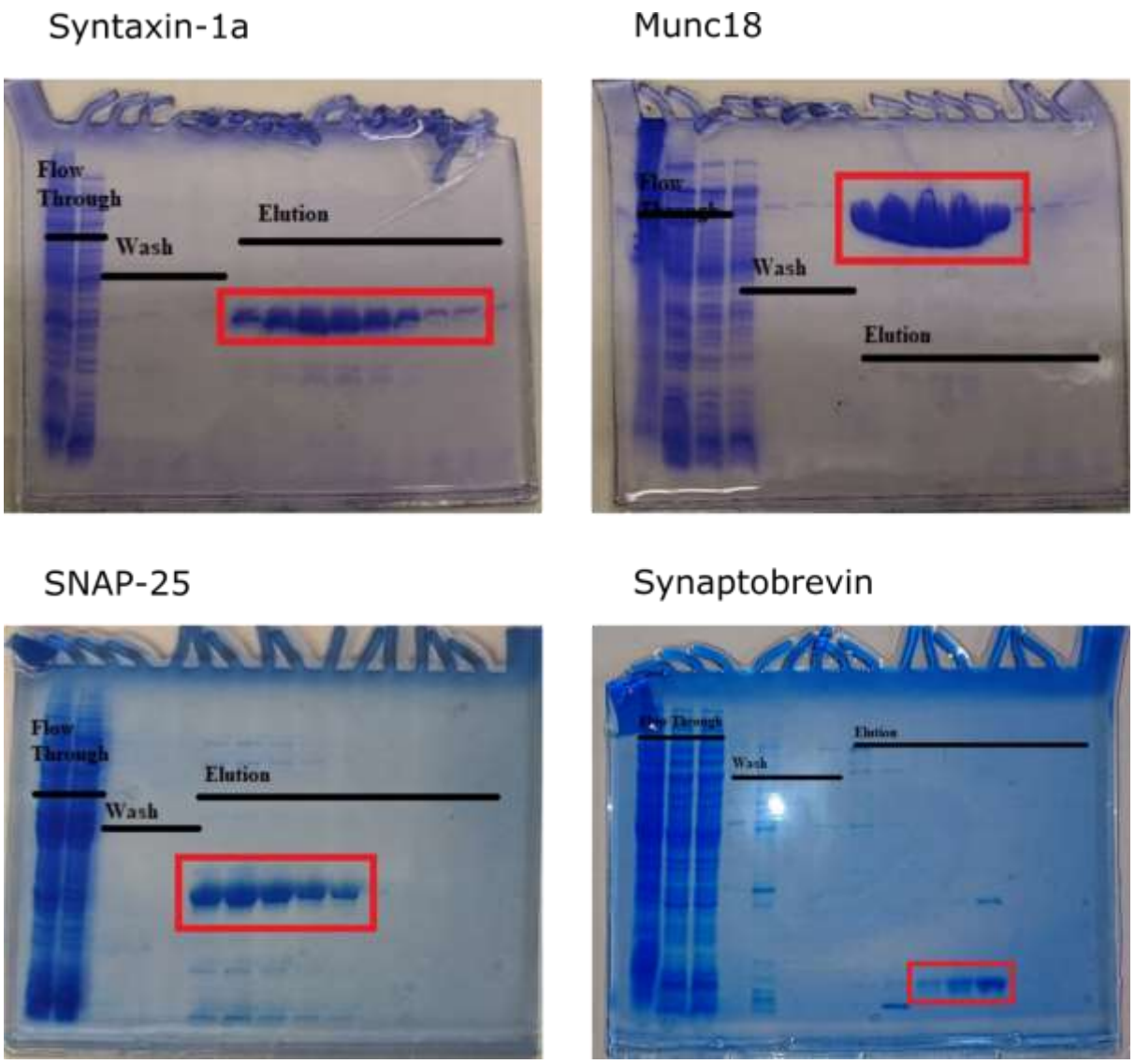


***Figure 26***. *Photographs of the typical SDS-PAGE gels (12 %) for individual proteins after purification on NiNTA agarose column. Here bands corresponding to the protein of interest are shown in the red boxes.*

Selected fractions of soluble syntaxin-1a, complexin-1, synaptobrevin-2, and SNAP25 were then combined in separate dialysis tubing with the proper molecular weight cut-off value for each protein and dialyzed against the Dialysis buffer (20mM HEPES, 200mM NaCl, 1Mm DTT, 1mM EDTA, pH = 7.4) with one buffer exchange. Before the next step, the amino-terminal His6 tag was removed by thrombin cleavage (250 µl of 5 mg/ml) during two-hour incubation at room temperature or overnight incubation in the cold room. All soluble proteins were further purified by ion-exchange chromatography on a HiTrap Q HP column or a HiTrap SP HP column using an ÄKTA Prime system with an increasing gradient of the salt buffer (20mM HEPES, 1M NaCl, pH = 7.4) (Figure 27A). Munc18-1 was purified in the same way as all soluble proteins with 10% glycerol in each buffer. Syntaxin-1a (1-288) was not dialyzed. Instead, the purest fractions were digested by thrombin (250µl of a 5mg/ml stock) at room temperature for 2 hours or in the cold room overnight. The sample was concentrated to 0.5 ml and was purified using the size exclusion column Superdex200 10/300 in the presence of 0.2% of DPC using ÄKTA Purifier systems (Figure 27B). All buffers were degassed beforehand by vacuum filtration through a 0.22 µm filter. The eluted fractions were monitored by UV absorbance at 280nm.

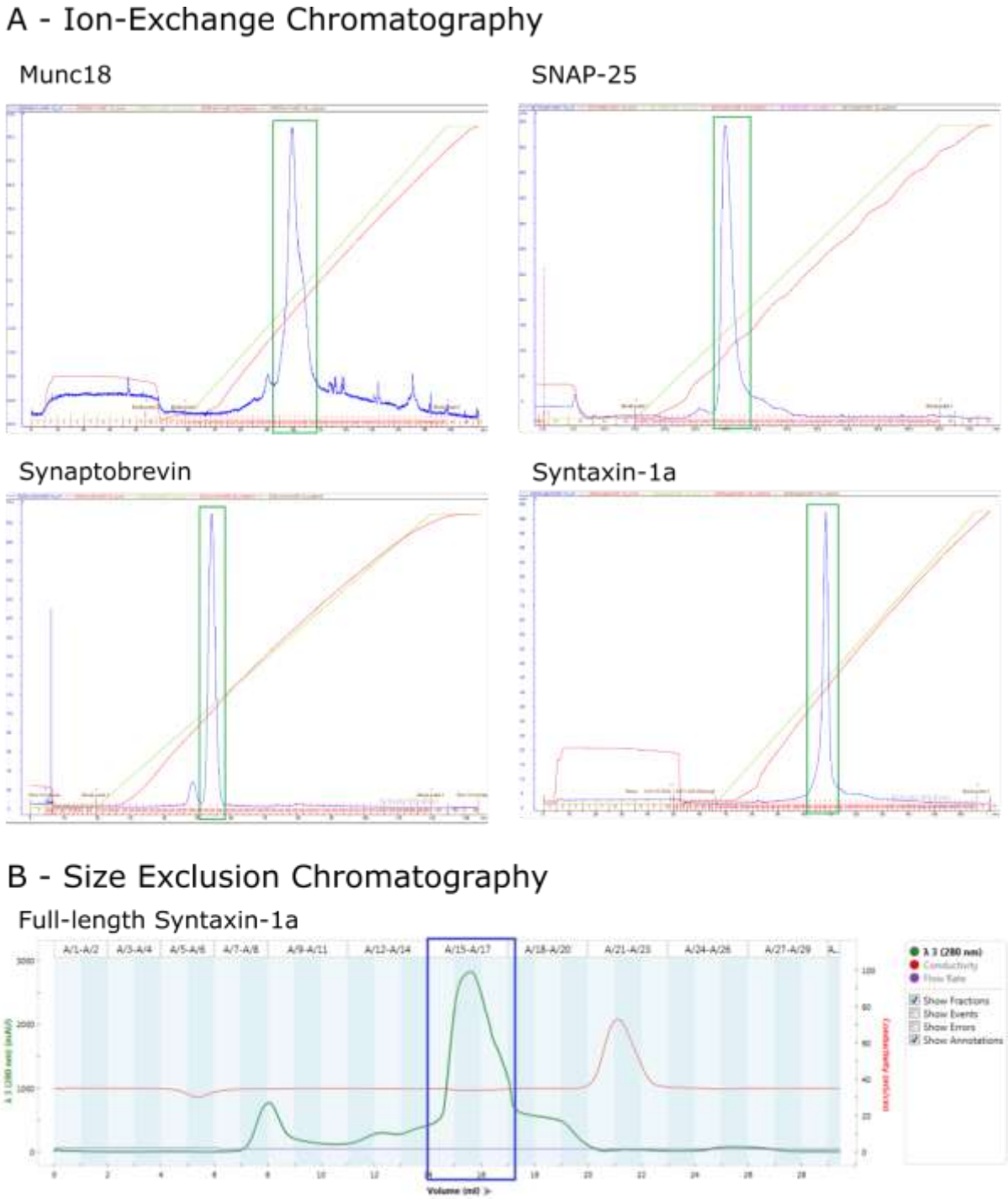


***Figure 27.*** *A. Typical chromatograms were obtained from a run on an ion-exchange column for Munc18, SNAP-25, Synaptobrevin, and a soluble fragment of Syntaxin-1a. B. The typical chromatogram was obtained by running on a size exclusion column for full-length Syntaxin-1a.*

The purity was checked with SDS polyacrylamide gel electrophoresis, followed by Coomassie staining (Figure 28). Samples containing the desired protein were mixed and concentrated in Amicon Ultra centrifugal filters by centrifugation. The protein concentration was measured by absorption at 280 nm and aliquots were flash frozen in liquid nitrogen and stored at −80°C.

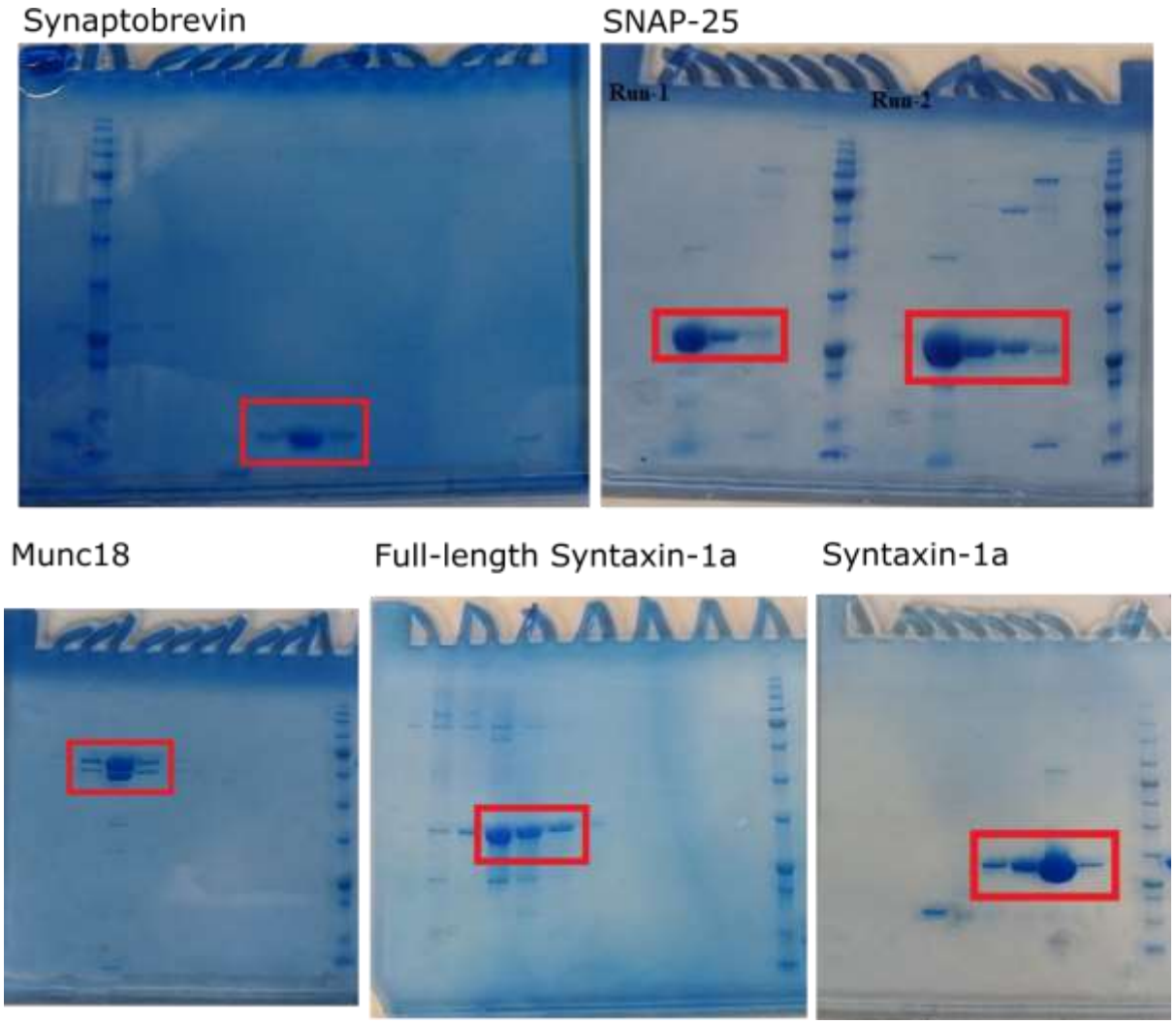


*Figure 28. Photographs of the typical SDS-PAGE gels (12 %) for individual proteins after purification on ion-exchange column (Synaptobrevin, SNAP-25, Munc18, Syntaxin-1a) and on size exclusion column (Full-length Syntaxin-1a). Here bands corresponding to the protein of interest are shown in the red boxes, samples tested on a gel had been chosen based on a chromatogram.*

### 3.2.3 Acceptor (or t-SNARE) complex assembly and purification

SNAP-25 and syntaxin-1 were mixed in a 1:1 ratio to assemble the t-SNARE complex. SNAP-25 was first combined with equal the Assembly buffer (20Mm HEPES, 150Mm NaCl, pH = 7.4) with 0.2% of DPC to make the final concentration of DPC at 0.1%. After this, an equal amount of syntaxin-1 (1-288) was added dropwise while stirring. The whole assembly was left on a rotating incubator in the cold room overnight. On the morning of the next day, the overnight assembly was diluted with two volumes of the assembly buffer with no salt to lower the salt concentration to 50mM. The acceptor complex was purified on a MonoQ 5/50 GL column in the salt gradient using the ÄKTA Purifier systems.

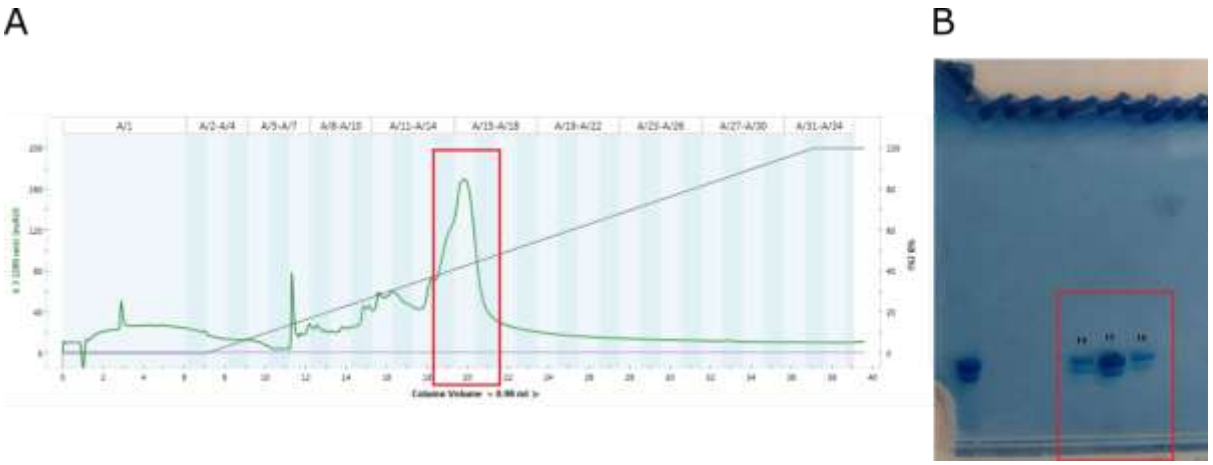


***Figure 29***. *A. The typical chromatogram is obtained from a MonoQ column run to purify the acceptor complex. B. Photograph of the typical SDS-PAGE gels (12 %) for the acceptor complex after purification on the ion-exchange column, samples tested on a gel were chosen based on a chromatogram. Peak and bands corresponding to the complex are shown in the red boxes.*

### 3.2.4 SNARE core complex assembly and purification

SNAP-25, syntaxin-1, and synaptobrevin-2 were mixed in a 1:1:1 ratio to assemble the SNARE core complex. SNAP-25 was first combined with an equal amount of synaptobrevin. The equivalent amount of the assembly buffer (20Mm HEPES, 150Mm NaCl, pH = 7.4) with 0.2% of DPC was added to the protein mixture to achieve the final concentration of DPC at 0.1% (in case of full-length syntaxin). After this, an equal amount of syntaxin-1 was added dropwise while stirring. The whole assembly was left on a rotating incubator in the cold room overnight. On the morning of the next day, sample was diluted with two volumes of the assembly buffer with no salt. This step was done to lower the salt concentration to 50mM. The SNARE complex was purified on a Mono Q 5/50 GL column in the salt gradient using the ÄKTA Purifier systems.

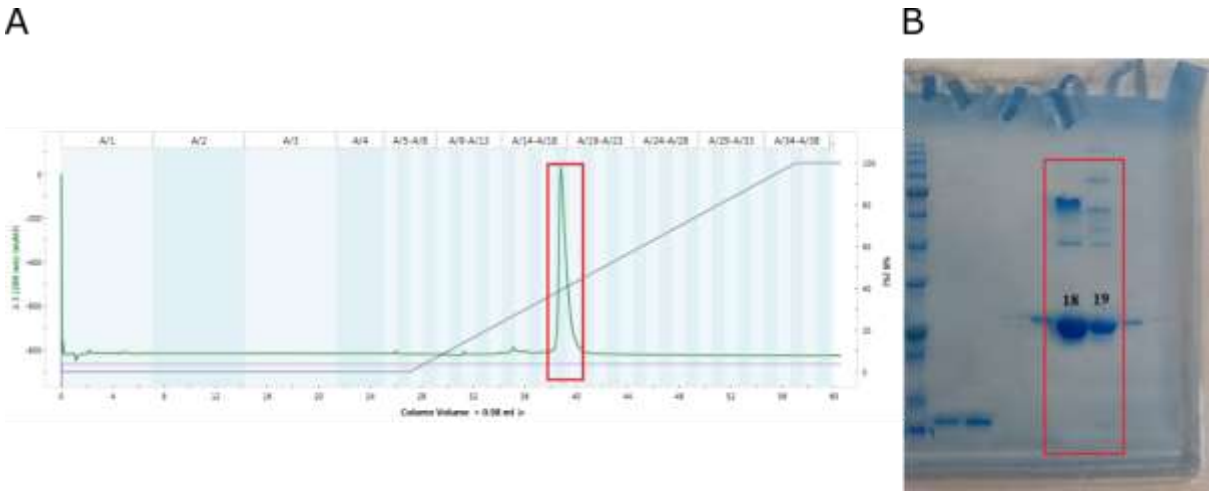


***Figure 30.*** *A. The typical chromatogram is obtained from a MonoQ column run to purify the SNARE complex. B. Photograph of the typical SDS-PAGE gels (12 %) for the SNARE complex after purification on the ion-exchange column, samples tested on a gel were chosen based on a chromatogram. Peak and bands corresponding to the complex are shown in the red boxes.*

### 3.2.5 Site-Directed Spin Labeling

All syntaxin-1a mutants were labeled with the cysteine specific spin-label – MTSL ((1-oxy-2,2,5,5-tetramethylpyrrolinyl-3methyl) methanethiosulfonate). After purification in Q-column (soluble syntaxin) or size exclusion column (full-length syntaxin), the protein sample was incubated with a 20-fold excess of DTT. After 2 hours, another 20-fold excess of DTT was added for another 2 hours. A PD10 column was used to separate unreacted DTT and activated syntaxin. Protein was eluted with the Spin label buffer (20Mm HEPES, 500Mm NaCl, 0.15% DPC, pH = 7.4) in 0.75 ml fractions. The purest fractions were collected, and 5-fold excess of MTSL was applied for 30 minutes of incubation. After this time, another 8-fold excess of MTSL was added for overnight incubation at 4ºC. On the morning of the next day, a PD10 column was used again to separate labeled protein from the free label. The protein was eluted with spin-label buffer in 0.75 ml fractions. Then each eluted fraction was checked on the NanoDrop. The eluted fractions of pure spin-labeled syntaxin were concentrated in Amicon Ultra centrifugal filters and stored at -80 ºC.

### 3.2.6 Lipid reconstitution

Lipids were mixed in chloroform according to desired composition (Table 4) in glass test tubes (13mm x 100mm). Lipids were evaporated under the vacuum in a desiccator for at least 1 hour. After the evaporation, the dried down lipids were solubilized in buffer (20Mm HEPES, 150Mm NaCl, pH = 7.4) containing 25Mm NaCl. A protein sample was added to solubilized lipids. The mixture was incubated for 60 minutes at room temperature, and then the sample was diluted with the buffer to obtain 16Mm NaCl. The sample was dialyzed in a dialyzer cassette

against the Dialysis buffer (20 Mm HEPES, 150 Mm NaCl, ph = 7.4) overnight with two buffer exchanges.

***Table 4**. Composition of lipid used in membrane reconstitution experiments*

| Name | Lipid composition |
|---|---|
| PO-PM1 | 34% PO-PC, 30% PO-PE, 15% PO-PS, 1% PIP2, 20% cholesterol |
| DO-PM1 | 34% DO-PC, 30% DO-PE, 15% DO-PS, 1% PIP2, 20% cholesterol |
| DP-PM1 | 34% DP-PC, 30% DP-PE, 15% DP-PS, 1% PIP2, 20% cholesterol |
| Brain-PM1 | 34% b-PC, 30% b-PE, 15% b-PS, 1% PIP2, 20% cholesterol |
| POPC-POPG | 80% PO-PC, 20% PO-PG |
| POPC-DOPS-DPPE | 85% POPC, 15% DOPS, 0,5% DPPE |

3.2.7 Continuous-wave Electron Paramagnetic Resonance

Measurements were performed using a 7µl sample of single or double spin-labeled syntaxin alone. They assembled into t-SNARE or SNARE complex under various conditions and with the addition of other proteins. The sample was loaded with a Hamilton syringe into the 0.6IDx0.84OD-100mm borosilicate glass capillaries that had been flame-sealed at one end before the experiment. The concentration of the spin-labeled protein was usually no lower than 25µM. Spectra were recorded on a Bruker EMX X-band EPR spectrometer at 2mW incident microwave power with a modulation amplitude of 1G and frequency of 100kHz. The magnetic field was swept through 100G, and up to 150 scans were performed to increase the signal/noise ratio. Spectra were then processed using LabVIEW programs provided by Christian Altenbach (University of California, Los Angeles, CA), normalized to enable comparison, and plotted in OriginPro 7.5 (The OriginLab Corporation) or in-house software provided by one of the labmates.

### 3.2.8 Double Electron-Electron Resonance

Pulsed EPR experiments were conducted on samples containing a single or double spin-labeled syntaxin alone. They assembled into t-SNARE or SNARE complex under various conditions and with the addition of other proteins. A 16 μL of protein sample was mixed with a 4uL of deuterated glycerol, loaded into 1.5 IDx1.8 OD-100 mm quartz capillaries, flash-frozen in liquid nitrogen, then ran at 60 K. DEER data wer collected using a dead time free four pulsed DEER sequence with an 8-10 ns $\pi/2$ pulse and 16-20 ns $\pi$ pulses. The separation between observing and pump frequencies was 75 MHz. All data were collected on a Bruker ELEXSYS E580 at Q-band with an EN5107D2 dielectric resonator. Data recorded for up to 24 hours were later analyzed using LongDistances version 771 by Christian Altenbach (University of California, Los Angeles, CA). The analyzed data were plotted using DavePlot (in-house software provided by one of the labmates) through Plotly and Dash frameworks developed by the Plotly corporation.

# IV. RESULTS

Elucidating conformational states of Syntaxin-1a requires identifying conditions under which Syntaxin-1a is in monomeric form and understanding how this condition might affect Syntaxin-1a interactions with other proteins. The Results section consists of three parts. Part 1 focuses on the effect of environment on Synaxin-1a. Part 2 describes the conformational states of Synaxin-1a during SNAREs assembly. Finally, Part 3 describes the interactions between Syntaxin-1a and two other SNARE-binding proteins, Munc18 and Complexin.

The CW-EPR and gel filtration experiments were performed at room temperature. In contrast, DEER experiments were performed at 56 K following rapid freezing from room temperature. The details of each experiment may be found in the Materials and Methods section.

## Part 1 – Environmental impact on Syntaxin-1a

### 1. DPC is affecting Syntaxin-1a in more than one way

1.1 DPC is minimizing protein aggregation

It is known that Syntaxin-1a tends to oligomerize when its concentration is higher than 2 μM[83,84]. However, there are also reports that the addition of the detergent DPC (dodecylphosphocholine) during syntaxin purification or even addition to the final sample places syntaxin in a monomeric state[227] (personal communication with Dr. Binyong Linag). I decided to test how solution environment, especially DPC, determines oligomerization first. Three different Syntaxin-1a constructs were examined to confirm that the presence of DPC leads to the monomeric state of Syntaxin-1a. The tested constructs were: H3 Syx (189-262) – this construct contains only the H3 domain of syntaxin-1a; Syx (1-262) – this construct contains both Habc and H3 domains but lacks a transmembrane domain; it is often referred to as soluble fragment; FL Syx (1-228) – this construct contains all three domains and is the full-length

protein. Each construct contains a single-point cysteine mutation to allow attachment of MTSSL spin-label: H3 Syx 242R1, Syx 240R1, and FL Syx 228R1. For the construct lacking the transmembrane domain, measurements were performed in the assembly buffer, containing 0.1% of DPC.

Measurements of the full-length construct were made using the protein reconstituted into lipid bilayers and suspended in an assembly buffer containing 0.1% of DPC. As is shown in Figure 24, the presence of DPC decreases protein aggregation, but does not completely eliminate it. The top panel shows the dipolar interaction data obtain from DEER experiments. Since these single labeled Syntaxin-1a mutants only contain one label; any dipolar interaction that is observed must arise from an interaction between two (or more) Syntaxin-1a molecules. The top panel in Figure 31 shows dipolar interaction in the presence of DPC (green) and the absence of DPC (grey). It is clear that DPC is decreasing the amplitude of the dipolar signal and hence protein aggregation, but it is not eliminating it. The best results were obtained with the soluble construct (Figure 24, Syx 240R1), where the signal in the presence of DPC is close to the expected intermolecular background.

When Syntaxin-1a was reconstituted into DPC micelles, the protein aggregation was insignificant in the full-length construct. On the other hand, in the case of the H3 construct, DPC had a much smaller effect on Syntaxin-1a aggregation, leaving a significant amount of aggregated protein in the sample. However, the present work focuses on the soluble construct containing Habc and H3 domain and the full-length construct, and in both these cases the reduction in the aggregation provided by the addition of DPC was satisfactory to allow a study of Syntain-1a. Syntaxin-1a in the membrane associated state is known to form clusters[86,87,88] and DEER data were obtained confirming protein aggregation in the membrane (Figure 31, FL Syx 228R1). Section 2 of this chapter presents a more detailed look at the protein behavior on the membrane and its dependence on the membrane composition. The bottom panels in

Figure 31 show the EPR lineshapes that were obtained, corresponding to DEER measurements in the top panels. The fact the lineshapes of each construct are different in the DPC buffer compared to the buffer without DPC suggests that DPC is not only minimizing aggregation, but is also affecting the local protein structure at the labeled site.

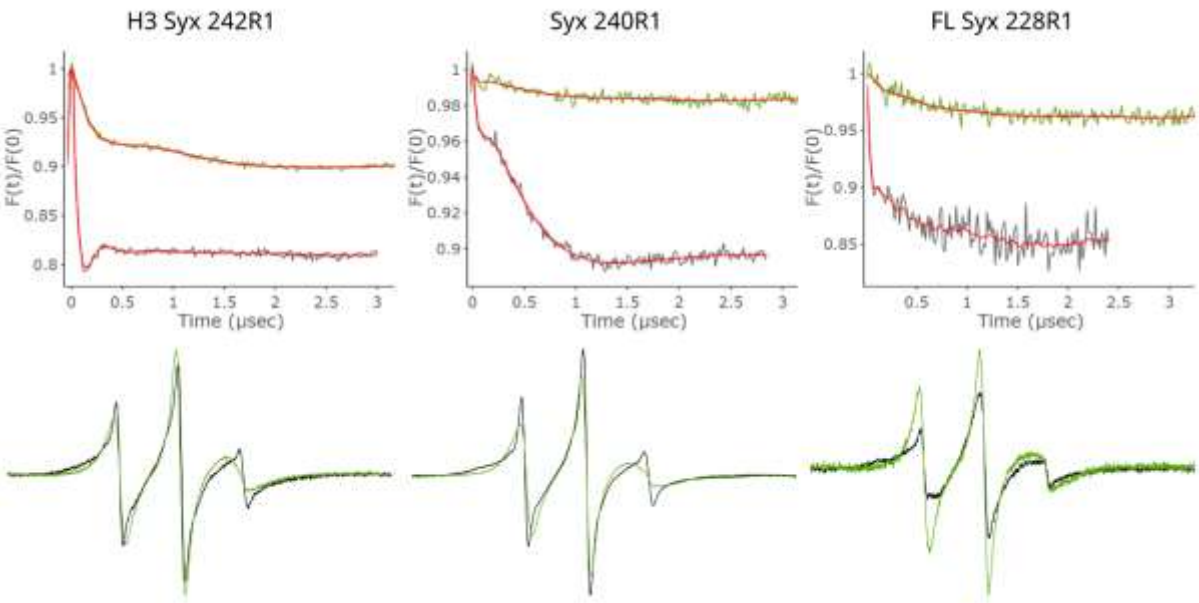


***Figure 31.*** *The DEER data collected on three different single-labeled Syntaxin-1a constructs: H3 Syx 242R, Syx 240R and FL Syx228R. For soluble constructs measurements were performed in buffer (grey) and in the presence of DPC micelles (green), for full length construct measurements we performed on the membrane (grey) and in the presence of DPC micelles (green). Top panel presents DEER dipolar data and the bottom panel corresponding CW's lineshapes.*

1.2 DPC (and SDS) is inducing helical structure after reaching CMC

During these experiments, where DPC was observed to reduce the aggregation of Syntaxin-1a, DPC was found to change the shapes of the EPR spectra. It is a known fact that anionic detergents like Sodium Dodecyl Sulfate or SDS may induce a helical structure in the protein[228,229,230,231]. To test this, EPR spectra of Syntaxin-1a were obtained with SDS and with DPC to compare two changes introduced into the structure by the two detergents. The EPR spectra, which reflect the local protein structure were the same in both cases. To investigate this further, a titration with detergent was performed to determine whether the changes in the EPR spectra were related to the CMC (Critical Micellization Concentration). Using the Syx (1-262) construct with a label at site 228, the DPC concentration was increased in the Syntaxin-1a sample until no further changes in the EPR spectra were observed. This occurred at the exact point of the CMC, indicating that the formation of helical structure in at the spin labeled site (site 228) was dependent on the DPC concentration (Figure 32).

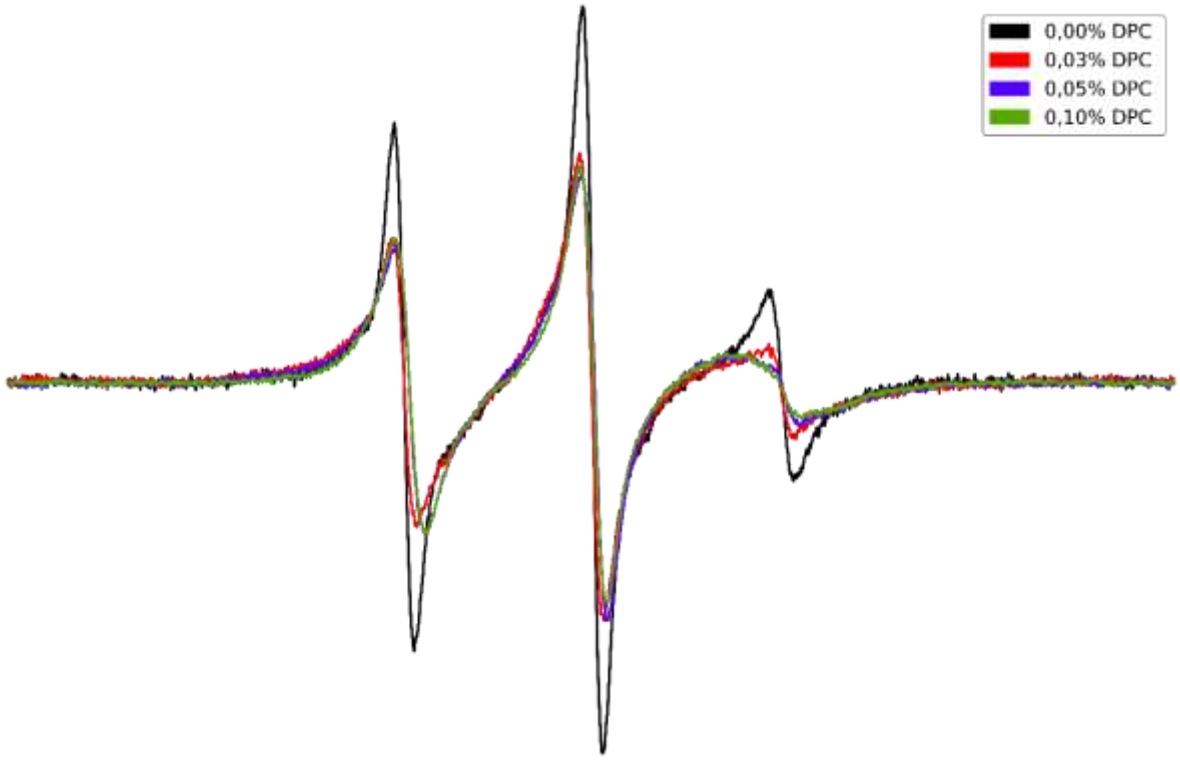


***Figure 32.*** *DPC titration into Syx 228R1.*

The induction of helical structure in Syntaxin-1a takes place only in those parts of the protein that are known to assume a helical structure at some point during SNARE assembly. The H3 domain of Syntaxin-1a is generally unstructured, but when bound to other proteins, i.e., Munc18 or other SNARE binding partners, it becomes helical. Cysteines and spin labels were introduced into the soluble Syntaxin-1a construct containing both Habc and H3 domains at the sties shown in Figure 33. These labels were examined in the presence of DPC and the resulting CW EPR spectra are shown Figure 34.

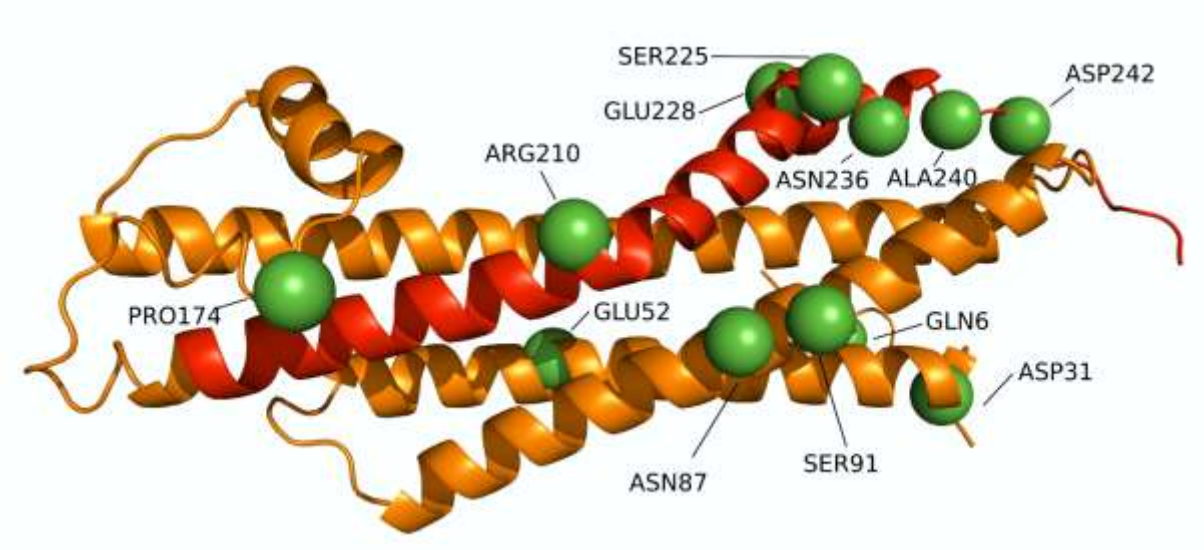


***Figure 33.*** *Graphic representation of tested mutation in Syntaxin-1a. The Syntaxin-1a model comes from the X-ray structure of Syntaxin-1a-Munc18 complex (PDB ID 3C98).*

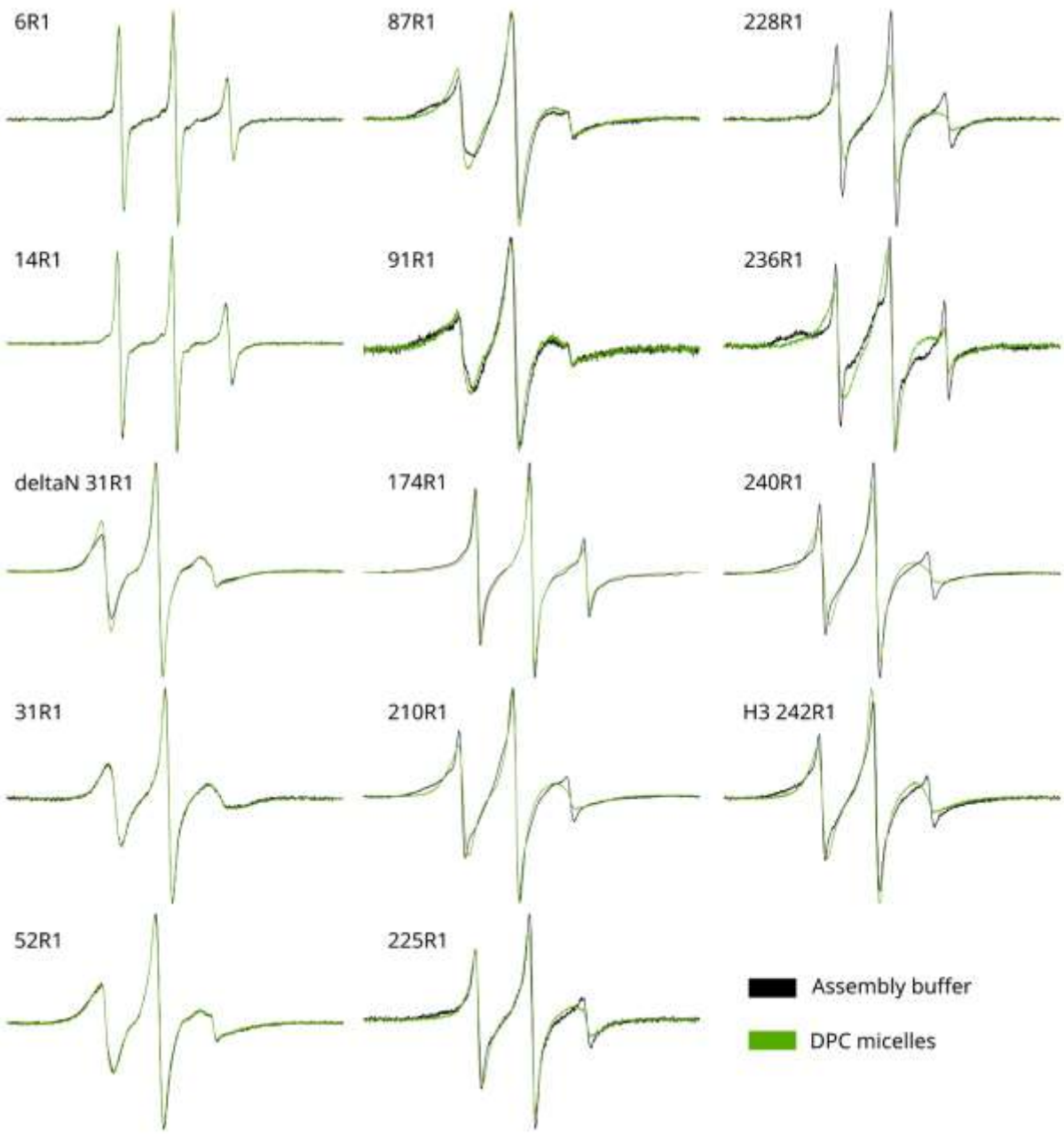


***Figure 34.*** *CW-EPR spectra for the corresponding mutants of Syntaxin-1a in the buffer (black) and in the presence of DPC micelles (green).*

1.3 DPC shifts equilibrium between the open and closed state of Syntaxin-1a towards open state

As it was already mentioned in the introduction part, Syntaxin-1a has two domains, a SNARE forming H3 domain and a regulatory Habc domain. When these domains are interacting, Syntaxin-1a is in a closed conformation. When they are dissociated from each other, Syntaxin-1a is in an open conformation. The open and closed conformations are in a dynamic equilibrium, and reports regarding which state dominates are not in agreement. Moreover, a specific mutation in the linker between Habc and H3 domains, called the LE mutation, is reported to lock Syntaxin-1a in the open state. I conducted preliminary experiments on the set of double mutants of the soluble construct of Syntaxin-1a, where I introduced one mutation into the Habc domain and the second into the H3 domain to study the distance between these two domains. Tested mutants were: Syx 31/240, Syx 52/210, Syx 105/216, Syx105/254, Syx 151/196, Syx 162/210, Syx LE 52/210, and ΔN Syx 52/210. Syx LE is a soluble construct of Syntaxin-1a with the LE mutation introduced into it to favor the open state of Syntaxin-1a, and ΔN is a soluble construct of Syntaxin-1a where the first 27 residues of the N-terminal region (referred to as N-peptide) have been deleted. From the previous work, a useful label pair tested in our laboratory was the 52/210 mutation. Because of that, I focused the rest of my research on this mutation. Knowing the addition of DPC was reducing the aggregation significantly, I wanted to determine whether DPC impacts the Syntaxin-1a conformation. I collected data on the three soluble variants of Syntaxin-1a: Syx 52/210, Syx LE 52/210, and ΔN Syx 52/210 in the regular assembly buffer and in the buffer with DPC addition above its CMC. In the case of measurements taken in the standard assembly buffer (Figure 35, grey traces), results indicated that Syntaxin-1a sampled open (the distance around 6nm) and closed state (the distance around 3 nm). The closed state was strongly favored as observed previously[105,130]. The two

states were also present in the LE mutant, and the equilibrium between the open and close conformation was shifted towards the open state. The addition of DPC to the protein sample shifted Syntaxin-1a towards the open conformation in each case.

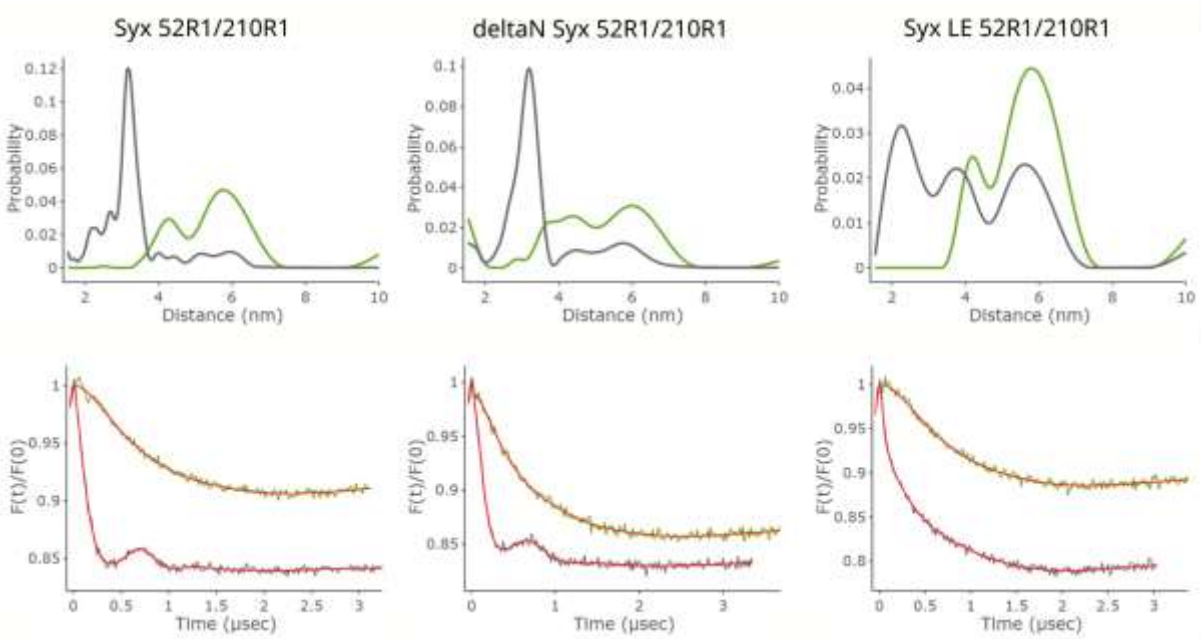


***Figure 35.*** *The DEER data collected on three different double-labeled soluble Syntaxin-1a constructs: Syx 1-262, ΔN Syx 27-262, SyxLE 1-262 165 166. All three constructs were labeled at positions 52 (Habc domain) and 210 (H3 domain). Measurements were performed in buffer (grey) and in the presence of DPC micelles (green). The top panel presents DEER distance distribution, and the bottom panel shows dipolar data.*

1.4 DPC addition affects binding affinity between Syntaxin-1a and Munc18

Munc18 binds to Syntaxin-1a with a high affinity and -upon binding- stabilizes Syntaxin-1a closed conformation. It has been proposed that LE mutation has little to no effect on the Munc18a–Syx1a binding mode[106]. Knowing that both the LE mutation and DPC shift Syntaxin-1a towards the open conformation, I decided to examine how Munc18 will act on the LE Syntaxin mutant in the presence of DPC. In the first step, I recorded a DEER spectrum on Syx LE 52/210 alone and equal molar addition of Munc18 in the assembly buffer. I observed total closure of Syntaxin-1a (Figure 36, top panel). In the next step, I performed a series of DEER measurements in the presence of DPC. The binding between Syntaxin-1a and Munc18 in the presence of DPC is weaker. Even 3-time excess of Mun18 did not result in full Syntaxin-1a closure.

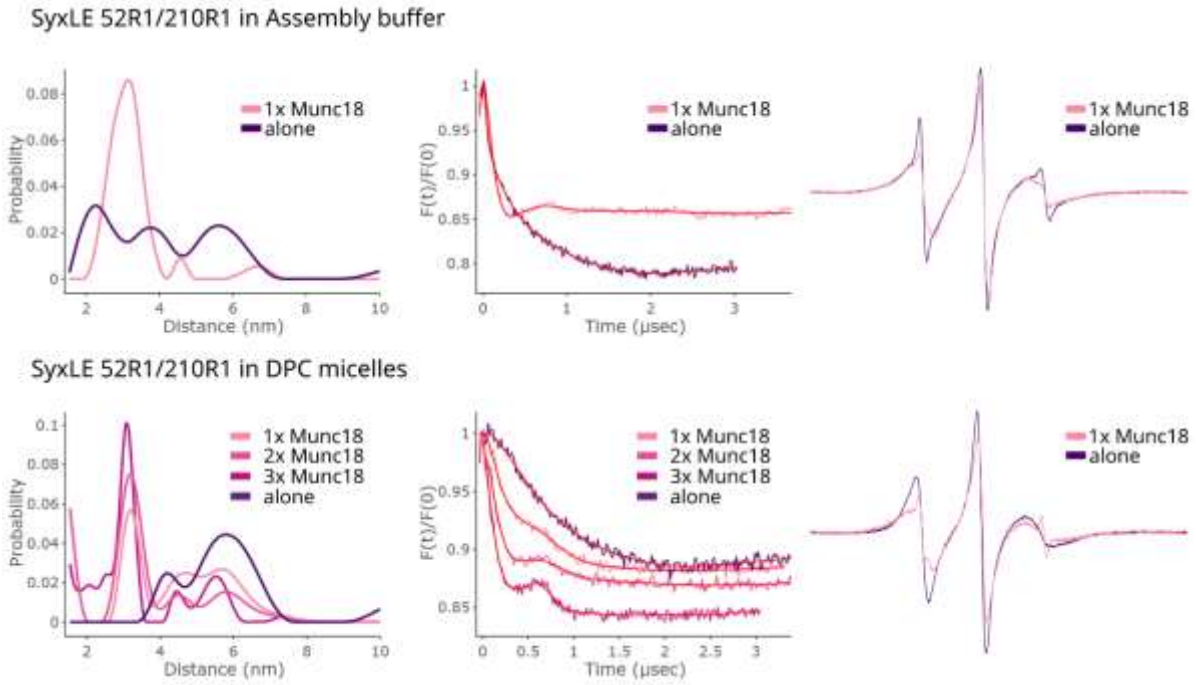


***Figure 36.*** *DEER data (DEER distance distribution, and the dipolar data) collected double-labeled soluble Syntaxin-1a constructs: SyxLE 52R1/210R1 in assembly buffer (top panel) and in DPC micelles (bottom panel) with the addition of Munc18.*

## 2. The buffer used to obtain crystal structure locks Syntaxin-1a in a different state than the physiological buffer.

During preliminary research exploring the effects of DPC on Syntaxin and Munc18 – Syntaxin-1a binding, I found that the Syntaxin-1a conformation obtained in the physiological buffer was different than expected based on the Syntaxin-1a - Munc18 crystal structure. I recorded CW spectra for Syx 87R1 and 97R1 in two buffer conditions (physiological and crystallization) and with and without equal molar addition of Munc18. As can be seen in Figure 37, I obtained different lineshapes for both buffer conditions. Under physiological conditions, clear evidence for tertiary contact of the spin labeled side chain, particularly at position 87, could be seen. The additional feature on the low-field resonance is due to incomplete averaging of Azz, which is known to occur when the label is not free to rotate. These spectra indicate an interaction between sites 87 and 91 on Syntaxin-1a with either Munc18 or another Syntaxin, while there was little sign of a strong interaction under crystallization conditions.

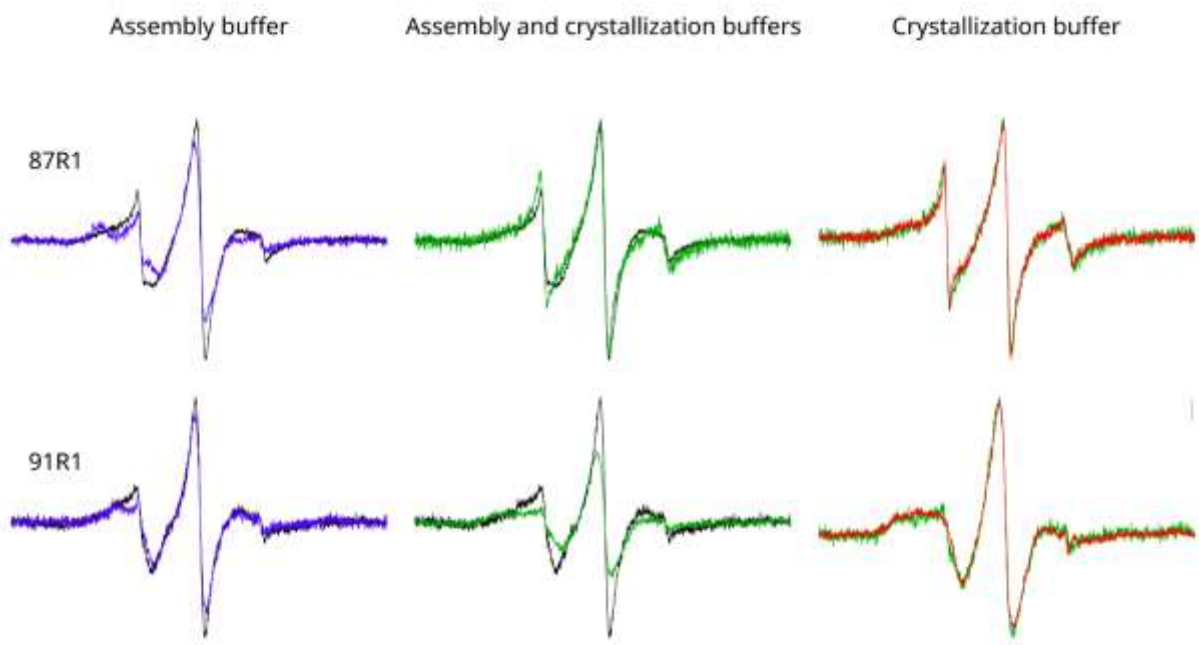


***Figure 37.*** *CW lineshapes of single cysteine mutants of soluble Syntaxin1-a in the assembly buffer (black) and the crystallization buffer (green), isolated and with the addition of Munc18 (in the assembly buffer – blue, in the crystallization buffer – red).*

I checked whether Syntaxin-1a – Munc18 complex could form a dimer or other higher organization structure with PISA[232]. As a result, I obtained that, another attainable and physiologically relevant structure is a dimer. Figure 38 presents a Syntaxin-1a – Munc18 complex dimer alongside both tested mutations. Even in dimer formation, both positions face outwards, and there is no interaction with Munc18. Possible dimer formation is not an explanation for different CW results.

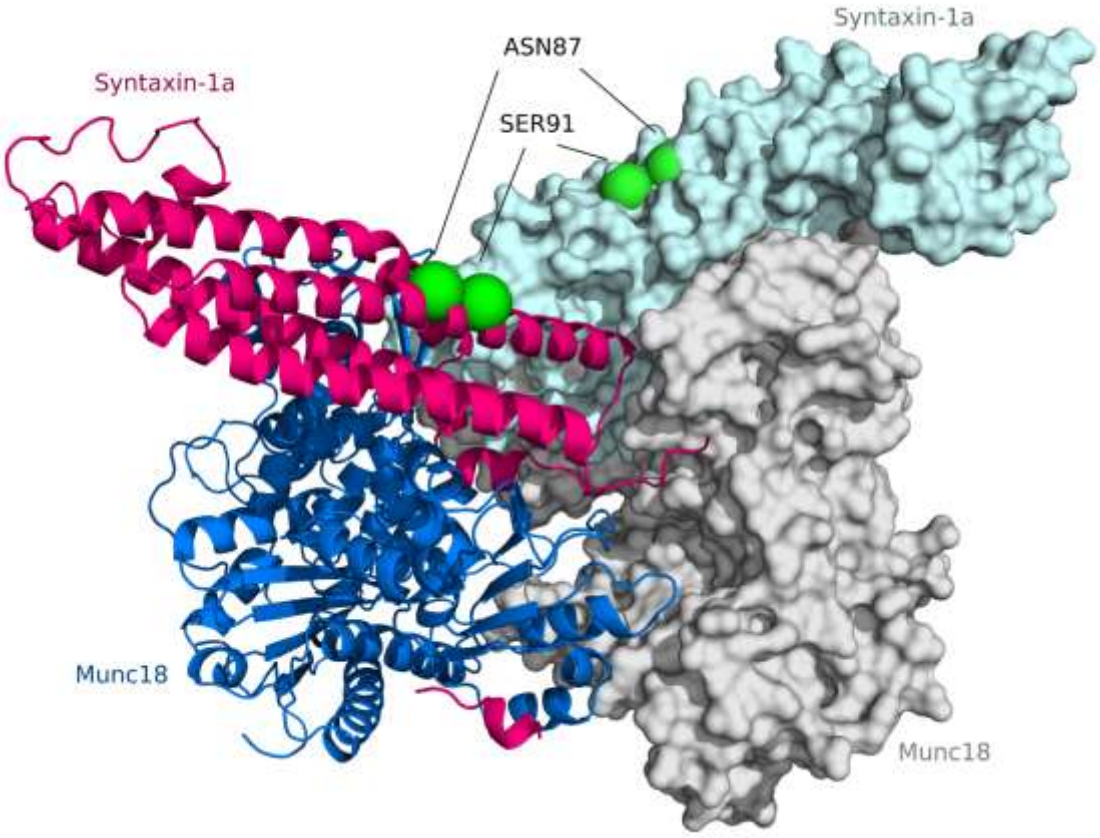


***Figure 38.*** *Possible dimer as predicted for PDB ID 3C98 by PISA*

In the second approach, I studied the *Chaetomium thermophilum* homolog structure of Syntaxin-1a-Munc18, Vps45–Tlg2 complex[233].

Munc18 binds to Syntaxin-1a tightly with nanomolar affinity[107]. The X-ray structures of a complex of the two proteins revealed that Munc18 interacts with the entire length of Syntaxin-1a's cytoplasmic domain[102] (Figure 39, PDB ID 3C98). The Syntaxin-1a interacts with Munc18 through its N-peptide, Habc domain, and H3 domain. Upon binding H3 domain interacts with both Munc18 and Habc domain. As a consequence, Munc18 inhibits SNARE assembly *in vitro*. Still, at the same time, the formation of the Munc18-Syntaxin-1a complex is considered essential for Syntaxin-1a trafficking to the membrane - a possible physiologically relevant starting point for SNARE complex assembly. The general idea that SM proteins interact with Qa-SNARE proteins and produce a closed conformation of Qa-SNARE has been confirmed in many cases with a couple of exceptions. Homologous structures lacking some part of Qa-SNARE protein and thus not fully supporting the closure idea are Sly-Sed5 which contains only N-peptide of Qa-SNARE, and Vsp33-Vam3, which has only H3 motif of Vam3. However, the recently resolved X-ray structure of Tlg2 (Qa-SNARE) bound to Vps45 (SM protein) contains almost complete Qa-SNARE (Figure 32, PDB ID 6XM1). Interestingly, Vps45 interacts with the same region of Qa-SNARE protein as Munc18, but it seems that the bound SNARE stays much more open than Syntaxin-1a. The main difference is in the interactions between Qa-SNARE's domain. In the case of Syntaxin-1a, H3 and Habc interact with each other, but in the case of Tlg2, the interaction between H3 and Habc is distanced. The H3 domain of Tlg2, similarly to the Syntaxin-1a H3 domain, is prone to oligomerization and the formation of tetramers. SM-bound Qa-SNAREs can adopt at least two conformations, one closed and one open, partially or more.

The existence of another binding model can explain the data I obtained for Syx 87 and Syx 91 mutants. In Syntaxin-1a – Munc18 bound structure, both residues face outwards but in the case

of Tlg2 – Vps45 bound structure. Both residues face inwards and this correlates to the CW data I obtained. I superpose both crystal structures using PyMol to show the main differences (Figure 39).

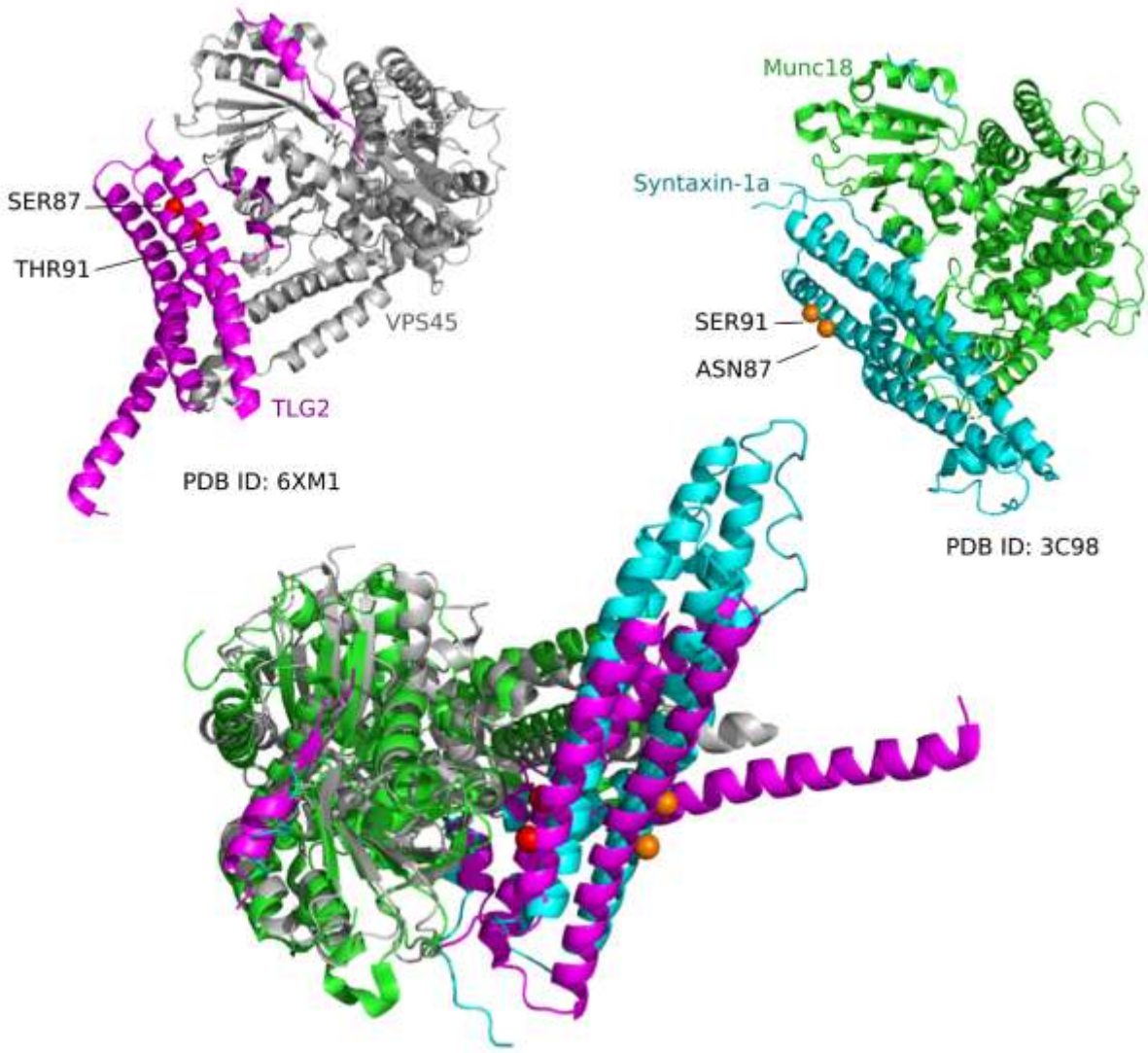


***Figure 39.*** *Crystal structures of Munc18 bound to Syntaxin (PDB ID3C98 rat structure – top, right corner) and Chaetomium thermophilum homolog (PDB ID 6XM1 – top, left corner), both Rattus norvegicus and Chaetomium thermophilum structure overlayed – bottom.*

## 3. Syntaxin-1a aggregation on the membrane depends on the lipid composition.

Syntaxin-1a molecules form aggregates that are 50 to 60 nm in diameter on the plasma membrane, and each aggregate contains about 90 molecules suggesting dense packing. The cluster's center is more tightly packed, and the density gradually decreases from the center to the periphery. Syntaxin-1a aggregation on the membrane may happen through two separate mechanisms. The first mechanism is driven by protein-protein interactions. The second driven by protein-lipid interactions, called 'lipid-mediated pre-clustering.' This mechanism is based on the ionic interactions between the polybasic linker region and lipids in the plasma membrane, especially PIP2. In addition to PIP2, cholesterol was reported to be active in Syntaxin-1a cluster formation. Moreover, different lipid compositions in the plasma membrane were reported to modulate the position of the SNARE complex towards the lipid bilayer[187]. It was in details described in the introduction section of this dissertation.

I reconstituted FL Syx228R into different lipid bilayers composed of different lipid mixtures: PO-PM1, DP-PM1, DO-PM1, brain-PM1, POPC-POPG, POPC-DOPS-DPPE, brain(PC-PS-PE), brain(PC-PS-PE) + cholesterol, and brain(PC-PS-PE) +PIP2. I used a full-length Syntaxin-1a in DPC micelles as a control experiment, which displayed the least aggregation. I prepared all samples from the same protein and lipid stocks to reduce the error from different labeling efficiency or variability of protein stocks. A single spin-labeled mutant was used in a DEER experiment to monitor aggregation, and any dipolar signal under these conditions arises from the interactions between other spin labeled Syntaxin. These experiments were used to identify the lipid composition having the lowest level of aggregation, which was used for further measurements. I observed that the lipid mixture, lipid acyl chain saturation, and head group composition are all essential factors in driving Syntaxin-1a aggregation in membranes.

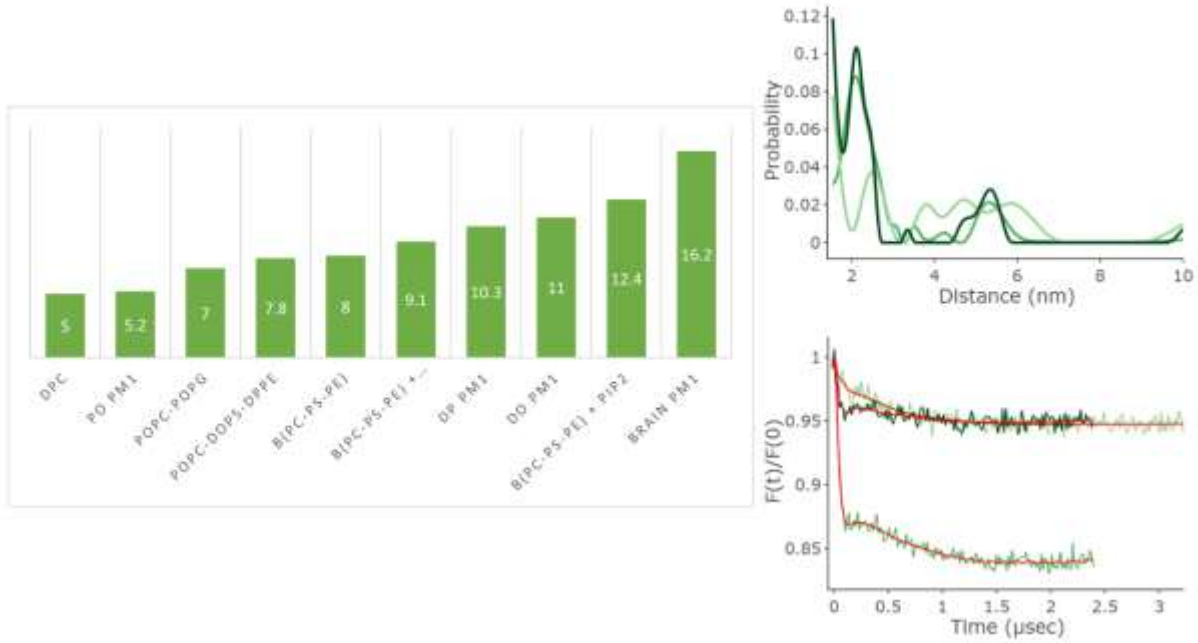


***Figure 40.*** *The DEER data collected on the full-length construct of Syntaxin-1a – FL Syx 228R. On the left bar graph is a representation of the dipolar data from all tested conditions. The numbers represent modulation depths (reference), which is the amplitude of the dipolar signal relative to the amplitude of the spin-echo in the DEER experiment. On the right side of the figure (top) are shown DEER distance distributions for the most extreme conditions. The corresponding dipolar data are shown on the bottom.*

As an extension of the above experiments, I decided to determine how the protein-to-lipid ratio modulates Syntaxin-1a aggregation. I reconstituted Syntaxin-1a into two different lipid compositions, and I chose one composition displaying the lowest state of aggregation, and one displaying the most significant aggregation. I tested both compositions at protein to lipid ratios of 1 to 300 and 1 to 1000. In both compositions, the higher protein to lipid ratio (1:1000) displayed greater aggregation than in the lower ratio (1 to 300).

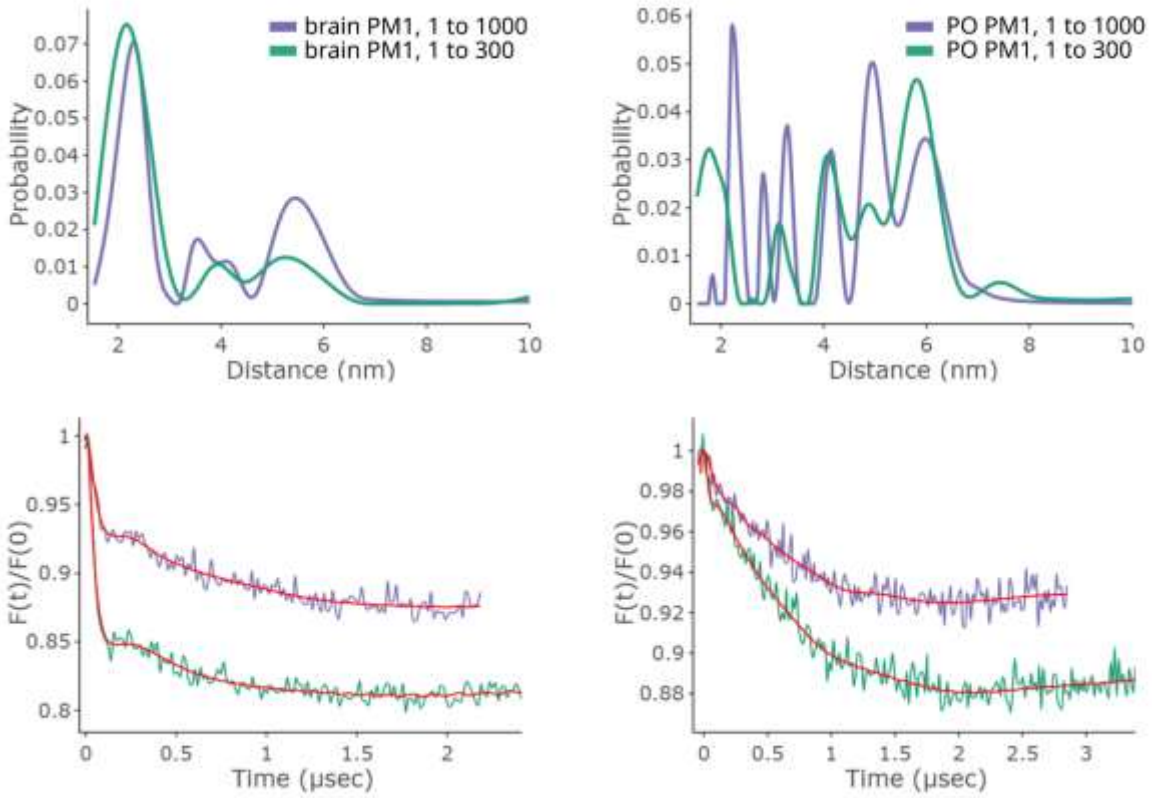


***Figure 41.*** *The DEER data (top: DEER distance distribution, bottom: the dipolar data) collected on the full-length construct of Syntaxin-1a FL Syx228R reconstituted into brain PM1 lipid mixture in protein to lipid ratio 1 to 300 (green) and 1 to 1000 (blue) on the left. On the right side of the figure, the DEER data collected on the full-length construct of Syntaxin (1-288) double-labeled on positions 52 and 210 (FL Syx52R/210R) reconstituted into PO PM1 lipid mixture in protein to lipid ratio 1 to 300 (green) and 1 to 1000 (blue).*

## 4. Screening to find conditions with minimized aggregation (Syntaxin-1a and SNARE complex)

The assembled SNARE complex has been observed to undergo oligomerizing[80,85,139], although neither the exact size of these oligomers nor the mechanism of oligomer formation are not fully known. Before examining the Syntaxin-1a structure and its role in directing the steps of SNAREs assembly, I decided to test a screen a set of conditions to determine which one might be best at reducing the aggregation of the SNARE complex. I used the SNARE complex with a single label in Syntaxin-1a (Syx 240R1) to screen for these conditions. The results indicate that the best condition is the same as that found for Syntaxin-1a, which is the case where the SNAREs are present in DPC micelles. I also observed different CW lineshapes for other buffer conditions, which suggest that there is a dependence of the state of the SNAREs on environment.

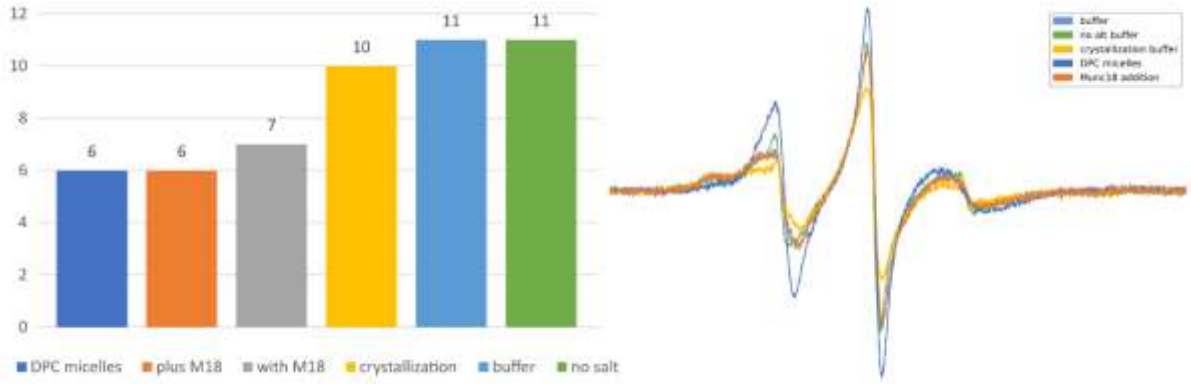


***Figure 42.*** *The DEER and CW data collected from soluble SNARE complex with the soluble construct of Syntaxin-1a Syx 240R under various conditions. On the left bar graph is a representation of the dipolar data from all tested conditions and on the right corresponding CW lineshapes.*

## Part 2 – Elucidating conformational states of Syntaxin-1a alone and assembled into t-SNARE and SNARE complex

### 1. Continuous-wave EPR measurements on Syntaxin-1a mutant proteins alone and assembled into a SNARE complex

Purified Syntaxin-1a mutants were spin-labeled with MTSL and analyzed using continuous-wave EPR spectroscopy. Single labeled Syntaxin-1a mutants were assembled into the SNARE complex, purified on the monoQ column, and CW-EPR spectra were recorded. Figure 43 presented the superposition of spectra for each spin-labeled Syntaxin-1a mutant alone and assembled into the SNARE complex.

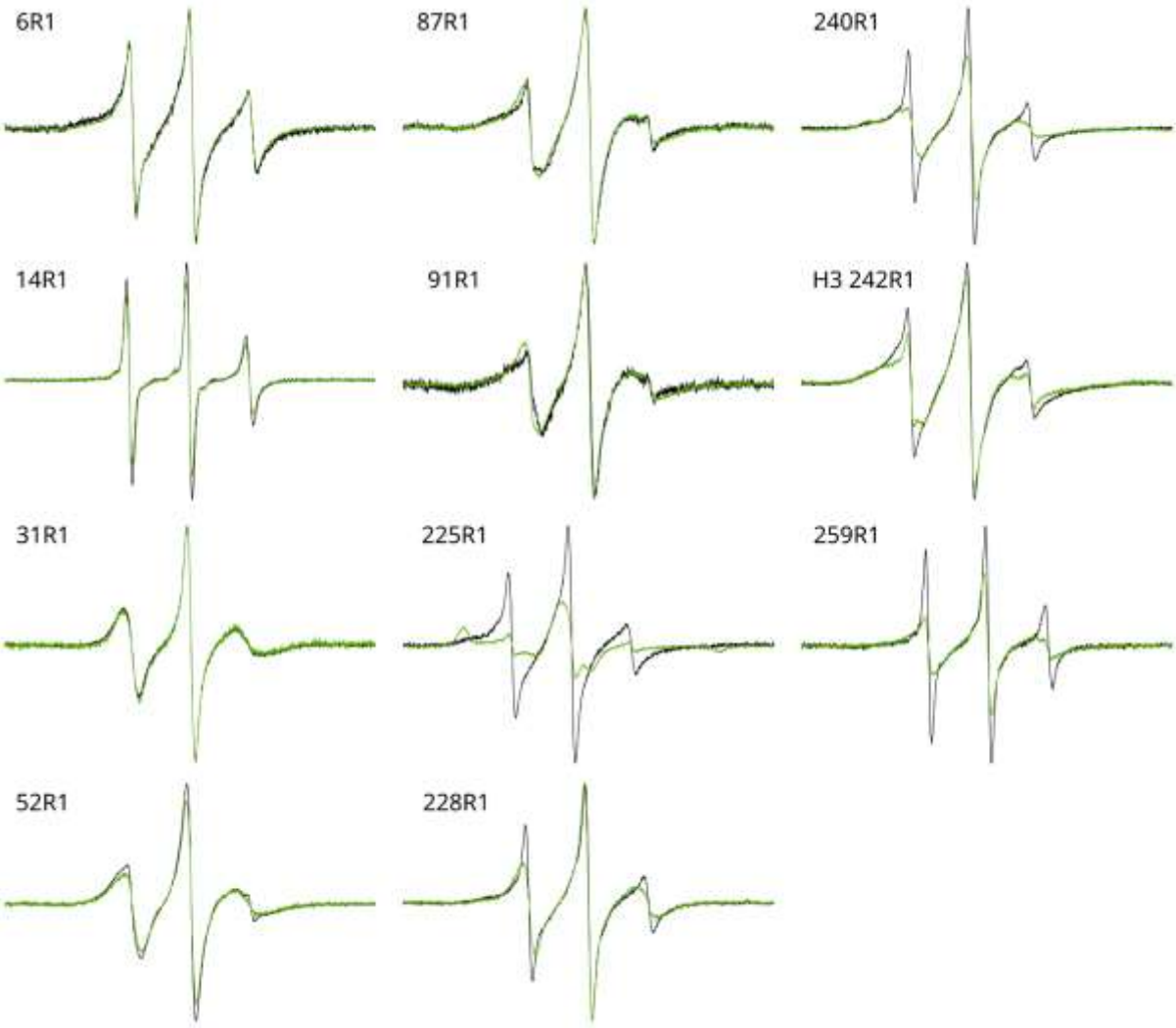


***Figure 43**. CW-EPR spectra for soluble mutants of Syntaxin-1a alone or assembled into a SNARE complex. Spectra recorded for samples composed of Syntaxin-1a alone are shown in black, while green traces correspond assembled SNARE complex samples.*

In each case, spin-labeling Syntaxin-1a yielded spectra having an excellent signal-to-noise ratio. The EPR lineshapes provide information about the behavior of Syntaxin-1a in solution, and they are consistent with previous reports[105,112,234]. Studies of spectral lineshapes of SNARE complex samples provide information regarding Syntaxin-1a behavior upon assembly, which in most cases confirms earlier findings that the H3 domain becomes structured upon assembly, and there is no change to the Habc domain. Surprising results were obtained for two sites in the Habc domain (Syx 87R and Syx 91R), suggesting that part of the Habc domain is affected by SNARE complex formation.

## 2. Equilibrium between an open and close state of Syntaxin-1a is shifted toward an open state for membrane reconstituted Syntaxin-1a

Going back to what was mentioned in the introduction part, there is a dynamic equilibrium between an open conformation of Syntaxin-1a where H3 and Habc domains are separated and a closed conformation where H3 and Habc domains interact. There is no clear information on which conformation is predominant. Moreover, the particular mutation in the linker between Habc and H3 domains, called LE mutation, was reported to lock soluble fragments of Syntaxin-1a in the open state. I demonstrated above that the addition of the detergent DPC opens Syntaxin-1a. Here I tested and compared our different Syntaxin-1a constructs, each labeled in two positions, 52 on the Habc domain and 210 on the H3 domain. I used soluble Syntaxin-1a fragment Syx (1-262), soluble Syntaxin-1a fragment lacking N-peptide domain ΔSyx (27-262), soluble Syntaxin-1a fragment bearing LE mutation Syx LE (1-262), and full-length Syntaxin-1a construct FL Syx (1-288). I collected the data for all soluble Syntaxin-1a fragments in the buffer and the full-length Syntaxin-1a sample was reconstituted into PO-PM1 lipid vesicles. For soluble fragments, except LE mutant, equilibrium between two Syntaxin-1a states is shifted

towards a closed state (as described above). Data obtained for LE mutant is consistent with those described above and reported previously[106] where Syntaxin-1a in an open state. In the case of full-length Syntaxin-1a reconstituted into a lipid bilayer, the equilibrium is shifted toward an open state (distance distribution around 6 nm) with a tiny population of a closed state (distance distribution around 3 nm). The shorter distance seen in the distribution (smaller than 2 nm) in the full-length protein sample corresponds to the formation of Syntaxin-1a aggregates in the form of dimers, as described previously[105].

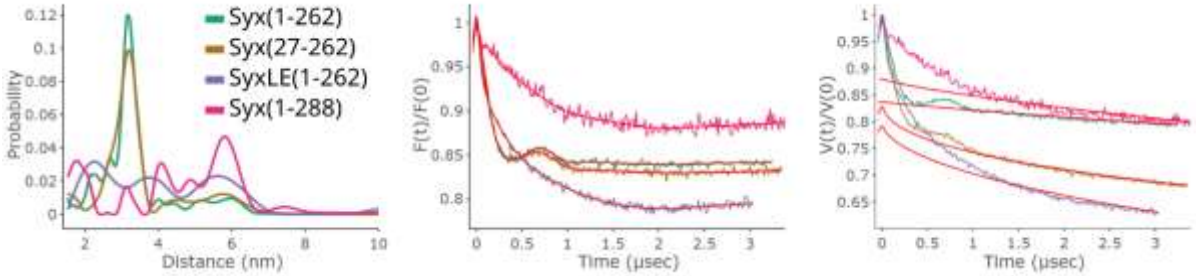


***Figure 44.*** *DEER data collected on four different double-labeled Syntaxin-1a constructs: Syx 1-262 (green), ΔN Syx 27-262 (brown), SyxLE 1-262 165 166 (blue) and FL Syx 1-288 (magenta). All three constructs were labeled at position 52 (Habc domain) and 210 (H3 domain). Measurements were performed in buffer (for soluble constructs) and full-length construct was reconstituted into PO-PM1 lipid vesicles.*

## 3. Syntaxin-1a opens up upon assembly into t-SNARE or SNARE complex

Most of the work done on the t-SNARE and SNARE complex includes only a short construct of Syntaxin-1a, which contains only the H3 domain (for work performed in solution) or H3 and transmembrane domains (for work performed in the presence of lipid bilayer). The main reason is that the Habc domain is not involved in any of the complex's formation and might inhibit assembly by putting Syntaxin-1a in a closed conformation. Since Syntaxin-1a needs to be open to form either acceptor or core complex, it is hypothesized that Syntaxin-1a stays open in those complexes after assembly. I decided to test that hypothesis by performing DEER measurements on various Syntaxin-1a constructs by attaching the R1 spin-label to the H3 and Habc domains when it is assembled into the t-SNARE and SNARE complex. I used Syx 52R1/210R1, ΔN Syx52R1/210R1, and Syx LE 52R1/210R1 in soluble constructs for these experiments. In each case, I observed that upon assembly Syntaxin-1a opens up (Figure 45). For the full-length construct, I decided to work only on FL Syx52R1/210R1 because I did not observe any significant differences between Syx 52R1/210R1 and ΔN Syx52R1/210R1 or Syx LE 52R1/210R1. For the full-length construct, I obtained similar results for measurements performed in DPC micelles and with lipid reconstituted samples. The only difference was that in the case of the protein samples reconstituted into a lipid bilayer, I detected a distance component consistent with protein aggregation, in addition to the distance reflecting the distance between the H3 and Habc domains.

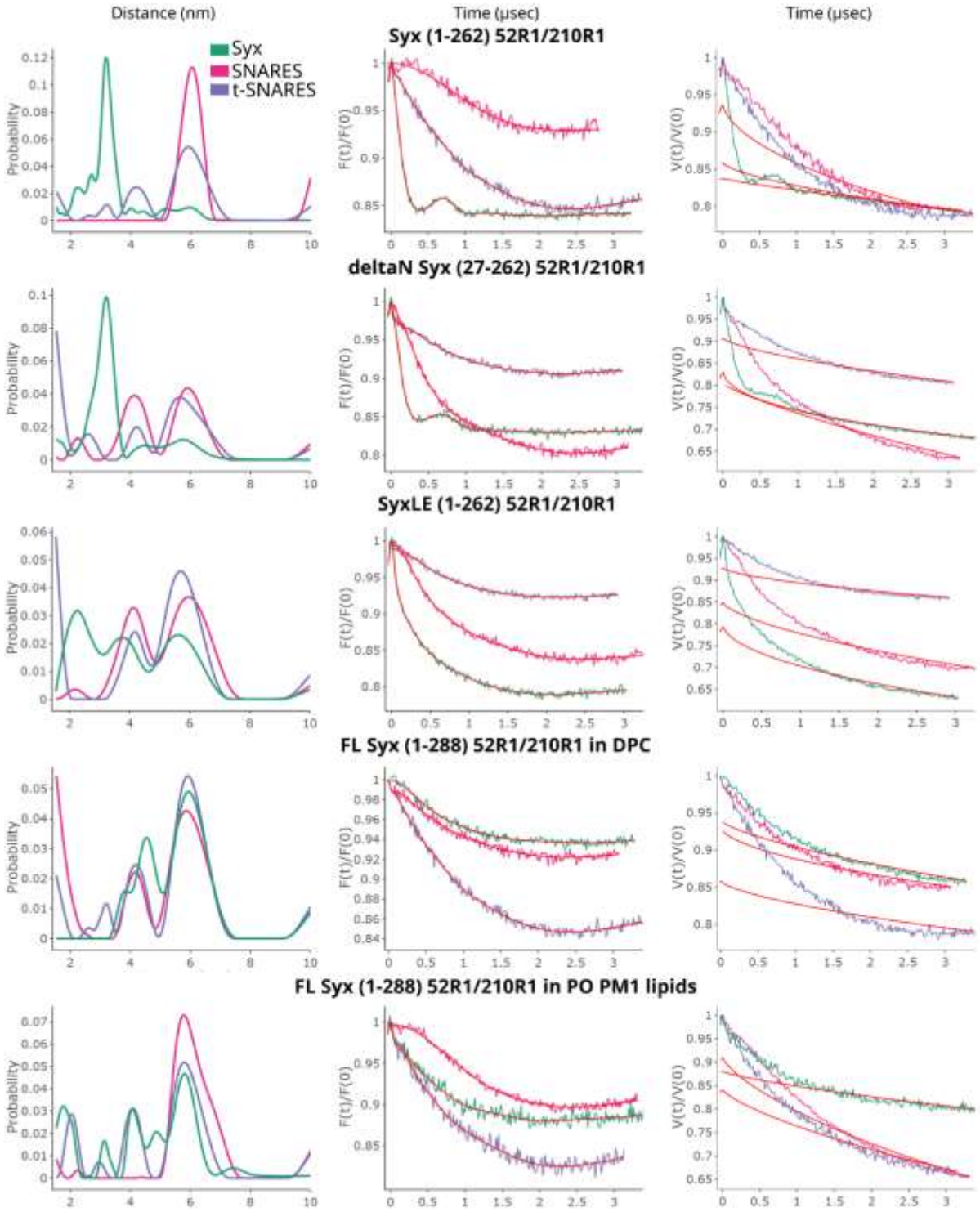


***Figure 45.*** *DEER data collected on three different doubles labeled Syntaxin-1a constructs: Syx 1-262 (left), ΔN Syx 27-262 (middle), SyxLE 1-262 (right) and one full-length construct. Data was collected on Syntaxin-1a alone (green), assembled into acceptor complex (purple) and assembled into SNARE complex (magenta). All four constructs were labeled at position 52 (Habc domain) and 210 (H3 domain). For the full-length construct on the left side protein sample is in DPC micelles and on the right is reconstituted into PO-PM1 lipids vesicles.*

## 4. Continuous-wave EPR measurements on full-length Syntaxinaxin-1a mutant proteins alone and assembled into SNARE complex in DPC micelles and reconstituted into lipid bilayer show that membrane affects Syntaxin-1a structure

I recorded CW-EPR spectra for full-length Syntaxin-1a alone and assembled them into either a t-SNARE or SNARE complex in the presence of DPC micelles or reconstituted into a lipid bilayer. Shown in Figure 46 are spectra obtained in DPC micelles with corresponding protein samples reconstituted into lipid vesicles. For every sample tested, I observed different lineshapes for both conditions. This result may indicate that in addition to lipid-mediated clustering, there is other membrane interactions of Syntaxin-1a that are not fully understood.

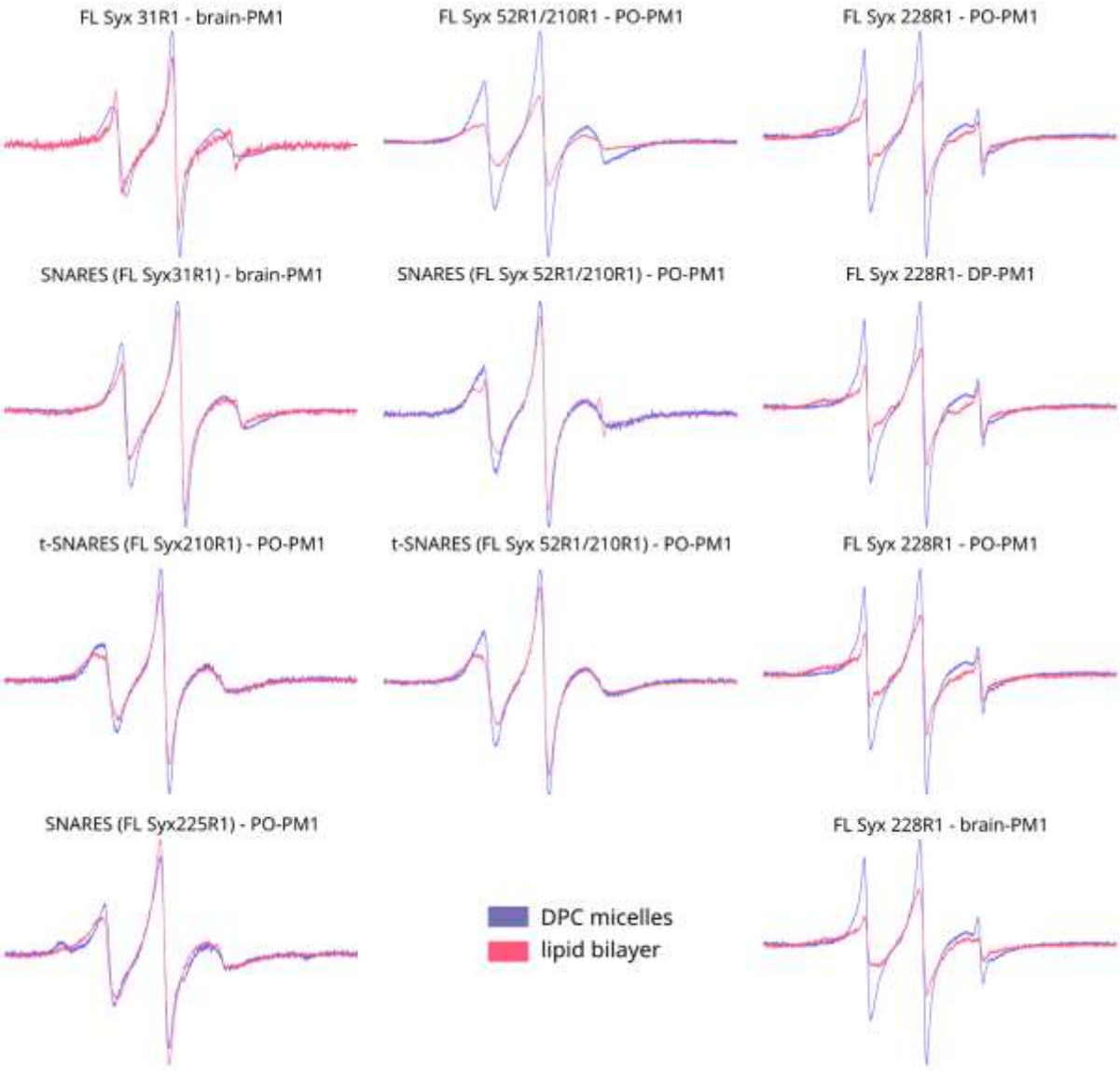


***Figure 46.*** *CW lineshapes of single cysteine mutants of full-length Syntaxin-1a, acceptor complex or snare complex in DPC micelles (blue) and reconstituted into lipid vesicles (magenta).*

## Part 3 – Study of the interactions between Syntaxin-1a on a different stages of SNAREs assembly with Munc18 and Complexin and its impact on Syntaxin-1a conformation

### 1. Continuous-wave EPR measurements on Syntaxin-1a mutant proteins alone and assembled into SNARE complex with and without the addition of Munc18

In order to further characterize Syntaxin-1a alone and during SNARE assembly in the presence of Munc18, I conducted EPR measurements on samples containing spin-labeled Syntaxin-1a alone and assembled into t-SNARE or SNARE complex mixed with one-to-one molar ratio of Munc18. Figures 47 - 49 shows spectra that I recorded for given samples.

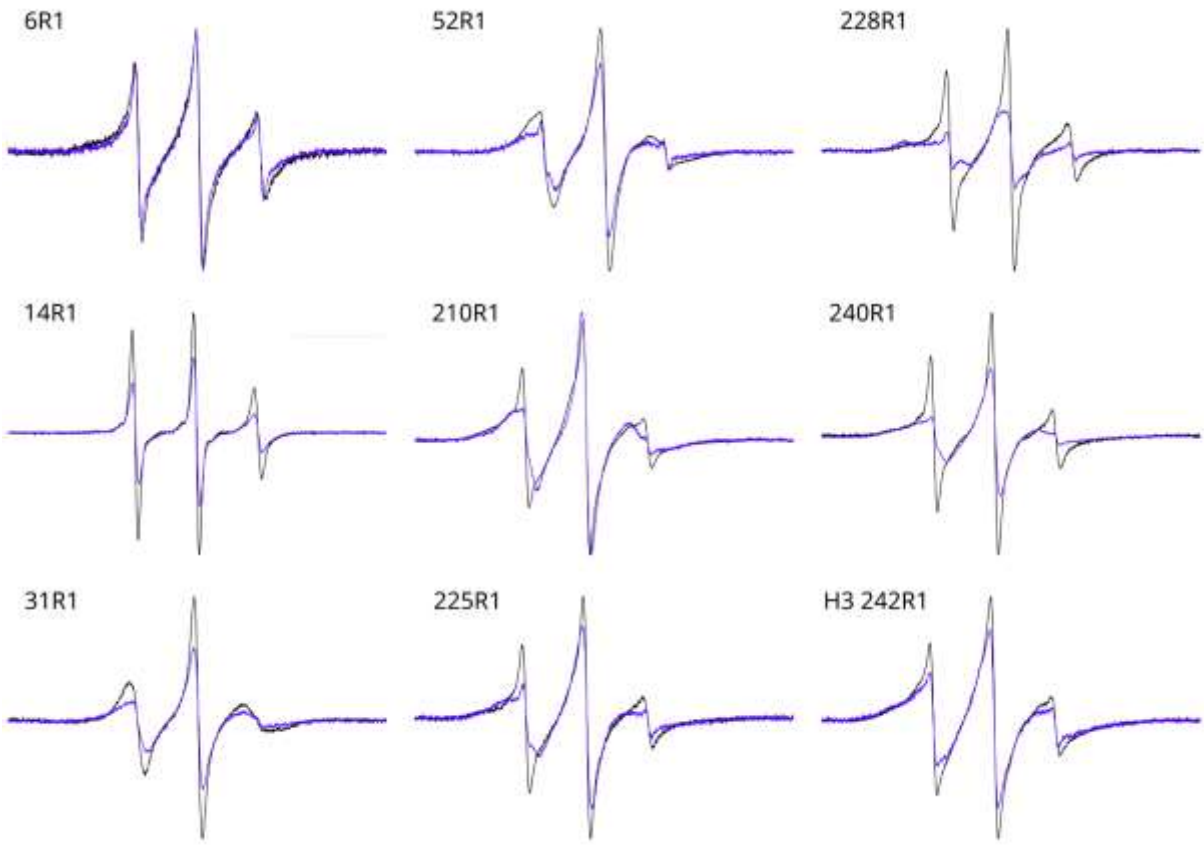


***Figure 47.*** *CW-EPR spectra for spin-labeled Syntaxin-1a mutants alone and incubated with the Munc18. Spectrum of free Syntaxin-1a in solution is shown in black, whereas spectrum of Syntaxin-1a incubated with Munc18 is presented in blue.*

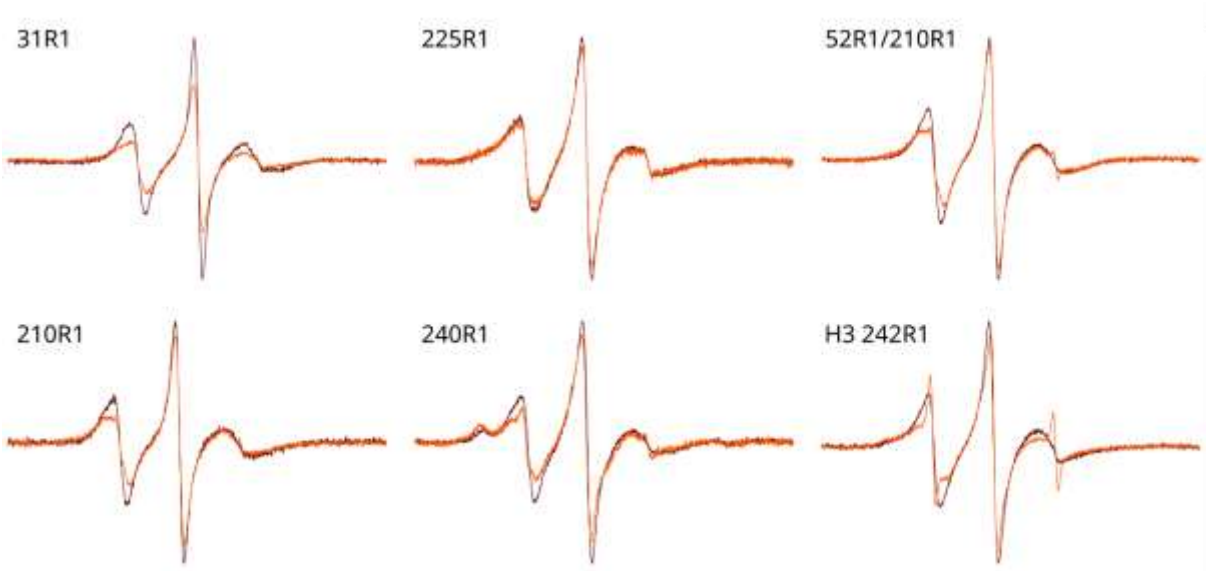


***Figure 48.*** *CW-EPR spectra for spin-labeled Syntaxin-1a mutants assembled into t-SNARE alone and with the Munc18. Spectrum of Syntaxin-1a assembled into t-SNARE complex is shown in brown and t-SNARE complex incubated with Munc18 is shown in orange.*

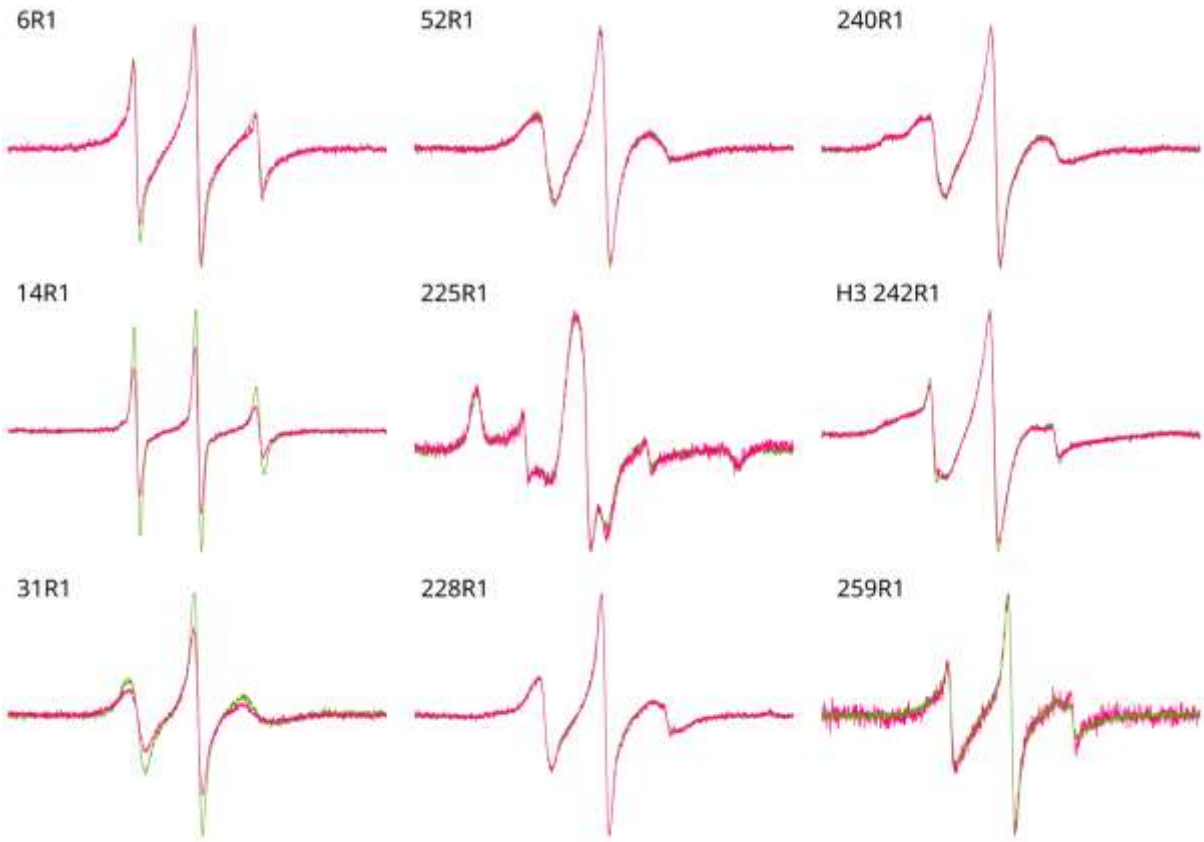


***Figure 49***. *CW-EPR spectra for spin-labeled Syntaxin-1a mutants assembled SNARE complex alone and incubated with the Munc18.Spectrum of SNARE complex sample in solution is presented in green, whereas spectrum of SNARE complex incubated with Munc18 is shown in magenta.*

EPR results obtained for Syntaxin-1a Munc18 binding (Figure 40) seem to be consistent with previous work[106,112] – the change in the EPR lineshapes after Munc18 addition is clear and visible in each tested position. EPR results obtained for t-SNARE Munc18 interactions (Figure 48) suggest that Munc18 binds to the acceptor complex through the Habc domain (label on position 31) and H3 domain (labels on positions 210, 240, 242). Data obtained for SNARE complex Munc18 (Figure 49) interactions suggest that Munc18 binds to Syntaxin-1a assembled into SNARE complex only through the N-peptide. The protein samples with spin-label located on the positions 52 (Habc domain), 225, 228, 240, and 242 (H3 domain) with the addition of Munc18 exhibit spectra that almost perfectly overlap with the spectra obtained without Munc18. The lack of any lineshapes changes obtained for positions placed in the H3 region of Syntaxin-1a suggests that if Munc18 interacts with the core complex, this interaction is not occurring through the Syntaxin-1a SNARE motif.

## 2. Munc18 disassociates Syntaxin-1a aggregates in solution and on the membrane, and Habc domain is essential for this process.

I used EPR spectroscopy to further explore the Munc18 – Syntaxin-1a interaction, and in particular, the ability of Munc18 to disassociate Syntaxin-1a aggregates. I collected the CW and DEER spectra for three single-labeled Syntaxin-1a constructs: H3 Syx 242R1, Syx 240R1, and FL Syx228R1 alone and with molar addition of Munc18. I performed the measurements on soluble Syntaxin-1a constructs: H3 Syx 242R1 and Syx 240R1 in the assembly buffer, whereas FL Syx228R1 I reconstituted into PO-PM1 lipid vesicles. I obtained results for the samples without and with the addition of Munc18 and pictured them in Figure 50.

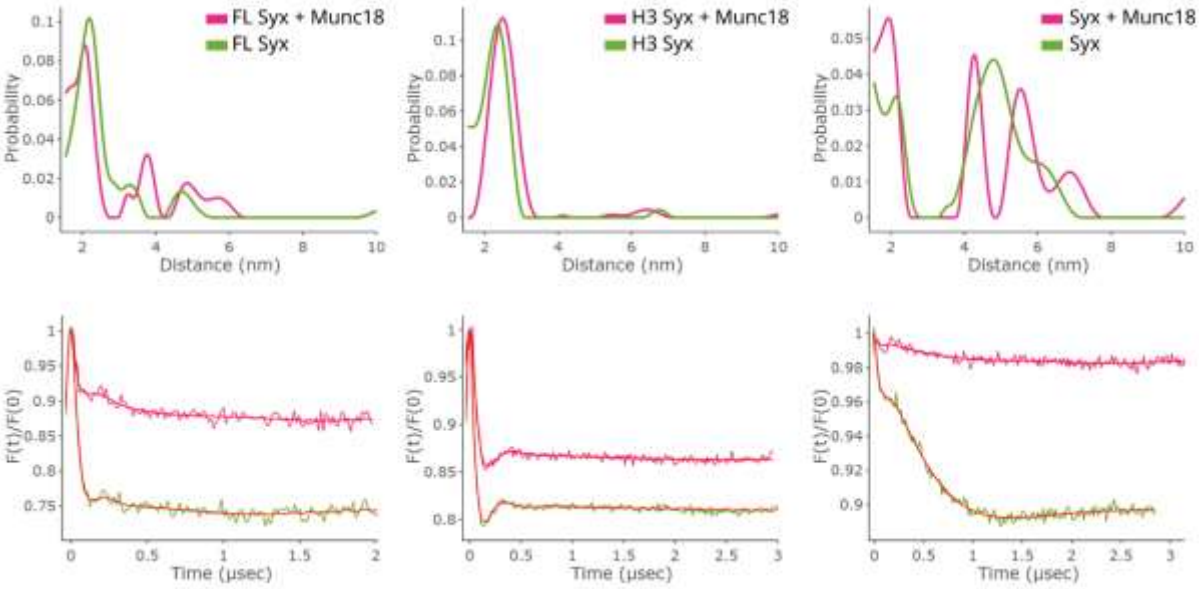


***Figure 50***. *DEER data collected on full length construct of Syntaxin (1-288) single labeled on position 228 reconstituted into brain PM1 lipid mixture (on the left) on soluble construct of Syntaxin (1-262) single labeled on position 240 (on the right) and on short soluble H3 construct of Syntaxin (183 – 262) single labeled on position 242 (in the middle); alone (green) and with Munc18 addition (pink).*

The results I obtained from EPR experiments regarding Syntaxin-1a and Munc18 binding (Figure 47) were presented above in the first section of this chapter and show that Munc18 binds to Syntaxin-1a in each case. However, the EPR spectrum for FL Syx228R1 with Munc18 shows less changes compared to the soluble construct spin-labeled in the same positions – Syx228R1 with Munc18 (Figure 47). The DEER experiments I performed on Syx240R1 in assembly buffer show that Syntaxin-1a in solution is aggregated and that Munc18 binding to Syntaxin-1a dissociates these aggregates. However, I noted a similar pattern with a much smaller effect for the SyxH3 242R1 variant of Syntaxin-1a. When I compared the results obtained for Syx240R1 and SyxH3 242R1, it appears that without the Habc domain, Syntaxin-1a is more prone to aggregation. My results indicate the Habc domain of Syntaxin-1a is essential for Munc18 to break apart clusters of Syntaxin-1a, even if Munc18 binds to the H3 motif of Syntaxin-1a. In the full-length construct, I also observed that Munc18 disassociated Syntaxin-1a aggregates upon binding to Syntaxin-1a, but some aggregation still persisted in the sample. The fact that there are still some aggregates left in the FL Syx228R sample confirms that Syntaxin-1a aggregation on the membrane might depend both on protein-protein and protein-lipid interactions.

### 3. Munc18 closes Syntaxin-1a upon binding to Syntaxin-1a and t-SNARE complex. Munc18 shifts the position of the Habc domain in the SNARE complex but does not close Syntaxin-1a in the core complex.

The interaction between Munc18 and Syntaxin-1a is well-researched, and it is known that Munc18 closes Syntaxin-1a upon binding[112]. Munc18 can also interact with the t-SNARE complex and SNARE complex[107]. Unfortunately, as previously mentioned in the introduction

part, neither the mode of these interactions nor the state of the Habc regulatory domain is well characterized in these complexes.

The previous section presented evidence for Munc18 binding to assembled t-SNARE or SNARE complex, along with an indication about regions that were associating. Here, I wanted to focus on how Munc18 affects the position of the Habc domain if Syntaxin-1a bears either LE mutation or is lacking the N-peptide, and to explore further how the Habc position changes in t-SNARE and SNARE complexes upon Munc18 binding for Syntaxin-1a in the absence of these mutations. I decided to examine the construct bearing the LE mutation and the construct lacking N-peptide, because both were reported to be important for Munc18 binding[106]. I conducted DEER experiments in the absence and presence of Munc18 to observe changes in the Habc domain (spin-label on position 52) relative to the H3 domain (spin-label on position 210) domain of Syntaxin-1a. The DEER data I obtained are presented in Figures 51 to 53.

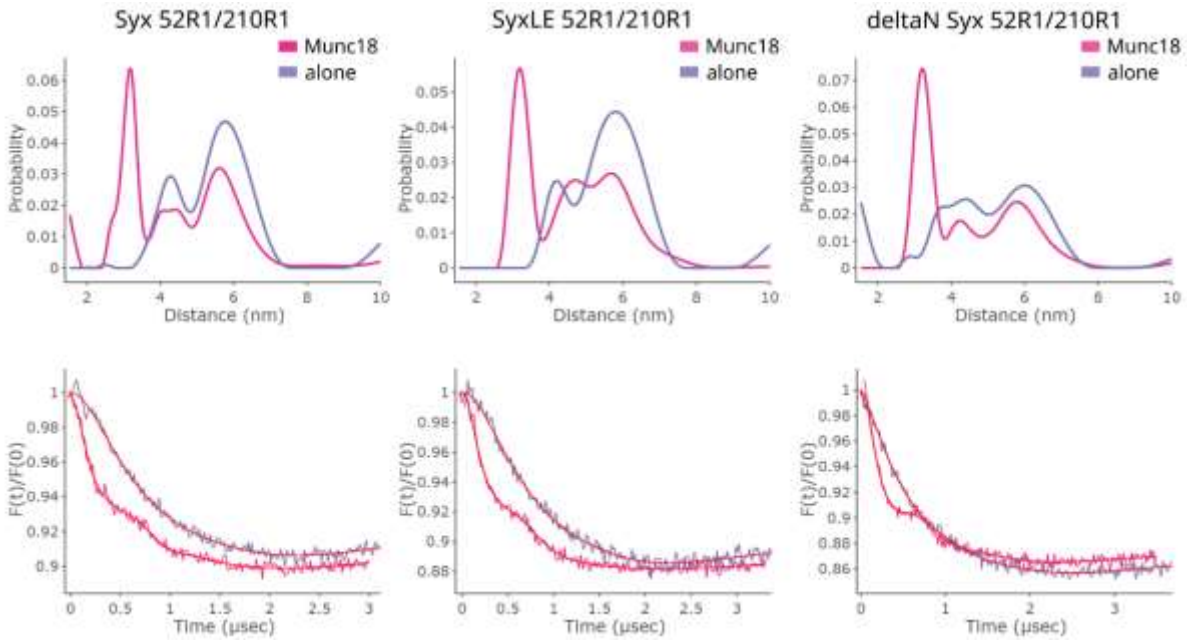


***Figure 51.*** *DEER data collected on three different double-labeled soluble Syntaxin-1a constructs: Syx 1-262 (left), SyxLE 1-262 165 166 (middle) and ΔN Syx 27-262 (right), alone (purple) and with Munc18 addition (magenta). All three constructs were labeled at positions 52 (Habc domain) and 210 (H3 domain). Measurements were performed in DPC micelles.*

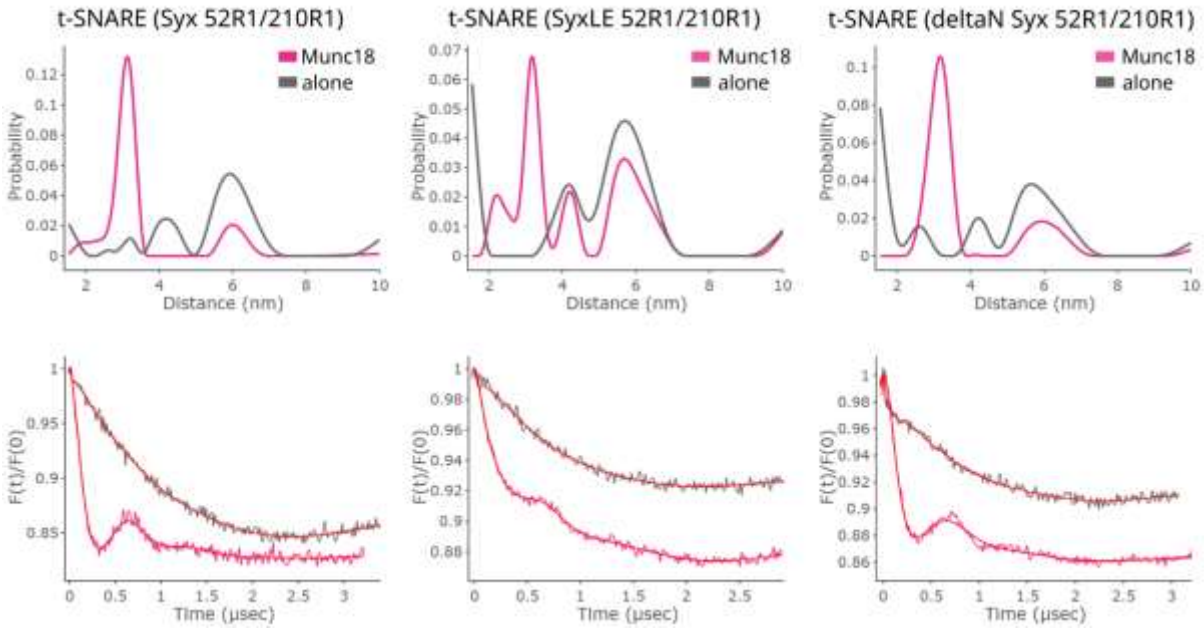


***Figure 52.*** *DEER data collected on the t-SNARE complex assembled with three different double-labeled soluble Syntaxin-1a constructs: Syx 1-262 (left), SyxLE 1-262 165 166 (middle) and ΔN Syx 27-262 (right), alone (grey) and with Munc18 addition (magenta). All three constructs were labeled at positions 52 (Habc domain) and 210 (H3 domain). Measurements were performed in DPC micelles. In all three cases, Syntaxinaxin-1a is in an open state (grey). Upon Munc18 addition, Habc and H3 domains are put closer and form the fully closed state (magenta).*

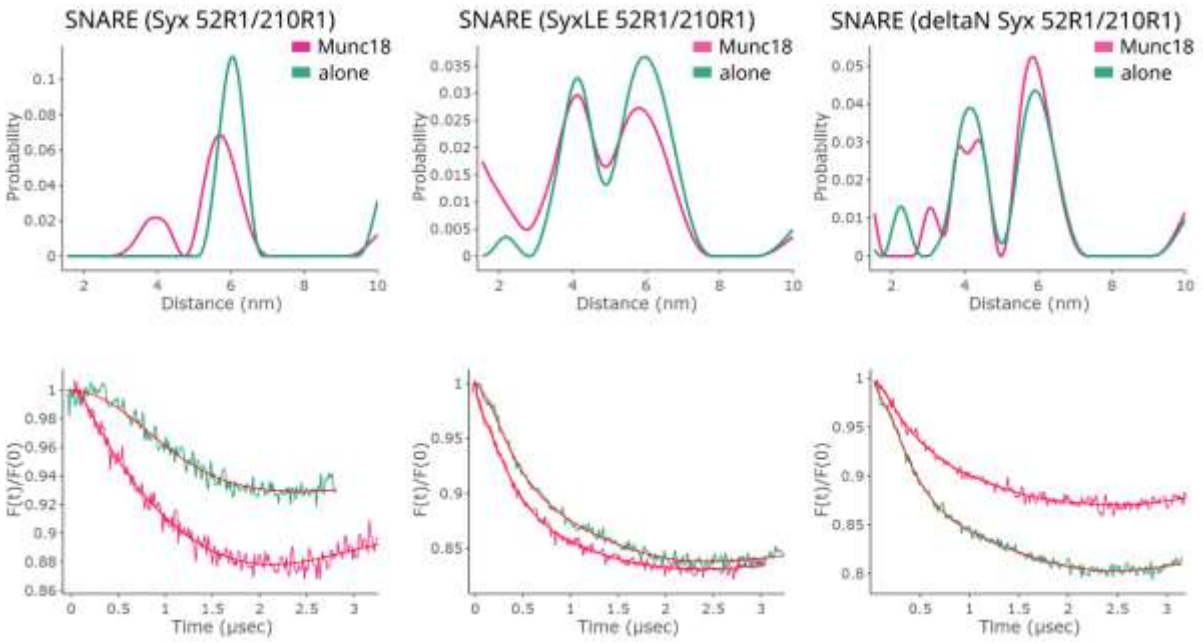


***Figure 53.*** *DEER data collected on the SNARE complex assembled with three different double-labeled soluble Syntaxin-1a constructs: Syx 1-262 (left), SyxLE 1-262 165 166 (middle) and ΔN Syx 27-262 (right), alone (green) and with Munc18 addition (magenta). All three constructs were labeled at positions 52 (Habc domain) and 210 (H3 domain). Measurements were performed in DPC micelles. In all three cases, Syntaxinaxin-1a is in an open state (green). Upon Munc18 addition (magenta), Habc and H3 domains are put closer but do not form the fully closed state. This change occurred only in the SNARE complex variant with an unchanged Habc domain (figure on the left). When any changes were introduced to the Habc domain like LE mutation or deletion of the first 27 residues (ΔN mutation), there was no interaction between Munc18 and SNARE complex. This leads to the conclusion that Munc18 – SNARE complex interaction is very sensitive to changes in the Habc domain. Again, the Habc domain of Syntaxin-1a is necessary for Munc18 to interact with the complex.*

The DEER data show that Munc18 closes Syntaxin-1a (Figure 51) regardless of construct. The DEER data I collected on three variants of the t-SNARE complex containing Syx52/210, SyxLE52/210, and ΔNSyx52/210 (Figure 52) shows that in all three cases, Syntaxin-1a is in an open state (grey). Upon the Munc18 addition, Habc and H3 domains move closer and form the fully closed state. I collected DEER data on three variants of SNARE complex (Figure 53) containing the same Syntaxin-1a variants. In all three cases, Syntaxin-1a is in an open state (green). Upon the Munc18 addition, Habc and H3 domains are brought closer together but do not form the fully closed state. This change occurred only in the SNARE complex variant with an unchanged Habc domain (Figure 53, left). When I introduced any changes into the Habc domain like LE mutation or deletion of the first 27 residues, I could not detect any interaction between Munc18 and SNARE complex. These findings show that Munc18 – SNARE complex interaction is very sensitive to changes in the Habc domain. Again, the Habc domain of Syntaxin-1a is necessary for Munc18 to interact with the complex.

## 4. Munc18 closes Syntaxin-1a on the membrane but does not close it in the t-SNARE and SNARE complex.

Next, I decided to explore the Munc18 interaction with Syntaxin-1a on the membrane using just the construct that contains two cysteine mutations but has no modifications to the N-peptide or Habc domain. I purified and labeled FL Syx52R1/210R1 and assembled it into a t-SNARE or SNARE complex. I reconstituted all three samples (FL Syx52R1/2101R, t-SNARE(FL Syx52R1/210R1), and SNARE complex(FL Syx52R1/210R1) into PO-PM1 lipid vesicles. I chose this particular lipid composition after performing a screening to find a lipid composition under which Syntaxin-1a aggregation is at the lowest level. DEER data obtained for all protein samples in the absence and presence of Munc18 are shown in Figure 54.

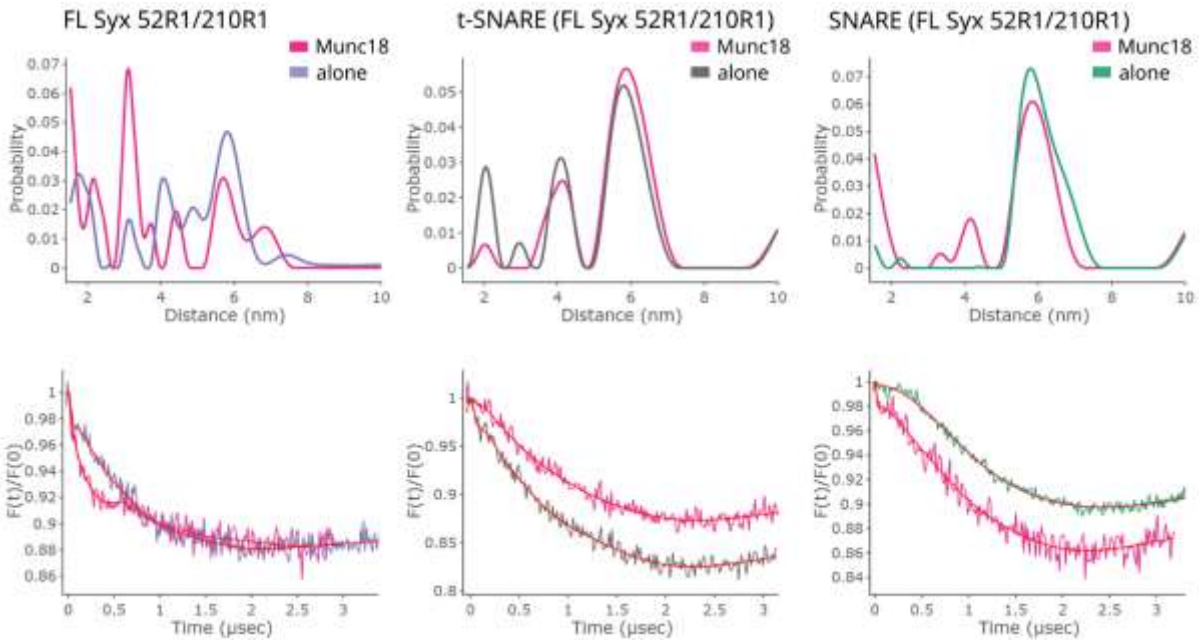


***Figure 54.*** *DEER data collected on the double labeled full-length Syntaxin-1a (52R/210R) construct alone (left, purple), assembled into t-SNARE complex (middle, grey) and assembled into SNARE complex (right, green) and with Munc18 addition (magenta). Measurements were performed in PO-PM1 lipid vesicles*

The DEER data shows that Munc18 closes Syntaxin-1a on the membrane. However, there is still a significant level of Syntaxin-1a in the open state. My DEER data for the SNARE complex (FL Syx52R/210R) are very similar to the DEER data I obtained for the corresponding soluble construct and show that upon Munc18 addition, the Habc and H3 domains are put into close proximity do not form the fully closed state. On the other hand, DEER data that I obtained for the t-SNARE (FL Syx52R/210R) complex indicates that Munc18 may not be able to close Syntaxin-1a on the membrane as it does for the soluble constructs.

## 5. Munc18 binds to the SNARE complex through N-peptide and Habc domain of Syntaxin-1a

I wanted to understand how Munc18 binds to the SNARE complex because the current binding modes between these two molecules are contradictory. To do that, I took a closer look at the CW-EPR lineshapes of single labeled SNARE complex samples with the addition of Munc18 that I already presented in Figure 55A. The CW-EPR experiments alone are not enough to fully characterize the binding mode between Munc18 and SNARE complex. To supplement them and be able to tell more about this interaction, I also performed DEER experiments on single labeled SNARE complexes using two different Syntaxin-1a constructs: H3 Syx 242R and Syx 240R (Figure 55B).

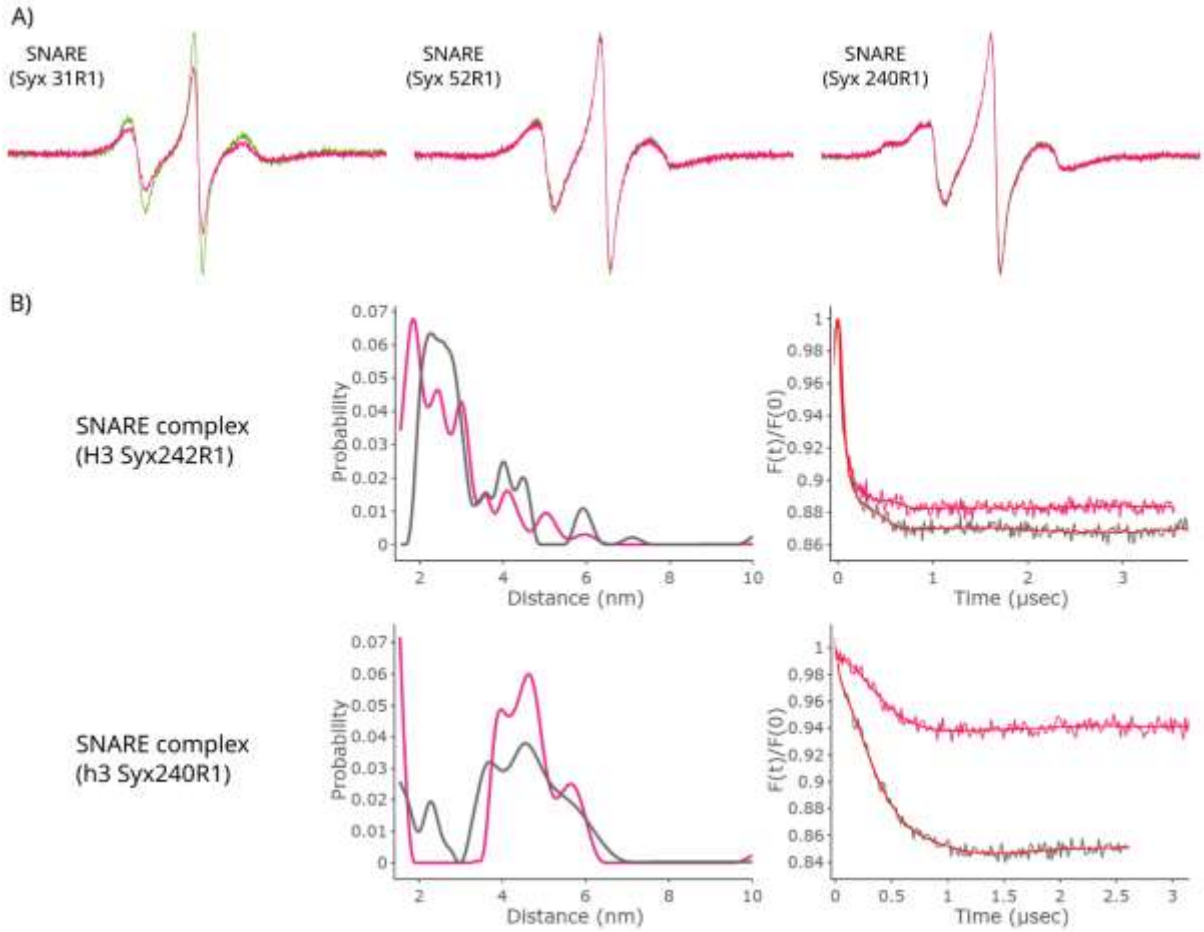


***Figure 55. A****. CW lineshapes of single cysteine mutants of soluble Syntaxin1-a assembled into SNARE complex (green) and with addition of Munc18 (magenta).*

***B.*** *DEER data collected on two variants of SNARE complex without (grey) and with Munc18 (pink) shows that Munc18 breaks apart SNARE complex aggregates only when Habc domain (bottom) of Syntaxin-1a is present. Habc domain of Syntaxin-1a in crucial for Munc18 – SNARE complex interactions.*

I obtained the three SNARE complexes with labeled Syntaxin-1a (soluble fragment with Habc and H3 domains) and prepared to run the CW measurements. In the first complex, Syntaxin-1a was labeled on position 31 in the Habc domain, in the second on position 52, and in the third on position 240 in the H3 domain. After the addition of Munc18 (magenta), I observed a change in the CW lineshapes only for the SNARE complex with Syntaxin-1a labeled on position 31, indicating Munc18 interaction with the SNARE complex occurs through the Habc domain of Syntaxin-1a and precisely through Ha domain.

The DEER data I collected on two variants of SNARE complex; one with only the H3 domain of Syntaxin-1a and the second with both Habc and H3 domains of Syntaxin-1a; without (grey) and with Munc18 (pink) shows that Munc18 breaks apart SNARE complex aggregates only when Habc the domain (right) of Syntaxin-1a is present. This result leads to the conclusion that the Habc domain of Syntaxin-1a is necessary for Munc18 – SNARE complex interactions.

## 6. Munc18 interacts with the t-SNARE complex through both H3 and Habc domains, and the Habc domain is unnecessary for interaction to occur. Munc18 does not disassociate t-SNARE complex aggregates.

Here, I looked closely at the interaction between the t-SNARE complex and Munc18. Figure 56 shows CW spectra obtained for single labeled t-SNARE complexes and corresponding DEER data.

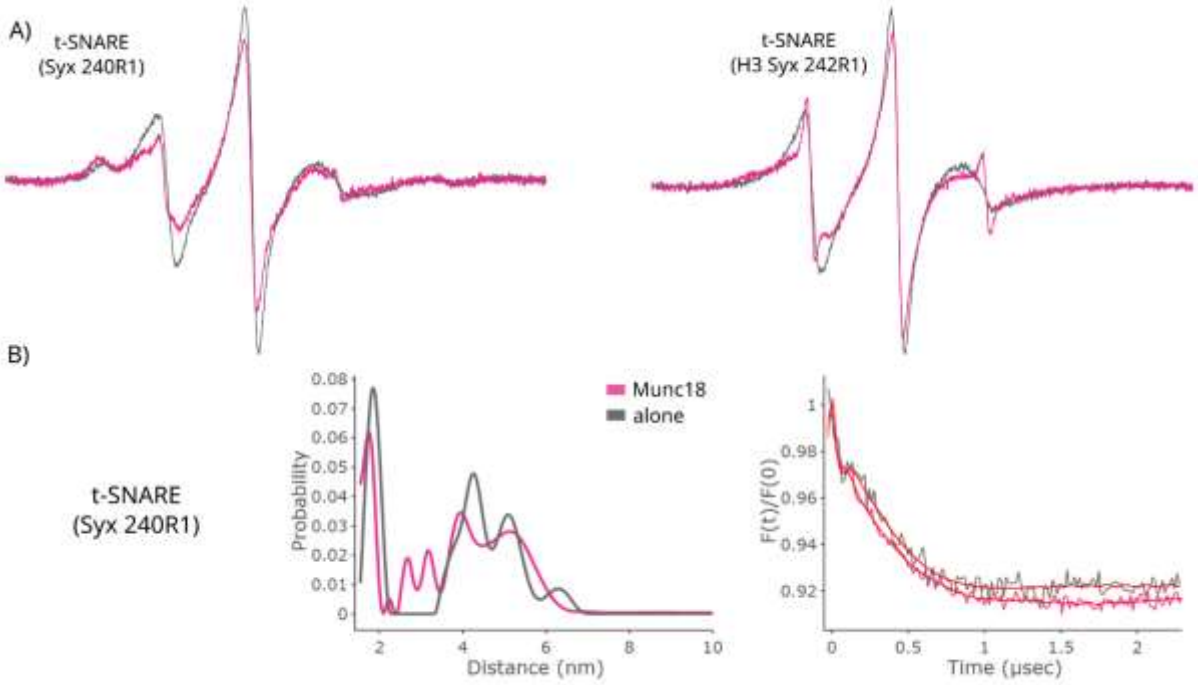


***Figure 56. A.*** *CW lineshapes of single cysteine mutants of soluble Syntaxin1-a assembled into t-SNARE complex (black) and with addition of Munc18 (magenta).*

***B.*** *DEER data collected on t-SNARE complex without (grey) and with Munc18 (pink) shows that Munc18 does not breaks apart t-SNARE complex aggregates.*

The change in the CW lineshapes after adding Munc18 (pink) to the acceptor complex (black) indicates that Munc18 binds to the acceptor complex through its interaction with the H3 domain of Syntaxin-1a. I tested the two variants of the acceptor complex, one containing just the H3 domain of Syntaxin-1a and the second with both domains of Syntaxin-1a. In both cases, I observed the binding, suggesting that the Habc domain is not necessary for Munc18 to bind to the acceptor complex. DEER data collected on the t-SNARE complex with Syx240R alone (grey) and with the addition of Munc18 (magenta) shows no change between these two samples, which means that Munc18 does not disassociate the aggregates upon binding to the t-SNARE complex as it does in case of Syntaxin-1a alone or for the SNARE complex.

## 7. Complexin binds to the SNARE complex and breaks its aggregates.

Complexin was reported to bind to the SNARE complex[182], and this interaction was described as one of the factors that can modulate SNARE complex oligomerization[146]. I decided to follow up on this hypothesis and run CW-EPR on all previously mentioned single-labeled SNARE complex samples in the presence of Complexin (data not shown). In only one case did I observe evidence for an interaction between Complexin and SNARE complex, and this was for a SNARE complex with Syx 225R1 (Figure 57).

Additionally, I ran DEER experiments on the SNARE complex alone and with Complexin (Figure 57). The results did not confirm the previous hypothesis and showed the opposite. I observe that the SNARE complex alone was already in oligomeric form, and upon Complexin binding, some of the oligomers were disassociated.

Knowing that Complexin binding occurs not only to the SNARE complex but also to the plasma membrane, I decided to check to see if I could observe a similar interaction between

the SNARE complex and Complexin in the presence of the membrane. I performed the same experiment for the SNARE complex with FL Syx225R as I did for the SNARE complex with Syx225R and the SNARE complex with FL Syx225R that I reconstituted into the PO-PM1 lipid vesicles. The data I obtained are shown in Figure 50, bottom panel. After the addition of Complexin to the sample, I observed a reduction in the overall aggregation in the SNARE complex sample as indicated by a decrease in the modulation depth in dipolar evolution data.

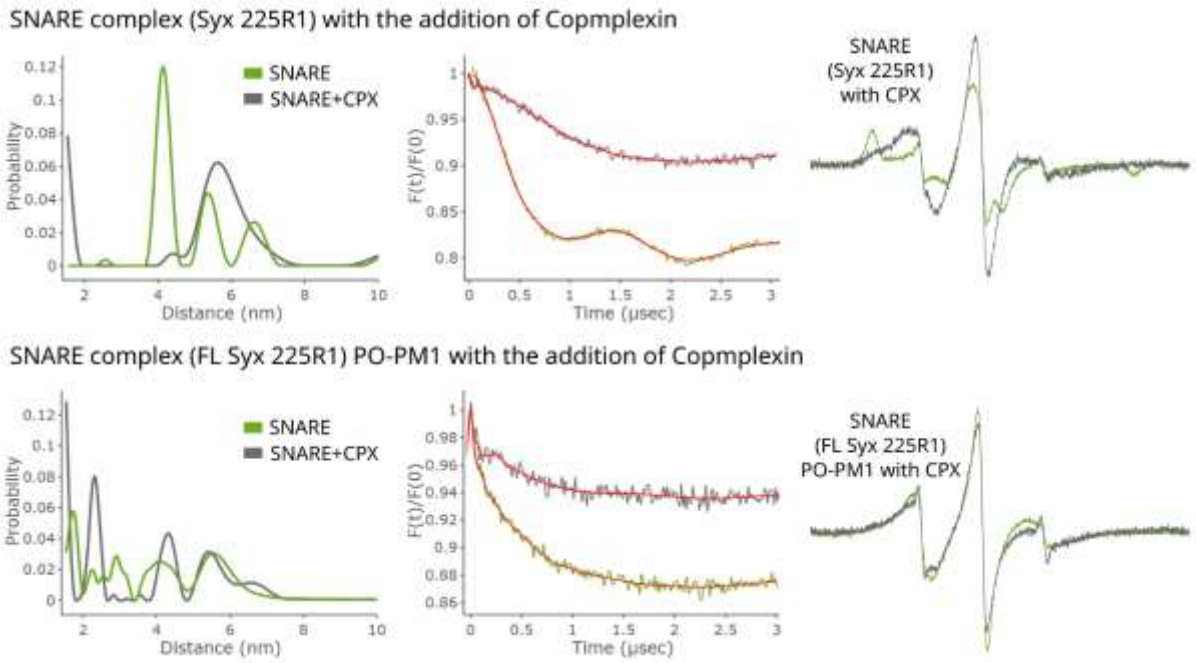


***Figure 57.*** *The DEER data (DEER distance distribution, and the dipolar data) and CW-EPR spectra for spin-labeled SNARE complex on Syx225R alone (green) incubated with the Complexin (green). The top panel shows data obtained in solution, and the bottom panel shows data obtain on the membrane.*

In addition to the DEER measurements, I performed an analytical run using size exclusion chromatography to better understand the nature of the oligomers that were formed without and with Complexin. The chromatographs I obtained from these two runs are shown in Figure 58. From size exclusion column molecules elute according to their sizes starting from the molecules that have the highest molecular weight. In the top panel of Figure 58 I show the elution profile of SNARE complex sample. There are two peaks. In the bottom panel I show the elution profile of SNARE complex sample after incubation with 1:1 molar ratio of Complexin. There are three peaks, first two peaks are the same as two peaks on the top panel but they are smaller. That means that the fraction of higher molecular structures is smaller. The biggest peak is observed for fraction 16 and it corresponds to the SNARE complex – Complexin bound molecule. Results obtained from runs on the size exclusion column agree with DEER findings that Complexin is disassociating SNARE complex aggregation.

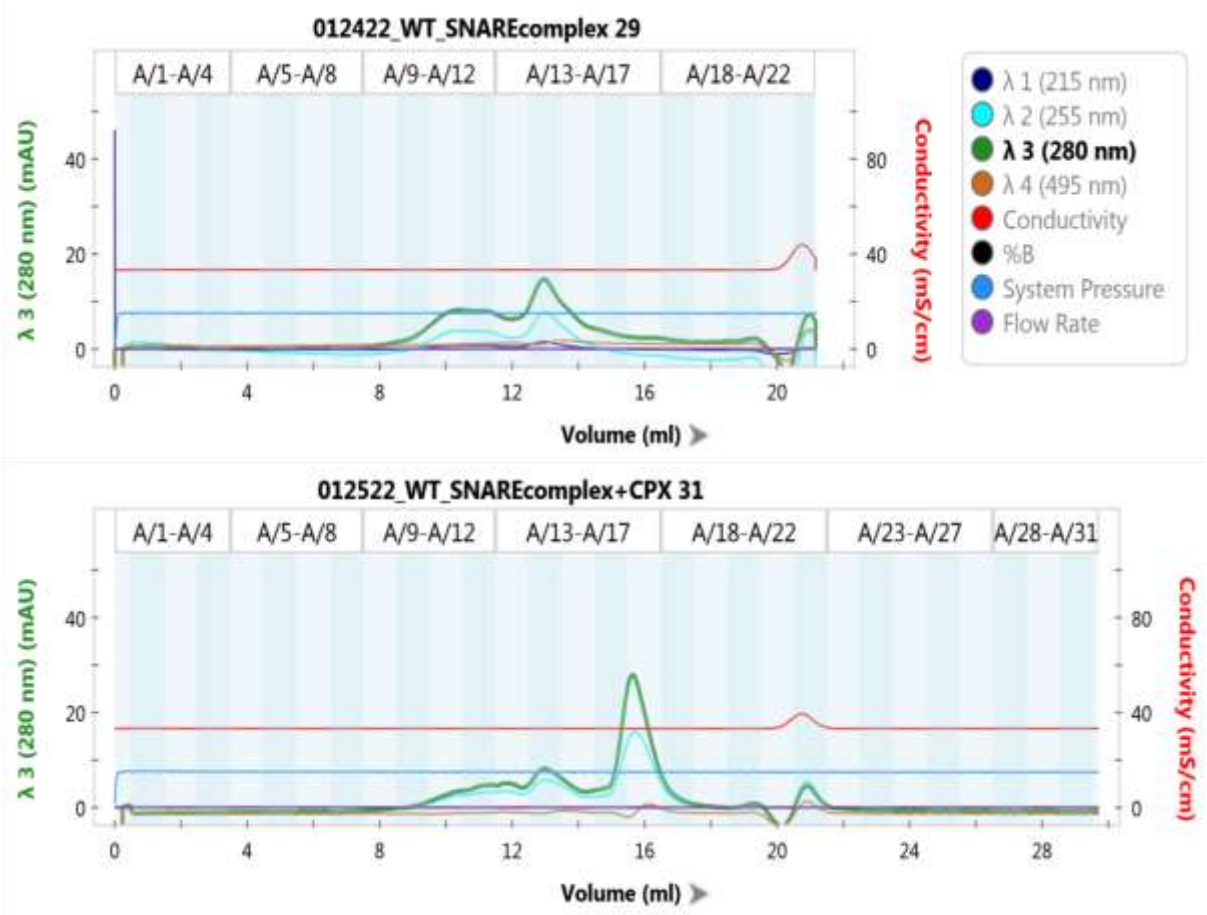


***Figure 58.*** *Chromatograms obtained from run on size exclusion column. Top panel shows chromatogram for SNARE complex sample run alone, and the bottom panel shows chromatogram for SNARE complex sample incubated wit Complexin prior to run on the column.*

# V. Discussion

The work described in this thesis aimed to determine the structural changes in Syntaxin-1a during SNAREs assembly as it is thought to participate in neuronal exocytosis. The chapters presented above step through an investigation of Syntaxin-1a as an essential component of the SNARE complex, which is crucial for neuronal exocytosis. Each chapter added to the complexity to the tested interactions, moving from work on the soluble construct to the full-length protein to investigating Syntaxin-1a interactions alone and assembled into the t-SNARE or SNARE complex with other proteins like Munc18 or Complexin. Future work should continue to add to the *in vitro* system piece-by-piece to understand how each component, lipid diversity, or added proteins, functions and changes within the system.

The first principal aim of this work was to determine how environment impacts the proteins that assemble into the SNARE complex and to determine the effect of environment on the aggregation of these proteins. It has been reported that Syntaxin-1a tends to oligomerize when its concentration is higher than 2 μM[83,84]. On the other hand, it has been proposed that adding the DPC detergent leads to their monomerization state[227] (personal communication with Dr Binyong Liang). In my work, I tested this hypothesis by the addition of DPC above critical micellar concentration (CMC). In Figure 31, the DEER data I obtained for Syx 240R1 shows a significant change in modulation depth for the dipolar evolution obtained by DEER upon the addition of DPC, where these depths decreased from 12% for Syx 240R1 in buffer to 1% for Syx 240R1 in DPC micelles. The modulation depth of the DEER signal depends upon the number of excited spin-pairs, and it can provide a rough estimate of the extent of dimerization as described previously (citation)[235]. One of the potential problems with the use of DPC is that this detergent causes Syntaxin-1a to adopt a more helical structure. I did a DPC titration for Syx 228R1 and observed that changes induced in the CW-EPR lineshapes continued until the

CMC of DPC was reached. At concentrations higher than the CMC, all the EPR lineshapes were identical.

Two mechanisms for Synraxin-1a aggregation have been proposed, and the first one focuses on protein-protein interactions; in particular, the interactions between H3 domains in neighboring Syntaxin-1a molecules. Interestingly, the Habc domain of Syntaxin-1a plays a role and appears to inhibit aggregation which has not been proposed earlier. In Figure 31, the dipolar evolution from DEER obtained for H3 Syx242R1 displays a larger modulation depth than does the data from Syx 240R1. The modulation depth obtained from H3 Syx 242R1 goes from 17% in buffer to 7% in DPC micelles. The fact that DPC addition was less effective at disassociating all the Syntaxin-1a aggregates for the shorter (H3) construct as compared to the construct having both H3 and Habc domains, suggests a role for the Habc domain in Syntaxin-1a aggregation. I observed a similar behavior for DPC at reducing aggregation in the assembled SNARE complex. I tested several different conditions and obtained the best results with the lowest aggregation of the complex when DPC was present in the tested sample.

The second mechanism for Syntaxin-1a aggregation is based on protein-lipid interactions. Previous work from our group and our collaborators shows the importance of the membrane composition and its impact on protein behavior[236]. I decided to test several lipid compositions and determine whether membrane composition has any effect on Syntaxin-1a aggregation. I focused on the lipid compositions previously tested by our collaborators (PO-PM1, DO-PM1, DP-PM1 brain-PM1) as well as on the presence of PIP2 and cholesterol because these two components were previously reported to play a crucial role in Syntaxin-1a aggregation[89,90,92,95]. First, I wanted to compare the full-length protein construct reconstituted into a lipid vesicle with a detergent sample (Figure 31). Here I observed that DPC also reduces aggregation in the case of the full-length protein. The modulation depth for membrane reconstituted protein is 15%, while for the detergent sample is 4%. However, the presence of the membrane alters not

only protein aggregation but also Syntaxin-1a itself. The CW-EPR lineshapes obtained in detergent differ from those obtained in membrane reconstituted samples (Figure 46). In every case of full-length Syntaxin-1a, I observed that the lineshapes were broader with features characteristic of an immobile spin label. I made a similar observation for the t-SNARE and SNARE complex except for the presence of an immobile component. One case that was different from that presented above was obtained for the SNARE complex having full-length Syntaxin-1a labeled on position 225. The reconstituted sample (magenta lineshape in Figure 46) does not show the immobile component in the DPC sample (blue lineshape).

Figure 40 shows all tested lipid compositions. From the data presented, it is evident that membrane composition is a crucial factor in Syntaxin-1a aggregation. I observed the lowest aggregation, similar to the aggregation level for the DPC sample, for the PO-PM1 composition. Brain-PM1 composition gave the most extensive level of aggregation. Eliminating cholesterol and PIP2 from brain-PM1 composition reduces aggregation by about 50%, the modulation depth changes from 16.2% for brain-PM1 to 8% brain(PC-PS-PE). Elimination of PIP2 gave 9.1% modulation depth, while cholesterol elimination resulted in 12.4% modulation depth. These results suggest that cholesterol and PIP2 are important for forming Syntaxin-1a clusters, but PIP2 has a more significant impact than cholesterol.

Syntaxin-1a in a solution can adopt two states, open and closed, and these two exist in a dynamic equilibrium, with a closed state being the dominant state[99,100,105]. Munc18 binds to Syntaxin-1a tightly with nM affinity[106,110] and locks it into the closed conformation. A high-resolution X-ray structure for Syntaxin-1a when bound to Munc18, represents the closed state (PDB ID 3C98)[102]. I used this structure as a starting point for my investigations using EPR, where I can employ different conditions than those used to obtain the X-ray crystallography structure. The buffer I used in my measurements (a physiological or assembly buffer) contains 150 mM NaCl, 20 mM HEPES, and pH 7.4.

In contrast, the buffer used for an X-ray experiment (referred to as crystallization buffer) contains PEG400, Ammonium Acetate, Sodium Acetate, EDTA, 2-mercaptoethanol, and pH 5.3. During my preliminary studies, I tested a series of positions along the Habc and H3 domains of Syntaxin-1a. For two of them, Syx 87R1 and Syx 91R1, I obtained results that did not correspond to data from the crystal structure. As shown in Figure 39, both 87 and 91 are facing outside of Mucn18, but the CW-EPR lineshapes obtained for these two mutants (Figure 37) show otherwise.

The lineshapes after Munc18 addition are broader and indicate the presence of an immobile component. This might have been a result of dimerization, and I decided to check whether the Syntaxin-1a – Munc18 complex could form a dimer or other higher oligomeric structure. I used an online tool - PDP-ePISA, and the results based on crystal structure 3C98 suggest that besides the monomer, another attainable and possible to form biological unit is a dimer (Figure 38). As shown in Figure 38, neither 87 nor 91 has any steric obstacles and both sites are facing towards the solution in this dimer structure. I already know that DPC has a significant impact on syntaxin-1a, so my second thought was that either the physiological (also called assembly) or crystallization buffer might be altering Syntaxin-1a, which results in different binding with Munc18. I dialyzed both mutants into a slightly modified crystallization buffer. I removed PEG400, EDTA, and 2-mercaptoethanol to keep protein and MTSL stable during CW-EPR measurements. The CW lineshapes for both mutants are slightly different under crystallization conditions compared to those obtained under physiological conditions. It suggests that there is a different conformation for Syntaxn-1a in the crystallization conditions. The EPR spectra for sites 87 and 91 obtained after addition and incubation with Munc18 do not change in lineshape (Figure 37), which correspond to data obtained under the conditions of protein crystallization. As my final step in this investigation, I analyzed and compared two crystal structures of homologues complexes. The first one is the crystal structure of the Munc18-Syntaxin-1a

complex from *Rattus norvegicus* (PDB ID 3C98)[102], and the second Tlg2 – Vps45 bound structure from *Chaetomium thermophilum* (PDB ID 6XM1)[233] where Tlg2 is Qa-SNARE and Vps45 is SM protein. Both crystal structures are presented in Figure 32.

Interestingly, Vps45 interacts with the same region of the Qa-SNARE protein as does Munc18, but the bound SNARE is in a much more open configuration than that for the Munc18 bound form of Syntaxin-1a. The main difference is in the interactions between Qa-SNARE's domain. In the case of Syntaxin-1a, H3 and Habc interact with each other and are roughly parallel, but in the case of Tlg2, the interaction between H3 and Habc is not as close and the H3 domain is lies at an angle relative to the Habc domain. I overlayed these two structures (Figure 39) using PyMOL. To ensure that both structures are aligned properly, I used 45 to 63 amino acid sequences from Munc18 (3C98) and 48 to 66 amino acid sequences from Vps45 (6XM1). This figure shows that Qa-SNAREs can adopt at least two conformations, one closed (Syntaxin-1a; blue) and one partially open (Tlg2; purple). The existence of another binding model might explain the data I obtained for Syx 87 and Syx 91 mutants. In Syntaxin-1a – Munc18 bound structure, both residues face outwards, but in the case of Tlg2 – Vps45 bound structure, both residues face inwards and labels at these sites could be motionally restricted. The position of these residues in the Tlg2 – Vps45 structure correlates to the CW data I obtained for the Syntaxin-1a – Munc18 complex, and it indicates that the Syntaxin-1a – Munc18 structure may sample a state similar to the *Chaetomium thermophilum* structure under physiological conditions. In summary, under physiological conditions I observed interaction between Munc18 and Syntaxin-1a that does not correspond to the X-ray structure obtained for this complex. The data I obtained for Syntaxin-1a-Munc18 complex fits into the X-ray structure of the *Chaetomium thermophilum* homolog. The fact that under two different conditions I obtained two completely different results and additionally the *Chaetomium thermophilum* homolog structure could potentially explain these results suggests at least two different binding

modes exist between these two proteins and what was captured in the X-ray structure is just one of the possibilities.

The second aim of this work focused on shedding light on the states of Syntaxin-1a in different stages of SNAREs assembly. It is a well-established fact that Syntaxin-1a exists in equilibrium between an open and a close state. I already discussed how DPC affects Syntaxin-1a, but in addition to these changes, DPC also opens up Syntaxin-1a in the solution. In Figure 35, I presented data for three constructs of Syntaxin-1a with spin labels on Glu52 (Habc domain) and Arg210 (H3 domain) each. In each case, both open (distance distribution ~ 6 nm) and closed states (distance distribution ~ 3 nm) are observed for Syntaxin-1a. In general, in the physiological buffer (grey trace) the equilibrium is shifted towards a closed state. Still, in the case of Syx LE 52R/210R, the population of an open state is significant, which is in agreement with previous reports[103,106]. When DPC is present (green trace in Figure 35), the equilibrium shifts toward an open state in each sample. Knowing how these different variants of Syntaxin-1a behave in the solution, I decided to test only the unmodified full-length construct. From the DEER data that I obtained for FL Syx52R/210R reconstituted into PO-PM1, I observed that on the membrane, in contrast to in a solution, the equilibrium between open and closed state is shifted towards an open state (Figure 44) meaning that Syntaxin-1a on the membrane is primarily open and available for interactions with other proteins.

However, the vast majority of the studies on t-SNARE and SNARE complexes use a short construct of Syntaxin-1a, which contains only the H3 domain (for work performed in solution) or H3 and transmembrane domains (for work performed in the presence of lipid bilayer). The reasoning for this decision is simple. There is a general belief that Syntaxin-1a must be open to be assembled into a complex so that other proteins can be accommodated when they bind. I decided to include the Habc domain in my research to test how the Habc domain of Syntaxin-1a is positioned relative to the H3 domain in either t-SNARE or SNARE complex. In

preliminary experiments, I screened a series of Syntaxin-1a double mutants with one spin-label placed on the Habc domain and the other on the H3 domain (data not shown). From that, I continued my work on three double mutants Syx 52R1/210R1, ΔN Syx 52R1/210R1, and Syx LE 52R1/210R1. In Figure 45, I present the DEER data I obtained for all three mutants assembled into t-SNARE and SNARE complexes. The results obtained confirm what has been hypothesized: Syntaxin-1a is open when it assembles into a SNARE complex. It is interesting to note that Syntaxin-1a is fully open only in the SNARE complex when no other mutations are introduced. For ΔN and LE variants, I also observed a distance component in the distribution near 4 nm, which might suggest a partially open state where both domains are slightly closer to each other but able to fully close.

These data also suggest that the Habc domain and linker between the Habc and H3 domains are important for an open state of Syntaxin-1a in the SNARE complex. I observed an equilibrium between fully open and partially open Syntaxin-1a states for the acceptor complex. Introducing a mutation in the Habc domain or linker region does not change this. For full-length protein again, I decided to work with just one construct. The DEER data (Figure 45) obtained for the reconstituted t-SNARE and SNARE complexes show the same results as did the soluble fragment. Syntaxin-1a is in an open state in the SNARE complex on the membrane. Furthermore, in the t-SNARE complex, there is a mixture of both fully- and partially open states of Syntaxin-1a.

The third aim of this work focused on the interaction between Munc18 and Syntaxin-1a during SNAREs assembly. Munc18 binds to Syntaxin-1a alone, and the CW-EPR spectra I obtained confirm this (Figure 47). The DEER data I got for three different single-labeled Syntaxin-1a mutants: H3 Syx 242R1, Syx 240R1, and FL Syx228R1 alone and with equimolar addition of Munc18 confirms that Munc18 is disassociating aggregated Syntaxin-1a in solution and on the membrane. The exciting observation I made is that the Habc domain is required for Munc18 to

disassociate Syntaxin-1a aggregates entirely. There is a significant difference in change in modulation depth for Syx 240R1 and H3 Syx 242R1 before and after Munc18 addition. In the case of Syx 240R1, Munc18 eliminates aggregation almost entirely. However, for H3 Syx 242R1, despite the apparent interaction between Munc18 and Syntaxin-1a short construct, there is still a significant amount of aggregated Syntaxin-1a in the sample. In the case of the full-length construct, Munc18 also did not disassociate Syntaxinaxin-1a entirely. Still, for full-length protein there are two mechanisms of aggregation, where one driven by protein-protein interaction. Munc18 can disassociate these aggregates, and the second one is driven by protein-lipid interaction. Overall, this allows us to conclude that the Habc domain is not required for Munc18 to bind to Syntain-1a, but it is necessary to disassociate Syntaxin-1a clusters.

While interactions between Munc18 and Syntaxin-1a in isolation have been well-investigated, there are many unanswered questions about the Munc18 interactions with Syntaxin-1a during SNAREs assembly. After SNARE assembly, there might not be enough space for Munc18 to bind to Syntaxin-1a through both the Habc and H3 domains, and it has been proposed that Munc18 interacts with the SNARE complex through the Habc domain alone[167]. In contrast, another study[114] suggests that there is competition between the Syntaxin-1a N-terminal region and the SNARE four-helix bundle for Munc18 binding. Unfortunately, there is no information about the position of the Habc domain relative to the H3 domain of Syntaxin-1a. I collected DEER data for three Syntaxin-1a constructs: Syx 52R1/210R1, ΔN Syx 52R1/210R1, and Syx LE 52R1/210R1 alone (as a reference) and assembled them into a t-SNARE or SNARE complex. It is worth mentioning that for Syntaxin-1a in the absence and presence of Munc18, in addition to the expected closure of Syntaxin-1a, DPC is changing the binding affinity between Munc18 and Syntaxin-1a. The DEER data in Figure 36 shows that without DPC, the addition of an equal molar amount of Munc18 is enough to fully close Syntaxin-1a, while in the case of DPC addition, even 3-time excess of Munc18 is not enough to fully close Syntaxin-

1a. I observed that in the presence of detergent binding between Syntaxin-1a and Munc18 might be much weaker than without detergent.

Munc18 interacts with the t-SNARE complex through Habc and H3 domains of Syntaxin-1a (Figure 48 & Figure 56A). The CW-EPR results I obtained for the t-SNARE Munc18 interaction suggests that Munc18 binds to the acceptor complex through the Habc domain (label on position 31) and H3 domain (labels on positions 210, 240, 242). The fact that I observed an interaction between the t-SNARE complex composed of the shorter H3 Syx 242R1 with Munc18 suggests that the Habc domain is not required for a Munc18-t-SNARE complex interaction. Upon binding, Munc18 closes Syntaxin-1a in the t-SNARE complex in a similar manner as observed for Syntaxin-1a alone (Figure 52). The DEER data obtain for the single-labeled t-SNARE complex suggest that this complex is not monomeric (Figure 56B). Munc18, despite binding to the complex, is not disassociating the aggregates. However, further exploration of the t-SNARE complex is required. Finally, although the Habc domain might not be crucial it is important for the Munc18-t-SNARE complex interaction.

A much lower binding affinity characterizes the binding of Munc18 to the SNARE complex than the binding of Munc18 binding to Syntaxin-1a[167]. This and the fact that the presence of DPC also weakens Munc18 binding affinity might be the reason why the changes observed in the DEER data (Figure 53) are minimal. The CW-EPR lineshapes for the single-labeled SNARE complex (Figure 49 & Figure 55) that were collected for the sample of SNARE complex alone and after incubation with Munc18 show that Munc18 binds only to N-peptide and Habc domains of Syntaxin-1a when Syntaxin-1a is assembled into the complex. Upon binding to the N-peptide and Habc domain, Munc18 shifts the Habc domain closer to the H3 domain but does not fully close Syntaxin-1a. However, this change occurred only for Syx 52R1/210R1. I did not observe any interaction for either ΔN Syx 52R1/210R1 or Syx LE 52R1/210R1. This finding suggests that interaction between Munc18 and SNARE

complex is not only weak but also very sensitive to any changes introduced into N-peptide or Habc domains. To test if Munc18 can interact with the SNARE complex through its core domain and not only through the N-peptide/Habc domains of Syntaxin-1a, I performed DEER experiments on two variants of the single-labeled SNARE complex, one with Syx 240R1 and the second with shorter Syntaxin-1a H3 Syx 242R1 (Figure 55). From the CW spectrum of the SNARE complex with a spin-label on Syx 240R1, I cannot determine if Munc18 interacts with the core complex. However, from the DEER data on this sample in the absence and presence of Munc18, it is apparent that in the presence of Munc18 the Habc domain shifts position and oligomers of the SNARE complex are dissociated. For the SNARE complex with H3 Syx 242R1, I did not observe changes in the CW spectrum or the DEER traces after Munc18 addition. The lack of changes suggests that the interaction between Munc18 and SNARE complex occurs only through N-peptide and Habc domains of Syntaxin-1a. Finally, all the above allows us to conclude that Munc18 – SNARE complex interaction is very sensitive to changes in the Habc domain and that the Habc domain of Syntaxin-1a is necessary for Munc18 to interact with the complex, as it was shown before by ITC measurments[107,167].

# VI. Outlook and Future directions

Syntaxin-1a is undeniably one of the essential elements of the neuronal fusion machinery. Its distinguishing feature is the presence of a separate regulatory domain (N-peptide and Habc domain) in addition to its SNARE motif. This domain enables Syntaxin-1a to be regulated by other components in the neuronal system. Indeed, critical regulatory proteins like Munc18 or Synaptotagmin[105,163,236,237], have been reported to interact with Syntaxin-1a during SNAREs assembly. Despite three decades of extensive research, the exact mechanism of Syntaxin-1a interactions and functions remains a mystery.

The work presented in this dissertation significantly expands our current knowledge regarding Syntaxin-1a and the SNAREs in the areas of:

- Syntaxin-1a conformational changes during SNAREs assembly.
- Impact on the Syntaxin-1a aggregation states and possible binding modes with Munc18.
- Interactions between Munc18 and Syntaxin-1a during SNAREs assembly
- Importance of cell membrane composition and its influence on SNARE proteins.

The progress made here will allow us to investigate other aspects of the regulatory mechanism that governs neuronal exocytosis by allowing us to tackle the following types of problems.

First, a necessary next step to this EPR study will be to add additional elements of complexity to the Syntaxin-1a interactions during SNARE assembly in the form of the lipid bilayer. While this study highlighted the importance of the membrane, the focus was only on one membrane composition. Additional experiments performed on samples reconstituted into different lipid bilayers would add valuable information on how membrane composition affects t-SNAREs, the SNARE complex, and its interaction with other proteins.

Second, in this work, I placed the main focus of the work on Syntaxin-1a. In the next step, it would be good to take a closer look at SNAP-25 or Synaptobrevin and examine the t-SNARE or SNARE complex by describing interactions made by different proteins in the complex. It might be especially interesting to investigate the t-SNARE complex by examining single or double spin-labeled mutants of Syntaxin-1a and SNAP-25 to better understand the stoichiometry and oligomerization state of this assembly.

Lastly, most of the work I preformed and presented was on soluble constructs of the SNAREs. For membrane interactions, I only looked at the full-length construct of Syntaxin-1a either alone or assembled into a complex. With just this one protein, I observed the importance of the membrane. The next logical step to further understand the neuronal exocytosis machinery would be to use palmitoylated SNAP-25 and Synaptobrevin anchored in the lipid bilayer. One could begin by examining protein-lipid interactions and adding membrane-bound protein to the system until all three SNAREs in the sample were assembled and membrane-associated. The CW-EPR experiments would allow observation of any local structural changes resulting from the presence of the membrane, while DEER experiments performed on single-labeled mutants would provide insight into the oligomerization state of the complex.

## List of References


1. Thorn P, Zorec R, Rettig J, Keating DJ. Exocytosis in non-neuronal cells. *J Neurochem*. Published online June 1, 2016:849-859. doi:10.1111/JNC.13602

2. Lauwers E, Goodchild R, Verstreken P. Membrane Lipids in Presynaptic Function and Disease. *Neuron*. 2016;90(1):11-25. doi:10.1016/J.NEURON.2016.02.033

3. Garland EL. Pain Processing in the Human Nervous System: A Selective Review of Nociceptive and Biobehavioral Pathways. Published online 2012. doi:10.1016/j.pop.2012.06.013

4. Margiotta A, Debanne D. cells Role of SNAREs in Neurodegenerative Diseases. Published online 2021. doi:10.3390/cells10050991

5. Wang Q, Wang Y, Ji W, et al. SNAP25 is associated with schizophrenia and major depressive disorder in the Han Chinese population. *J Clin Psychiatry*. 2015;76(1):e76-e82. doi:10.4088/JCP.13M08962

6. Bin NR, Huang M, Sugita S. Investigating the Role of SNARE Proteins in Trafficking of Postsynaptic Receptors using Conditional Knockouts. *Neuroscience*. 2019;420:22-31. doi:10.1016/J.NEUROSCIENCE.2018.11.027

7. Chen F, Chen H, Chen Y, et al. Dysfunction of the SNARE complex in neurological and psychiatric disorders. *Pharmacol Res*. 2021;165:105469. doi:10.1016/J.PHRS.2021.105469

8. Maton A. *Human Biology and Health*. 1st ed. Prentice Hall; 1993.

9. Nieuwenhuys R, Voogd J, van Huijzen C. The Human Central Nervous System. *Hum Cent Nerv Syst*. Published online 1988. doi:10.1007/978-3-662-10343-2

10. Fillingim RB, Loeser JD, Baron R, Edwards RR. Assessment of Chronic Pain: Domains, Methods, and Mechanisms HHS Public Access. *J Pain*. 2016;17(9):10-20. doi:10.1016/j.jpain.2015.08.010

11. From neurotransmission to neuronal disorders. Published online 2021. doi:10.1111/bph.v178.4/issuetoc

12. Azevedo FAC, Carvalho LRB, Grinberg LT, et al. Equal numbers of neuronal and nonneuronal cells make the human brain an isometrically scaled-up primate brain. *J Comp Neurol*. 2009;513(5):532-541. doi:10.1002/CNE.21974

13. Piccolino M, Strettoi E, Laurenzi E. Santiago Ramón Y Cajal, the retina and the neuron theory. *Doc Ophthalmol 1989 712*. 1989;71(2):123-141. doi:10.1007/BF00163466

14. Zeng H, Sanes JR. Neuronal cell-type classification: challenges, opportunities and the path forward. *Nat Publ Gr*. 2017;18. doi:10.1038/nrn.2017.85

15. Leonard BE. Principles of neural science, third edition. By E. R. Kandel, J. H. Schwartz and T. M. Jessell. Appleton & Lange, 1991. pp. 1135 + xxxvii. ISBN 0-8385-8068-8. *Hum Psychopharmacol Clin Exp*. 1993;8(4):294-294. doi:10.1002/HUP.470080412

16. Hirano T. Purkinje Neurons: Development, Morphology, and Function. doi:10.1007/s12311-018-0985-7

17. Hodgkin AL, Huxley AF. *A Quantitative Description of Membrane Current and Its*

*Application to Conduction and Excitation in Nerve*.; 1952.

18. Foster M. *A Textbook of Physiology. With C.S. Sherrington. Part 3. The Central Nervous System.* Macmillan,; 1897.

19. Nagy JI, Pereda AE, Rash JE. Electrical synapses in mammalian CNS: Past eras, present focus and future directions. *Biochim Biophys Acta - Biomembr*. 2018;1860(1):102-123. doi:10.1016/J.BBAMEM.2017.05.019

20. Connors BW, Long MA. Electrical synapses in the mammalian brain. *Annu Rev Neurosci*. 2004;27:393-418. doi:10.1146/ANNUREV.NEURO.26.041002.131128

21. Pereda AE, Purpura DP. Electrical synapses and their functional interactions with chemical synapses. *Nat Publ Gr*. 2014;15. doi:10.1038/nrn3708

22. Bennett MVL, Zukin RS. Electrical coupling and neuronal synchronization in the Mammalian brain. *Neuron*. 2004;41(4):495-511. doi:10.1016/S0896-6273(04)00043-1

23. O'Brien J. Design principles of electrical synaptic plasticity. *Neurosci Lett*. 2019;695:4-11. doi:10.1016/J.NEULET.2017.09.003

24. Cowan WM, Südhof TC, Stevens CF, Howard Hughes Medical Institute. Synapses. Published online 2001:767.

25. ECCLES JC, JAEGER JC. The relationship between the mode of operation and the dimensions of the junctional regions at synapses and motor end-organs. *Proc R Soc Lond B Biol Sci*. 1958;148(930):38-56. doi:10.1098/RSPB.1958.0003

26. Biederer T, Kaeser PS, Blanpied TA. Transcellular Nanoalignment of Synaptic Function. *Neuron*. 2017;96(3):680-696. doi:10.1016/J.NEURON.2017.10.006

27. Südhof TC, Rizo J. Synaptic vesicle exocytosis. *Cold Spring Harb Perspect Biol*. 2011;3(12). doi:10.1101/CSHPERSPECT.A005637

28. Harris K m., Sultan P. Variation in the number, location and size of synaptic vesicles provides an anatomical basis for the nonuniform probability of release at hippocampal CA1 synapses. *Neuropharmacology*. 1995;34(11):1387-1395. doi:10.1016/0028-3908(95)00142-S

29. Takamori S, Holt M, Stenius K, et al. Molecular anatomy of a trafficking organelle. *Cell*. 2006;127(4):831-846. doi:10.1016/J.CELL.2006.10.030

30. Jahn R, Fasshauer D. Molecular machines governing exocytosis of synaptic vesicles. *Nature*. 2012;490(7419):201-207. doi:10.1038/nature11320

31. Murthy VN, De Camilli P. Cell biology of the presynaptic terminal. *Annu Rev Neurosci*. 2003;26:701-728. doi:10.1146/ANNUREV.NEURO.26.041002.131445

32. Ruiz R, Cano R, Casañas JJ, Gaffield MA, Betz WJ, Tabares L. Cellular/Molecular Active Zones and the Readily Releasable Pool of Synaptic Vesicles at the Neuromuscular Junction of the Mouse. Published online 2011. doi:10.1523/JNEUROSCI.4663-10.2011

33. Abraham C, Bai L, Leube RE. Synaptogyrin-dependent modulation of synaptic neurotransmission in Caenorhabditis elegans. *Neuroscience*. 2011;190:75-88. doi:10.1016/J.NEUROSCIENCE.2011.05.069

34. Hammarlund M, Palfreyman MT, Watanabe S, Olsen S, Jorgensen EM. Open syntaxin docks synaptic vesicles. *PLoS Biol*. 2007;5(8):1695-1711. doi:10.1371/JOURNAL.PBIO.0050198

35. Lin XG, Ming M, Chen MR, et al. UNC-31/CAPS docks and primes dense core vesicles in C. elegans neurons. *Biochem Biophys Res Commun*. 2010;397(3):526-531. doi:10.1016/J.BBRC.2010.05.148

36. Saheki Y, De Camilli P. Synaptic vesicle endocytosis. *Cold Spring Harb Perspect Biol*. 2012;4(9). doi:10.1101/CSHPERSPECT.A005645

37. Südhof TC. Neurotransmitter release: The last millisecond in the life of a synaptic vesicle. *Neuron*. 2013;80(3):675-690. doi:10.1016/j.neuron.2013.10.022

38. Chapman ER. How does synaptotagmin trigger neurotransmitter release? *Annu Rev Biochem*. 2008;77:615-641. doi:10.1146/ANNUREV.BIOCHEM.77.062005.101135

39. Rizzoli SO, Jahn R. Kiss-and-run, collapse and "readily retrievable" vesicles. *Traffic*. 2007;8(9):1137-1144. doi:10.1111/j.1600-0854.2007.00614.x

40. Jung N, Haucke V. Clathrin-mediated endocytosis at synapses. *Traffic*. 2007;8(9):1129-1136. doi:10.1111/j.1600-0854.2007.00595.x

41. Kaksonen M, Roux A. Mechanisms of clathrin-mediated endocytosis. *Nat Rev Mol Cell Biol*. 2018;19(5):313-326. doi:10.1038/NRM.2017.132

42. Mueller VJ, Wienisch M, Nehring RB, Klingauf J. Monitoring clathrin-mediated endocytosis during synaptic activity. *J Neurosci*. 2004;24(8):2004-2012. doi:10.1523/JNEUROSCI.4080-03.2004

43. Murthy VN, Stevens CF. Synaptic vesicles retain their identity through the endocytic cycle. *Nature*. 1998;392(6675):497-501. doi:10.1038/33152

44. Lira RB, Robinson T, Dimova R, Riske KA. Highly Efficient Protein-free Membrane Fusion: A Giant Vesicle Study. *Biophys J*. 2019;116(1):79-91. doi:10.1016/J.BPJ.2018.11.3128

45. Kozlovsky Y, Chernomordik L V., Kozlov MM. Lipid intermediates in membrane fusion: formation, structure, and decay of hemifusion diaphragm. *Biophys J*. 2002;83(5):2634-2651. doi:10.1016/S0006-3495(02)75274-0

46. Hernández JM, Podbilewicz B. The hallmarks of cell-cell fusion. *Development*. 2017;144(24):4481-4495. doi:10.1242/DEV.155523

47. Witkowska A, Spindler S, Mahmoodabadi RG, Sandoghdar V, Jahn R. Differential Diffusional Properties in Loose and Tight Docking Prior to Membrane Fusion. *Biophys J*. 2020;119(12):2431-2439. doi:10.1016/J.BPJ.2020.10.033

48. Broadie K, Prokop A, Bellen HJ, O'Kane CJ, Schulze KL, Sweeney ST. Syntaxin and synaptobrevin function downstream of vesicle docking in Drosophila. *Neuron*. 1995;15(3):663-673. doi:10.1016/0896-6273(95)90154-X

49. Hess SD, Doroshenko PA, Augustine GJ. A functional role for GTP-binding proteins in synaptic vesicle cycling. *Science*. 1993;259(5098):1169-1172. doi:10.1126/SCIENCE.8438167

50. Imig C, Min SW, Krinner S, et al. The morphological and molecular nature of synaptic

vesicle priming at presynaptic active zones. *Neuron*. 2014;84(2):416-431. doi:10.1016/J.NEURON.2014.10.009

51. Richmond JE, Davis WS, Jorgensen EM. Unc-13 is required for synaptic vesicle fusion in C. elegans. *Nat Neurosci*. 1999;2(11):959-964. doi:10.1038/14755

52. Song L, Ahkong QF, Georgescauld D, Lucy JA. Membrane fusion without cytoplasmic fusion (hemi-fusion) in erythrocytes that are subjected to electrical breakdown. *BBA - Biomembr*. 1991;1065(1):54-62. doi:10.1016/0005-2736(91)90010-6

53. Yavuz H, Kattan I, Hernandez JM, et al. Arrest of trans-SNARE zippering uncovers loosely and tightly docked intermediates in membrane fusion. *J Biol Chem*. 2018;293(22):8645-8655. doi:10.1074/JBC.RA118.003313

54. Witkowska A, Heinz LP, Grubmüller H, Jahn R. Tight docking of membranes before fusion represents a metastable state with unique properties. *Nat Commun*. 2021;12(1). doi:10.1038/S41467-021-23722-8

55. Chernomordik L V., Kozlov MM, Melikyan GB, Abidor IG, Markin VS, Chizmadzhev YA. The shape of lipid molecules and monolayer membrane fusion. *BBA - Biomembr*. 1985;812(3):643-655. doi:10.1016/0005-2736(85)90257-3

56. Chernomordik L V, Kozlov MM. Mechanics of membrane fusion. doi:10.1038/nsmb.1455

57. Sabatini BL, Regehr WG. Timing of neurotransmission at fast synapses in the mammalian brain. Published online 1996.

58. Brenner S. *THE GENETICS OF CAENORHABDZTZS ELEGANS*. https://academic.oup.com/genetics/article/77/1/71/5991065

59. Novick P, Field C, Schekman R. Identification of 23 complementation groups required for post-translational events in the yeast secretory pathway. *Cell*. 1980;21(1):205-215. doi:10.1016/0092-8674(80)90128-2

60. Balch WE, Dunphy WG, Braell WA, Rothman JE. Reconstitution of the transport of protein between successive compartments of the Golgi measured by the coupled incorporation of N-acetylglucosamine. *Cell*. 1984;39(2 Pt 1):405-416. doi:10.1016/0092-8674(84)90019-9

61. Weber T, Zemelman B V., McNew JA, et al. SNAREpins: minimal machinery for membrane fusion. *Cell*. 1998;92(6):759-772. doi:10.1016/S0092-8674(00)81404-X

62. Link E, Edelmann L, Chou JH, et al. Tetanus toxin action: Inhibition of neurotransmitter release linked to synaptobrevin proteolysis. *Biochem Biophys Res Commun*. 1992;189(2):1017-1023. doi:10.1016/0006-291X(92)92305-H

63. Schiavo GG, Benfenati F, Poulain B, et al. Tetanus and botulinum-B neurotoxins block neurotransmitter release by proteolytic cleavage of synaptobrevin. *Nature*. 1992;359(6398):832-835. doi:10.1038/359832A0

64. Blasi J, Chapman ER, Link E, et al. Botulinum neurotoxin A selectively cleaves the synaptic protein SNAP-25. *Nature*. 1993;365(6442):160-163. doi:10.1038/365160A0

65. Jahn R, Scheller RH. SNAREs - Engines for membrane fusion. *Nat Rev Mol Cell Biol*. 2006;7(9):631-643. doi:10.1038/nrm2002

66. Dietrich LEP, Boeddinghaus C, LaGrassa TJ, Ungermann C. Control of eukaryotic membrane fusion by N-terminal domains of SNARE proteins. *Biochim Biophys Acta*. 2003;1641(2-3):111-119. doi:10.1016/S0167-4889(03)00094-6

67. Antonin W, Fasshauer D, Becker S, Jahn R, Schneider TR. Crystal structure of the endosomal SNARE complex reveals common structural principles of all SNAREs. *Nat Struct Biol*. 2002;9(2):107-111. doi:10.1038/NSB746

68. Sutton RB, Fasshauer D, Jahn R, Brunger AT. Crystal structure of a SNARE complex involved in synaptic exocytosis at 2.4 A resolution. *Nature*. 1998;395(6700):347-353. doi:10.1038/26412

69. Hanson PI, Heuser JE, Jahn R. Neurotransmitter release — four years of SNARE complexes. *Curr Opin Neurobiol*. 1997;7(3):310-315. doi:10.1016/S0959-4388(97)80057-8

70. Li F, Pincet F, Perez E, et al. Energetics and dynamics of SNAREpin folding across lipid bilayers. *Nat Struct Mol Biol*. 2007;14(10):890-896. doi:10.1038/NSMB1310

71. Pobbati A V., Stein A, Fasshauer D. N- to C-terminal SNARE complex assembly promotes rapid membrane fusion. *Science (80- )*. 2006;313(5787):673-676. doi:10.1126/SCIENCE.1129486

72. Sørensen JB, Wiederhold K, Müller EM, et al. Sequential N- to C-terminal SNARE complex assembly drives priming and fusion of secretory vesicles. *EMBO J*. 2006;25(5):955. doi:10.1038/SJ.EMBOJ.7601003

73. Stein A, Weber G, Wahl MC, Jahn R. Helical extension of the neuronal SNARE complex into the membrane. *Nature*. 2009;460(7254):525-528. doi:10.1038/NATURE08156

74. Ossig R, Schmitt HD, De Groot B, et al. Exocytosis requires asymmetry in the central layer of the SNARE complex. *EMBO J*. 2000;19(22):6000-6010. doi:10.1093/EMBOJ/19.22.6000

75. Scales SJ, Yoo BY, Scheller RH. The ionic layer is required for efficient dissociation of the SNARE complex by-SNAP and NSF. *PNAS December*. 2001;4:14262-14267. Accessed June 15, 2022. www.pnas.orgcgidoi10.1073pnas.251547598

76. Fasshauer D, Sutton RB, Brunger AT, Jahn R. Conserved structural features of the synaptic fusion complex: SNARE proteins reclassified as Q- and R-SNAREs. *Proc Natl Acad Sci U S A*. 1998;95(26):15781-15786. doi:10.1073/PNAS.95.26.15781

77. Söllner T, Bennett MK, Whiteheart SW, Scheller RH, Rothman JE. A protein assembly-disassembly pathway in vitro that may correspond to sequential steps of synaptic vesicle docking, activation, and fusion. *Cell*. 1993;75(3):409-418. doi:10.1016/0092-8674(93)90376-2

78. Lin RC, Scheller RH. Structural organization of the synaptic exocytosis core complex. *Neuron*. 1997;19(5):1087-1094. doi:10.1016/S0896-6273(00)80399-2

79. Kroch AE, Fleming KG. Alternate interfaces may mediate homomeric and heteromeric assembly in the transmembrane domains of SNARE proteins. *J Mol Biol*. 2006;357(1):184-194. doi:10.1016/J.JMB.2005.12.060

80. Fasshauer D, Eliason WK, Brünger AT, Jahn R. Identification of a minimal core of the

synaptic SNARE complex sufficient for reversible assembly and disassembly. *Biochemistry*. 1998;37(29):10354-10362. doi:10.1021/BI980542H

81. Risselada HJ, Kutzner C, Grubmüller H. Caught in the Act: Visualization of SNARE-Mediated Fusion Events in Molecular Detail. *ChemBioChem*. 2011;12(7):1049-1055. doi:10.1002/CBIC.201100020

82. Knecht V, Grubmüller H. Mechanical Coupling via the Membrane Fusion SNARE Protein Syntaxin 1A: A Molecular Dynamics Study. *Biophys J*. 2003;84(3):1527-1547. doi:10.1016/S0006-3495(03)74965-0

83. Misura KMS, Scheller RH, Weis WI. Self-association of the H3 region of syntaxin 1A. Implications for intermediates in SNARE complex assembly. *J Biol Chem*. 2000;276(16):13273-13282. doi:10.1074/JBC.M009636200

84. Lerman JC, Robblee J, Fairman R, Hughson FM. Structural analysis of the neuronal SNARE protein syntaxin-1A. *Biochemistry*. 2000;39(29):8470-8479. doi:10.1021/BI0003994

85. Margittai M, Fasshauer D, Pabst S, Jahn R, Langen R. Homo- and heterooligomeric SNARE complexes studied by site-directed spin labeling. *J Biol Chem*. 2001;276(16):13169-13177. doi:10.1074/JBC.M010653200

86. Mertins J, Finke J, Sies R, Rink KM, Hasenauer J, Lang T. The mesoscale organization of syntaxin 1A and SNAP25 is determined by SNARE-SNARE interactions. *Elife*. 2021;10. doi:10.7554/ELIFE.69236

87. Sieber JJ, Willig KI, Kutzner C, et al. Anatomy and dynamics of a supramolecular membrane protein cluster. *Science (80- ).* 2007;317(5841):1072-1076. doi:10.1126/science.1141727

88. Bar-On D, Wolter S, Van De Linde S, et al. Super-resolution imaging reveals the internal architecture of nano-sized syntaxin clusters. *J Biol Chem*. 2012;287(32):27158-27167. doi:10.1074/JBC.M112.353250

89. Van Den Bogaart G, Meyenberg K, Risselada HJ, et al. Membrane protein sequestering by ionic protein–lipid interactions. *Nat 2011 4797374*. 2011;479(7374):552-555. doi:10.1038/nature10545

90. Merklinger E, Schloetel JG, Weber P, et al. The packing density of a supramolecular membrane protein cluster is controlled by cytoplasmic interactions. *Elife*. 2017;6. doi:10.7554/ELIFE.20705

91. Van Den Bogaart G, Holt MG, Bunt G, Riedel D, Wouters FS, Jahn R. One SNARE complex is sufficient for membrane fusion. *Nat Struct Mol Biol*. 2010;17(3):358-364. doi:10.1038/NSMB.1748

92. Khuong TM, Habets RLP, Kuenen S, et al. Synaptic PI(3,4,5)P3 is required for Syntaxin1A clustering and neurotransmitter release. *Neuron*. 2013;77(6):1097-1108. doi:10.1016/J.NEURON.2013.01.025

93. Lang T, Bruns D, Wenzel D, et al. SNAREs are concentrated in cholesterol-dependent clusters that define docking and fusion sites for exocytosis. *EMBO J*. 2001;20(9):2202-2213. doi:10.1093/EMBOJ/20.9.2202

94. Murray DH, Tamm LK. Clustering of Syntaxin-1A in Model Membranes is Modulated

by Phosphatidylinositol-4,5-bisphosphate and Cholesterol. *Biochemistry*. 2009;48(21):4617. doi:10.1021/BI9003217

95. Murray DH, Tamm LK. Molecular mechanism of cholesterol- and polyphosphoinositide-mediated syntaxin clustering. *Biochemistry*. 2011;50(42):9014-9022. doi:10.1021/BI201307U/ASSET/IMAGES/LARGE/BI-2011-01307U_0007.JPEG

96. Sieber JJ, Willig KI, Heintzmann R, Hell SW, Lang T. The SNARE motif is essential for the formation of syntaxin clusters in the plasma membrane. *Biophys J*. 2006;90(8):2843-2851. doi:10.1529/BIOPHYSJ.105.079574

97. Vardar G, Salazar-Lázaro A, Brockmann M, et al. Reexamination of N-terminal domains of syntaxin-1 in vesicle fusion from central murine synapses. *Elife*. 2021;10. doi:10.7554/ELIFE.69498

98. Fernandez I, Ubach J, Dulubova I, Zhang X, Südhof TC, Rizo J. Three-dimensional structure of an evolutionarily conserved N-terminal domain of syntaxin 1A. *Cell*. 1998;94(6):841-849. doi:10.1016/S0092-8674(00)81742-0

99. Margittai M, Widengren J, Schweinberger E, et al. Single-molecule fluorescence resonance energy transfer reveals a dynamic equilibrium between closed and open conformations of syntaxin 1. *Proc Natl Acad Sci U S A*. 2003;100(26):15516-15521. doi:10.1073/PNAS.2331232100

100. Chen X, Lu J, Dulubova I, Rizo J. NMR analysis of the closed conformation of syntaxin-1. *J Biomol NMR*. 2008;41(1):43-54. doi:10.1007/S10858-008-9239-1

101. Ma C, Li W, Xu Y, Rizo J. Munc13 mediates the transition from the closed syntaxin-Munc18 complex to the SNARE complex. *Nat Struct Mol Biol*. 2011;18(5):542-549. doi:10.1038/nsmb.2047

102. Misura KMS, Scheller RH, Weis WI. Three-dimensional structure of the neuronal-Sec1-syntaxin 1a complex. *Nature*. 2000;404(6776):355-362. doi:10.1038/35006120

103. Dulubova I, Sugita S, Hill S, et al. A conformational switch in syntaxin during exocytosis: Role of munc18. *EMBO J*. 1999;18(16):4372-4382. doi:10.1093/emboj/18.16.4372

104. Magdziarek M, Bolembach AA, Stepien KP, Quade B, Liu X, Rizo J. Re-examining how Munc13-1 facilitates opening of syntaxin-1. *Protein Sci*. 2020;29(6):1440-1458. doi:10.1002/PRO.3844

105. Dawidowski D, Cafiso DS. Allosteric control of syntaxin 1a by munc18-1: Characterization of the open and closed conformations of syntaxin. *Biophys J*. 2013;104(7):1585-1594. doi:10.1016/J.BPJ.2013.02.004

106. Colbert KN, Hattendorf DA, Weiss TM, Burkhardt P, Fasshauer D, Weis WI. Syntaxin1a variants lacking an N-peptide or bearing the LE mutation bind to Munc18a in a closed conformation. *Proc Natl Acad Sci U S A*. 2013;110(31):12637-12642. doi:10.1073/pnas.1303753110

107. Burkhardt P, Hattendorf DA, Weis WI, Fasshauer D. Munc18a controls SNARE assembly through its interaction with the syntaxin N-peptide. *EMBO J*. 2008;27(7):923-933. doi:10.1038/emboj.2008.37

108. Richmond JE, Weimer RM, Jorgensen EM. An open form of syntaxin bypasses the requirement for UNC-13 in vesicle priming. *Nature*. 2001;412(6844):338-341. doi:10.1038/35085583

109. Margittai M, Fasshauer D, Jahn R, Langen R. The Habc domain and the SNARE core complex are connected by a highly flexible linker. *Biochemistry*. 2003;42(14):4009-4014. doi:10.1021/BI027437Z

110. Khvotchev M, Dulubova I, Sun J, Dai H, Rizo J, Südhof TC. Dual modes of Munc18-1/SNARE interactions are coupled by functionally critical binding to syntaxin-1 N terminus. *J Neurosci*. 2007;27(45):12147-12155. doi:10.1523/JNEUROSCI.3655-07.2007

111. Rickman C, Medine CN, Bergmann A, Duncan RR. Functionally and spatially distinct modes of munc18-syntaxin 1 interaction. *J Biol Chem*. 2007;282(16):12097-12103. doi:10.1074/JBC.M700227200

112. Dawidowski D, Cafiso DS. Munc18-1 and the Syntaxin-1 N Terminus Regulate Open-Closed States in a t-SNARE Complex. *Structure*. 2016;24(3):392-400. doi:10.1016/j.str.2016.01.005

113. Dulubova I, Khvotchev M, Liu S, Huryeva I, Südhof TC, Rizo J. Munc18-1 binds directly to the neuronal SNARE complex. *Proc Natl Acad Sci U S A*. 2007;104(8):2697-2702. doi:10.1073/pnas.0611318104

114. Xu Y, Su L, Rizot J. Binding of Munc18-1 to synaptobrevin and to the SNARE four-helix bundle. *Biochemistry*. 2010;49(8):1568-1576. doi:10.1021/BI9021878

115. Bennett MK, Calakos N, Scheller RH. Syntaxin: a synaptic protein implicated in docking of synaptic vesicles at presynaptic active zones. *Science*. 1992;257(5067):255-259. doi:10.1126/SCIENCE.1321498

116. Vardar G, Chang S, Arancillo M, Wu YJ, Trimbuch T, Rosenmund C. Distinct functions of syntaxin-1 in neuronal maintenance, synaptic vesicle docking, and fusion in mouse neurons. *J Neurosci*. 2016;36(30):7911-7924. doi:10.1523/JNEUROSCI.1314-16.2016

117. Kádková A, Radecke J, Sørensen JB. The SNAP-25 Protein Family. *Neuroscience*. 2019;420:50-71. doi:10.1016/J.NEUROSCIENCE.2018.09.020

118. Gonzalo S, Greentree WK, Linder ME. SNAP-25 is targeted to the plasma membrane through a novel membrane-binding domain. *J Biol Chem*. 1999;274(30):21313-21318. doi:10.1074/JBC.274.30.21313

119. Oyler GA, Higgins GA, Hart RA, et al. The identification of a novel synaptosomal-associated protein, SNAP-25, differentially expressed by neuronal subpopulations. *J Cell Biol*. 1989;109(6 I):3039-3052. doi:10.1083/JCB.109.6.3039

120. Rickman C, Medine CN, Dun AR, et al. t-SNARE protein conformations patterned by the lipid microenvironment. *J Biol Chem* . 2010;285(18):13535-13541. doi:10.1074/JBC.M109.091058

121. Fasshauer D, Bruns D, Shen B, Jahn R, Brünger AT. A structural change occurs upon binding of syntaxin to SNAP-25. *J Biol Chem*. 1997;272(7):4582-4590. doi:10.1074/JBC.272.7.4582

122. Weninger K, Bowen ME, Choi UB, Chu S, Brunger AT. Accessory proteins stabilize

the acceptor complex for synaptobrevin, the 1:1 syntaxin/SNAP-25 complex. *Structure*. 2008;16(2):308-320. doi:10.1016/J.STR.2007.12.010

123. Bark IC. Structure of the chicken gene for SNAP-25 reveals duplicated exon encoding distinct isoforms of the protein. *J Mol Biol*. 1993;233(1):67-76. doi:10.1006/JMBI.1993.1485

124. Johansson JU, Ericsson J, Janson J, et al. An ancient duplication of exon 5 in the Snap25 gene is required for complex neuronal development/function. *PLoS Genet*. 2008;4(11):e1000278. doi:10.1371/JOURNAL.PGEN.1000278

125. Delgado-Martínez I, Nehring RB, Sørensen JB. Differential abilities of SNAP-25 homologs to support neuronal function. *J Neurosci*. 2007;27(35):9380-9391. doi:10.1523/JNEUROSCI.5092-06.2007

126. Williams D, Vicôgne J, Zaitseva I, McLaughlin S, Pessin JE. Evidence that electrostatic interactions between vesicle-associated membrane protein 2 and acidic phospholipids may modulate the fusion of transport vesicles with the plasma membrane. *Mol Biol Cell*. 2009;20(23):4910-4919. doi:10.1091/MBC.E09-04-0284

127. Brewer KD, Li W, Horne BE, Rizo J. Reluctance to membrane binding enables accessibility of the synaptobrevin SNARE motif for SNARE complex formation. *Proc Natl Acad Sci U S A*. 2011;108(31):12723-12728. doi:10.1073/PNAS.1105128108

128. Bowen M, Brunger AT. Conformation of the synaptobrevin transmembrane domain. *Proc Natl Acad Sci U S A*. 2006;103(22):8378-8383. doi:10.1073/PNAS.0602644103

129. Ellena JF, Liang B, Wiktor M, et al. Dynamic structure of lipid-bound synaptobrevin suggests a nucleation-propagation mechanism for trans-SNARE complex formation. *Proc Natl Acad Sci U S A*. 2009;106(48):20306-20311. doi:10.1073/PNAS.0908317106

130. Liang B, Dawidowski D, Ellena JF, Tamm LK, Cafiso DS. The SNARE motif of synaptobrevin exhibits an aqueous-interfacial partitioning that is modulated by membrane curvature. *Biochemistry*. 2014;53(9):1485-1494. doi:10.1021/BI401638U

131. Darios F, Wasser C, Shakirzyanova A, et al. Sphingosine Facilitates SNARE Complex Assembly and Activates Synaptic Vesicle Exocytosis. *Neuron*. 2009;62(5):683-694. doi:10.1016/J.NEURON.2009.04.024

132. Lakomek NA, Yavuz H, Jahn R, Pérez-Lara Á. Structural dynamics and transient lipid binding of synaptobrevin-2 tune SNARE assembly and membrane fusion. *Proc Natl Acad Sci U S A*. 2019;116(18):8699-8708. doi:10.1073/PNAS.1813194116

133. Walter AM, Wiederhold K, Bruns D, Fasshauer D, Sørensen JB. Synaptobrevin N-terminally bound to syntaxin-SNAP-25 defines the primed vesicle state in regulated exocytosis. *J Cell Biol*. 2010;188(3):401-413. doi:10.1083/JCB.200907018

134. Montecucco C. How do tetanus and botulinum toxins bind to neuronal membranes? *Trends Biochem Sci*. 1986;11(8):314-317. doi:10.1016/0968-0004(86)90282-3

135. McMahon HT, Sudhof TC. Synaptic core complex of synaptobrevin, syntaxin, and SNAP25 forms high affinity alpha-SNAP binding site. *J Biol Chem*. 1995;270(5):2213-2217. doi:10.1074/JBC.270.5.2213

136. Hanson PI, Roth R, Morisaki H, Jahn R, Heuser JE. Structure and conformational changes in NSF and its membrane receptor complexes visualized by quick-freeze/deep-

etch electron microscopy. *Cell*. 1997;90(3):523-535. doi:10.1016/S0092-8674(00)80512-7

137. Lin RC, Scheller RH. Mechanisms of synaptic vesicle exocytosis. *Annu Rev Cell Dev Biol*. 2000;16:19-49. doi:10.1146/ANNUREV.CELLBIO.16.1.19

138. Zhao M, Wu S, Zhou Q, et al. Mechanistic insights into the recycling machine of the SNARE complex. *Nature*. 2015;518(7537):61-67. doi:10.1038/NATURE14148

139. Xu D, Joglekar AP, Williams AL, Hay JC. Subunit structure of a mammalian ER/Golgi SNARE complex. *J Biol Chem*. 2000;275(50):39631-39639. doi:10.1074/JBC.M007684200

140. Poirier MA, Hao JC, Malkus PN, et al. Protease resistance of syntaxin·SNAP-25-VAMP complexes: Implications for assembly and structure. *J Biol Chem*. 1998;273(18):11370-11377. doi:10.1074/JBC.273.18.11370

141. Hua Y, Scheller RH. Three SNARE complexes cooperate to mediate membrane fusion. *Proc Natl Acad Sci U S A*. 2001;98(14):8065-8070. doi:10.1073/PNAS.131214798

142. Laage R, Rohde J, Brosig B, Langosch D. A conserved membrane-spanning amino acid motif drives homomeric and supports heteromeric assembly of presynaptic SNARE proteins. *J Biol Chem*. 2000;275(23):17481-17487. doi:10.1074/JBC.M910092199

143. Gerona RRL, Larsen EC, Kowalchyk JA, Martin TFJ. The C terminus of SNAP25 is essential for Ca(2+)-dependent binding of synaptotagmin to SNARE complexes. *J Biol Chem*. 2000;275(9):6328-6336. doi:10.1074/JBC.275.9.6328

144. Troy Littleton J, Bai J, Vyas B, et al. Synaptotagmin mutants reveal essential functions for the C2B domain in Ca2+-triggered fusion and recycling of synaptic vesicles in vivo. *J Neurosci*. 2001;21(5):1421-1433. doi:10.1523/JNEUROSCI.21-05-01421.2001

145. Chen YA, Scales SJ, Patel SM, Doung YC, Scheller RH. SNARE complex formation is triggered by Ca2+ and drives membrane fusion. *Cell*. 1999;97(2):165-174. doi:10.1016/S0092-8674(00)80727-8

146. Tokumaru H, Umayahara K, Pellegrini LL, et al. SNARE complex oligomerization by synaphin/complexin is essential for synaptic vesicle exocytosis. *Cell*. 2001;104(3):421-432. doi:10.1016/S0092-8674(01)00229-X

147. Hua SY, Charlton MP. Activity-dependent changes in partial VAMP complexes during neurotransmitter release. *Nat Neurosci*. 1999;2(12):1078-1083. doi:10.1038/16005

148. Xu T, Rammner B, Margittai M, Artalejo AR, Neher E, Jahn R. Inhibition of SNARE complex assembly differentially affects kinetic components of exocytosis. *Cell*. 1999;99(7):713-722. doi:10.1016/S0092-8674(00)81669-4

149. Wiederhold K, Kloepper TH, Walter AM, et al. A Coiled Coil Trigger Site Is Essential for Rapid Binding of Synaptobrevin to the SNARE Acceptor Complex. *J Biol Chem*. 2010;285(28):21549. doi:10.1074/JBC.M110.105148

150. Xiao W, Poirier MA, Bennett MK, Shin YK. The neuronal t-SNARE complex is a parallel four-helix bundle. *Nat Struct Biol*. 2001;8(4):308-311. doi:10.1038/86174

151. Fasshauer D, Margittai M. A Transient N-terminal Interaction of SNAP-25 and Syntaxin Nucleates SNARE Assembly. *J Biol Chem*. 2004;279(9):7613-7621.

doi:10.1074/JBC.M312064200

152. Baker RW, Hughson FM. Chaperoning SNARE assembly and disassembly. *Nat Rev Mol Cell Biol*. 2016;17(8):465-479. doi:10.1038/NRM.2016.65

153. Weber T, Parlati F, McNew JA, et al. Snarepins Are Functionally Resistant to Disruption by Nsf and αSNAP. *J Cell Biol*. 2000;149(5):1063-1072. doi:10.1083/JCB.149.5.1063

154. Ma C, Su L, Seven AB, Xu Y, Rizo J. Reconstitution of the vital functions of Munc18 and Munc13 in neurotransmitter release. *Science*. 2013;339(6118):421-425. doi:10.1126/SCIENCE.1230473

155. Wiedelhold K, Fasshauer D. Is Assembly of the SNARE Complex Enough to Fuel Membrane Fusion? *J Biol Chem*. 2009;284(19):13143-13152. doi:10.1074/JBC.M900703200

156. Verhage M, Maia AS, Plomp JJ, et al. Synaptic assembly of the brain in the absence of neurotransmitter secretion. *Science (80- )*. 2000;287(5454):864-869. doi:10.1126/science.287.5454.864

157. Varoqueaux F, Sigler A, Rhee JS, et al. Total arrest of spontaneous and evoked synaptic transmission but normal synaptogenesis in the absence of Munc13-mediated vesicle priming. *Proc Natl Acad Sci U S A*. 2002;99(13):9037-9042. doi:10.1073/PNAS.122623799

158. Rizo J, Südhof TC. The membrane fusion enigma: SNAREs, Sec1/Munc18 proteins, and their accomplices--guilty as charged? *Annu Rev Cell Dev Biol*. 2012;28:279-308. doi:10.1146/ANNUREV-CELLBIO-101011-155818

159. Lee Y Il, Kim YG, Pyeon HJ, et al. Dysregulation of the SNARE-binding protein Munc18-1 impairs BDNF secretion and synaptic neurotransmission: a novel interventional target to protect the aging brain. *GeroScience*. 2019;41(2):109-123. doi:10.1007/S11357-019-00067-1

160. Lee S, Shin J, Jung Y, et al. Munc18-1 induces conformational changes of syntaxin-1 in multiple intermediates for SNARE assembly. *Sci Rep*. 2020;10(1):11623-11623. doi:10.1038/S41598-020-68476-3

161. Jiang X, Zhang Z, Cheng K, et al. Membrane-mediated disorder-to-order transition of SNAP25 flexible linker facilitates its interaction with syntaxin-1 and SNARE-complex assembly. *FASEB J*. 2019;33(7):7985-7994. doi:10.1096/fj.201802796R

162. Romaniello R, Saettini F, Panzeri E, Arrigoni F, Bassi MT, Borgatti R. A de-novo STXBP1 gene mutation in a patient showing the Rett syndrome phenotype. *Neuroreport*. 2015;26(5):254-257. doi:10.1097/WNR.0000000000000337

163. Zhou P, Pang ZP, Yang X, et al. Syntaxin-1 N-peptide and Habc-domain perform distinct essential functions in synaptic vesicle fusion. *EMBO J*. 2013;32(1):159-171. doi:10.1038/EMBOJ.2012.307

164. Gong J, Wang X, Cui C, et al. Exploring the Two Coupled Conformational Changes That Activate the Munc18-1/Syntaxin-1 Complex. *Front Mol Neurosci*. 2021;14. doi:10.3389/FNMOL.2021.785696/FULL

165. Stepien KP, Xu J, Zhang X, Bai X-C, Rizo J. SNARE assembly enlightened by cryo-EM structures of a synaptobrevin-Munc18-1-syntaxin-1 complex. *Sci Adv*. 2022;8(25).

doi:10.1126/SCIADV.ABO5272

166. Sitarska E, Xu J, Park S, et al. Autoinhibition of munc18-1 modulates synaptobrevin binding and helps to enable munc13-dependent regulation of membrane fusion. *Elife*. 2017;6:e24278. doi:10.7554/ELIFE.24278

167. Meijer M, Burkhardt P, de Wit H, Toonen RF, Fasshauer D, Verhage M. Munc18-1 mutations that strongly impair SNARE-complex binding support normal synaptic transmission. *EMBO J*. 2012;31(9):2156-2168. doi:10.1038/emboj.2012.72

168. Zilly FE, Sørensen JB, Jahn R, Lang T. Munc18-bound syntaxin readily forms SNARE complexes with synaptobrevin in native plasma membranes. *PLoS Biol*. 2006;4(10):1789-1797. doi:10.1371/journal.pbio.0040330

169. Brose N, Petrenko AG, Sudhof TC, Jahn R. Synaptotagmin: A calcium sensor on the synaptic vesicle surface. *Science (80- )*. 1992;256(5059):1021-1025. doi:10.1126/SCIENCE.1589771

170. Fernández-Chacón R, Königstorfer A, Gerber SH, et al. Synaptotagmin I functions as a calcium regulator of release probability. *Nature*. 2001;410(6824):41-49. doi:10.1038/35065004

171. Walter AM, Groffen AJ, Sørensen Jakob B. JB, Verhage M. Multiple Ca2+ sensors in secretion: teammates, competitors or autocrats? *Trends Neurosci*. 2011;34(9):487-497. doi:10.1016/J.TINS.2011.07.003

172. Shin OH, Xu J, Rizo J, Südhof TC. Differential but convergent functions of Ca2+ binding to synaptotagmin-1 C2 domains mediate neurotransmitter release. *Proc Natl Acad Sci U S A*. 2009;106(38):16469-16474. doi:10.1073/PNAS.0908798106/SUPPL_FILE/0908798106SI.PDF

173. Kuo W, Herrick DZ, Ellena JF, Cafiso DS. The calcium-dependent and calcium-independent membrane binding of synaptotagmin 1: two modes of C2B binding. *J Mol Biol*. 2009;387(2):284-294. doi:10.1016/J.JMB.2009.01.064

174. Pérez-Lara Á, Thapa A, Nyenhuis SB, et al. PtdInsP 2 and PtdSer cooperate to trap synaptotagmin-1 to the plasma membrane in the presence of calcium. *Elife*. 2016;5(OCTOBER2016). doi:10.7554/ELIFE.15886

175. Nyenhuis SB, Karandikar N, Kiessling V, et al. Conserved arginine residues in synaptotagmin 1 regulate fusion pore expansion through membrane contact. *Nat Commun 2021 121*. 2021;12(1):1-13. doi:10.1038/s41467-021-21090-x

176. Brewer KD, Bacaj T, Cavalli A, et al. Dynamic binding mode of a Synaptotagmin-1-SNARE complex in solution. *Nat Struct Mol Biol*. 2015;22(7):555-564. doi:10.1038/NSMB.3035

177. Zhou Q, Lai Y, Bacaj T, et al. Architecture of the synaptotagmin-SNARE machinery for neuronal exocytosis. *Nature*. 2015;525(7567):62-67. doi:10.1038/NATURE14975

178. Zhou Q, Zhou P, Wang AL, et al. The Primed SNARE-Complexin-Synaptotagmin Complex for Neuronal Exocytosis. *Nature*. 2017;548(7668):420. doi:10.1038/NATURE23484

179. Söllner T, Whiteheart SW, Brunner M, et al. SNAP receptors implicated in vesicle targeting and fusion. *Nature*. 1993;362(6418):318-324. doi:10.1038/362318A0

180. Lai AL, Huang H, Herrick DZ, Epp N, Cafiso DS. Synaptotagmin 1 and SNAREs Form a Complex That Is Structurally Heterogeneous. *J Mol Biol*. 2011;405(3):696-706. doi:10.1016/J.JMB.2010.11.015

181. Park Y, Seo JB, Fraind A, et al. Synaptotagmin-1 binds to PIP(2)-containing membrane but not to SNAREs at physiological ionic strength. *Nat Struct Mol Biol*. 2015;22(10):815-823. doi:10.1038/NSMB.3097

182. Ishizuka T, Saisu H, Odani S, Abe T. Synaphin: a protein associated with the docking/fusion complex in presynaptic terminals. *Biochem Biophys Res Commun*. 1995;213(3):1107-1114. doi:10.1006/BBRC.1995.2241

183. Chen X, Tomchick DR, Kovrigin E, et al. Three-dimensional structure of the complexin/SNARE complex. *Neuron*. 2002;33(3):397-409. doi:10.1016/S0896-6273(02)00583-4

184. Heinig M, Frishman D. STRIDE: a web server for secondary structure assignment from known atomic coordinates of proteins. *Nucleic Acids Res*. 2004;32(Web Server issue):W500. doi:10.1093/NAR/GKH429

185. Seiler F, Malsam J, Krause JM, Söllner TH. A role of complexin-lipid interactions in membrane fusion. *FEBS Lett*. 2009;583(14):2343-2348. doi:10.1016/J.FEBSLET.2009.06.025

186. Wragg RT, Snead D, Dong Y, et al. Synaptic vesicles position complexin to block spontaneous fusion. *Neuron*. 2013;77(2):323-334. doi:10.1016/J.NEURON.2012.11.005

187. Zdanowicz R, Kreutzberger A, Liang B, Kiessling V, Tamm LK, Cafiso DS. Complexin Binding to Membranes and Acceptor t-SNAREs Explains Its Clamping Effect on Fusion. *Biophys J*. 2017;113(6):1235. doi:10.1016/J.BPJ.2017.04.002

188. Brose N. For better or for worse: complexins regulate SNARE function and vesicle fusion. *Traffic*. 2008;9(9):1403-1413. doi:10.1111/J.1600-0854.2008.00758.X

189. Trimbuch T, Rosenmund C. Should I stop or should I go? The role of complexin in neurotransmitter release. *Nat Rev Neurosci*. 2016;17(2):118-125. doi:10.1038/NRN.2015.16

190. An SJ, Grabner CP, Zenisek D. Real-time visualization of complexin during single exocytic events. *Nat Neurosci*. 2010;13(5):577-583. doi:10.1038/NN.2532

191. Lin MY, Rohan JG, Cai H, Reim K, Ko CP, Chow RH. Complexin facilitates exocytosis and synchronizes vesicle release in two secretory model systems. *J Physiol*. 2013;591(10):2463-2473. doi:10.1113/JPHYSIOL.2012.244517

192. Jasniewski A, Hu Y, Ribbe MW. Chapter 13 Electron Paramagnetic Resonance Spectroscopy of Metalloproteins. doi:10.1007/978-1-4939-8864-8_13

193. Nohr D, Weber S, Schleicher E. EPR spectroscopy on flavin radicals in flavoproteins. doi:10.1016/bs.mie.2019.03.013

194. Stone TJ, Buckman T, Nordio PL, McConnell HM. Spin-labeled biomolecules. *Proc Natl Acad Sci U S A*. 1965;54(4):1010-1017. doi:10.1073/PNAS.54.4.1010

195. Fanucci GE, Cafiso DS. Recent advances and applications of site-directed spin labeling.

*Curr Opin Struct Biol*. 2006;16(5):644-653. doi:10.1016/J.SBI.2006.08.008

196. Klug CS, Feix JB. Methods and Applications of Site-Directed Spin Labeling EPR Spectroscopy. *Methods Cell Biol*. 2008;84:617-658. doi:10.1016/S0091-679X(07)84020-9

197. Jeschke G, Polyhach Y. Distance measurements on spin-labelled biomacromolecules by pulsed electron paramagnetic resonance. doi:10.1039/b614920k

198. Hubbell WL, Cafiso DS, Altenbach C. *Review Site-Directed Spin Labeling Identifying Conformational Changes with Site-Directed Spin Labeling*.; 2000. http://structbio.nature.com

199. Acharya KR, Lloyd MD. The advantages and limitations of protein crystal structures. *Trends Pharmacol Sci*. 2005;26(1):10-14. doi:10.1016/J.TIPS.2004.10.011

200. Wüthrich K, Wüthrich K. NMR Studies of Structure and Function of Biological Macromolecules (Nobel Lecture). *Angew Chemie Int Ed*. 2003;42(29):3340-3363. doi:10.1002/ANIE.200300595

201. Gupta U, Joshi MD, Criscuolo D, et al. Advantages and Limitations of Current Imaging Techniques for Characterizing Liposome Morphology. Published online 2018. doi:10.3389/fphar.2018.00080

202. Czogalla A, Pieciul A, Jezierski A, Sikorski AF. Attaching a spin to a protein - Site-directed spin labeling in structural biology. *Acta Biochim Pol*. 2007;54(2):235-244. doi:10.18388/abp.2007_3243

203. Schreier S, Polnaszek CF, Smith ICP. Spin labels in membranes problems in practice. *Biochim Biophys Acta - Rev Biomembr*. 1978;515(4):395-436. doi:10.1016/0304-4157(78)90011-4

204. Kivelson D. Theory of ESR Linewidths of Free Radicals. *J Chem Phys*. 2004;33(4):1094. doi:10.1063/1.1731340

205. Berliner LJ. *Spin Labeling Theory and Applications. Molecular Biology.* Academic press inc; 1976.

206. ESR Spectroscopy in Membrane Biophysics. *ESR Spectrosc Membr Biophys*. Published online 2007. doi:10.1007/978-0-387-49367-1

207. Jeschke G. Instrumentation and Experimental Setup. *ESR Spectrosc Membr Biophys*. Published online August 13, 2007:17-47. doi:10.1007/978-0-387-49367-1_2

208. Sealy RC, Hyde JS, Antholine WE. Chapter 2 Electron spin resonance. *New Compr Biochem*. 1985;11(PA):69-148. doi:10.1016/S0167-7306(08)60561-X

209. Vicino MF, Hett T, Schiemann O. Spin Labeling of RNA Using "Click" Chemistry for Coarse-grained Structure Determination via Pulsed Electron-electron Double Resonance Spectroscopy. *Bio-protocol*. 2021;11(9). doi:10.21769/BIOPROTOC.4004

210. Becker CFW, Lausecker K, Balog M, et al. Incorporation of spin-labelled amino acids into proteins. *Magn Reson Chem*. 2005;43(SPEC. ISS.). doi:10.1002/MRC.1688

211. Cornish VW, Benson DR, Altenbach CA, Hideg K, Hubbell WL, Schultz PG. Site-specific incorporation of biophysical probes into proteins. *Proc Natl Acad Sci U S A*. 1994;91(8):2910-2914. doi:10.1073/pnas.91.8.2910

212. Berliner LJ, Grunwald J, Hankovszky HO, Hideg K. A novel reversible thiol-specific spin label: papain active site labeling and inhibition. *Anal Biochem*. 1982;119(2):450-455. doi:10.1016/0003-2697(82)90612-1

213. Altenbach, C., Flitsch, S. L., Khorana, H. G., & Hubbell WL. Structural studies on transmembrane proteins. 2. Spin labeling of bacteriorhodopsin mutants at unique cysteinesNo Title. *Biochemistry*. 1989;28(19):7806–7812.

214. Altenbach, C., Marti, T., Khorana, H. G., & Hubbell WL. Transmembrane protein structure: spin labeling of bacteriorhodopsin mutantsNo Title. *Science (80- )*. 1990;248(4959):1088–92.

215. Cattani J, Subramaniam V, Drescher M. Room-temperature in-cell EPR spectroscopy: alpha-Synuclein disease variants remain intrinsically disordered in the cell. *Phys Chem Chem Phys*. 2017;19(28):18147-18151. doi:10.1039/C7CP03432F

216. Dockter C, Volkov A, Bauer C, et al. Refolding of the integral membrane protein light-harvesting complex II monitored by pulse EPR. *Proc Natl Acad Sci U S A*. 2009;106(44):18485-18490. doi:10.1073/PNAS.0906462106/SUPPL_FILE/0906462106SI.PDF

217. Fielding AJ, Concilio MG, Heaven G, Hollas MA. New Developments in Spin Labels for Pulsed Dipolar EPR. *Molecules*. 2014;19(10):16998. doi:10.3390/MOLECULES191016998

218. Haugland MM, Anderson EA, Lovett JE. Tuning the properties of nitroxide spin labels for use in electron paramagnetic resonance spectroscopy through chemical modification of the nitroxide framework. doi:10.1039/9781782629436-00001

219. Jeschke G. DEER Distance Measurements on Proteins. *http://dx.doi.org/101146/annurev-physchem-032511-143716*. 2012;63:419-446. doi:10.1146/ANNUREV-PHYSCHEM-032511-143716

220. Klare JP, Steinhoff HJ. Spin labeling EPR. *Photosynth Res*. 2009;102(2):377-390. doi:10.1007/s11120-009-9490-7

221. Klare JP. Site-Directed Spin Labeling and Electron Paramagnetic Resonance (EPR) Spectroscopy: A Versatile Tool to Study Protein-Protein Interactions. Accessed May 13, 2022. www.intechopen.com

222. Mchaourab HS, Lietzow MA, Hideg K, Hubbell WL. *Motion of Spin-Labeled Side Chains in T4 Lysozyme. Correlation with Protein Structure and Dynamics †.*; 1996. https://pubs.acs.org/sharingguidelines

223. Reginsson GW, Schiemann O. Pulsed electron-electron double resonance: beyond nanometre distance measurements on biomacromolecules. *Biochem J*. 2011;434:353-363. doi:10.1042/BJ20101871

224. Jeschke G. Distance Measurements in the Nanometer Range by Pulse EPR. *ChemPhysChem*. 2002;3(11):927-932. doi:10.1002/1439-7641(20021115)3:11<927::AID-CPHC927>3.0.CO;2-Q

225. Fajer PG. Electron Spin Resonance Spectroscopy Labeling in Peptide and Protein Analysis. *Encycl Anal Chem*. Published online September 15, 2006. doi:10.1002/9780470027318.A1609

226. Steinhoff HJ. Inter- and intra-molecular distances determined by EPR spectroscopy and site-directed spin labeling reveal protein-protein and protein-oligonucleotide interaction. *Biol Chem*. 2004;385(10):913-920. doi:10.1515/BC.2004.119

227. Liang B, Kiessling V, Tamm LK. Prefusion structure of syntaxin-1A suggests pathway for folding into neuronal trans-SNARE complex fusion intermediate. *Proc Natl Acad Sci U S A*. 2013;110(48):19384-19389. doi:10.1073/PNAS.1314699110

228. Khan JM, Malik A, Ahmed A, Alghamdi OHA, Ahmed M. SDS induces cross beta-sheet amyloid as well as alpha-helical structure in conconavalin A. *J Mol Liq*. 2020;319:114154. doi:10.1016/J.MOLLIQ.2020.114154

229. Takaramoto S, Nakasone Y, Sadakane K, Maruta S, Terazima M. Time-resolved detection of SDS-induced conformational changes in α-synuclein by a micro-stopped-flow system. *RSC Adv*. 2020;11(2):1086. doi:10.1039/D0RA09614H

230. Zhang X, Adda CG, Low A, et al. Role of the helical structure of the N-terminal region of Plasmodium falciparum merozoite surface protein 2 in fibril formation and membrane interaction. *Biochemistry*. 2012;51(7):1380-1387. doi:10.1021/BI201880S

231. Jurczak P, Sikorska E, Czaplewska P, Rodziewicz-Motowidlo S, Zhukov I, Szymanska A. The Influence of the Mixed DPC:SDS Micelle on the Structure and Oligomerization Process of the Human Cystatin C. *Membranes (Basel)*. 2020;11(1):1-22. doi:10.3390/MEMBRANES11010017

232. Krissinel E, Henrick K. Inference of macromolecular assemblies from crystalline state. *J Mol Biol*. 2007;372(3):774-797. doi:10.1016/J.JMB.2007.05.022

233. Eisemann TJ, Allen F, Lau K, Shimamura GR, Jeffrey PD, Hughson FM. The Sec1/Munc18 protein Vps45 holds the Qa-SNARE Tlg2 in an open conformation. *Elife*. 2020;9:1-18. doi:10.7554/ELIFE.60724

234. Zhang F, Chen Y, Kweon DH, Kim CS, Shin YK. The four-helix bundle of the neuronal target membrane SNARE complex is neither disordered in the middle nor uncoiled at the C-terminal region. *J Biol Chem*. 2002;277(27):24294-24298. doi:10.1074/JBC.M201200200

235. Hilger D, Jung H, Padan E, et al. Assessing Oligomerization of Membrane Proteins by Four-Pulse DEER: pH-Dependent Dimerization of NhaA Na+/H+ Antiporter of E. coli. *Biophys J*. 2005;89(2):1328. doi:10.1529/BIOPHYSJ.105.062232

236. Kiessling V, Kreutzberger AJB, Liang B, et al. A molecular mechanism for calcium-mediated synaptotagmin-triggered exocytosis. *Nat Struct Mol Biol*. 2018;25(10):911-917. doi:10.1038/S41594-018-0130-9

237. Park S, Bin N-R, Michael Rajah M, et al. Conformational states of syntaxin-1 govern the necessity of N-peptide binding in exocytosis of PC12 cells and *Caenorhabditis elegans*. Glick BS, ed. *Mol Biol Cell*. 2016;27(4):669-685. doi:10.1091/mbc.E15-09-0638